Genetic studies on transcriptional regulation and pleiotropy of the body pigmentation-associated gene *ebony* in *Drosophila melanogaster*

Noriyoshi Akiyama

Department of Biological Sciences

Tokyo Metropolitan University

2022

CONTENTS

Page

GENERAL INTRODUCTION 1

LITERATURE CITED 5

Part I 10

INTRODUCTION 11

MATERIALS AND METHODS 15

RESULTS 23

DISCUSSION 30

LITERATURE CITED 37

TABLE 47

FIGURES 50

Part II 74

INTRODUCTION 75

MATERIALS AND METHODS 78

RESULTS 84

DISCUSSION 89

LITERATURE CITED 93

TABLE 101

FIGURES 104

GENERAL DISCUSSION 115

LITERATURE CITED 118

COMPLIANCE STATEMENT IN DISSERTATIONS 121

ACKNOWLEDGEMENTS 122

GENERAL INTRODUCTION

Organisms have acquired a wide variety of phenotypes, including the size, shape and color of organs, through their evolution. To understand the evolutionary process of these various traits, two parallel studies have long been conducted, one focusing on genotypic diversity and the other on phenotypic diversity (Lewontin, 1974). These biological areas are currently being integrated, and many studies link genotype and phenotype by identifying the molecular changes that cause phenotypic evolution (e.g., Carroll *et al*., 2001; Nachman *et al*., 2003; Brakefield *et al*., 2003; Carroll, 2008). However, for a proper understanding, more in-depth studies are required, such as spatiotemporal regulatory systems of the causative gene expression and pleiotropic effects of the genetic changes on other traits.

Pigmentation traits represent one of the most suitable research materials for a deeper understanding of the association between genotypes and phenotypes. It was clearly demonstrated by the Mendelian inheritance in one of the earliest studies in genetics, using the albino phenotype in animals and "depigmentation" in plants (Castle and Allen, 1903). More importantly, body color and pigment patterns are quantifiable and often show dramatic variation within and between species, both vertebrate and invertebrate (e.g., Endler, 1990; Parchem *et al*., 2007). This property has led to the identification of causative genes for color variation and/or diversity in many organisms (e.g., Schlager and Dickie, 1966; Miyagi and Terai, 2013). In particular, the pigment biosynthesis pathways are well-studied in animals (reviewed in Jackson, 1994; Sugumaran, 2002), and the major genes involved in the pathway in insects have been known for a long time (Wright, 1987).

Drosophila, a model genus in insects used for biological research, has a wide variation in body color within and between species. For example, within-species variation in abdominal and thoracic cuticle pigment intensity has been reported in many species (reviewed in Pétavy *et al*., 2002; Wittkopp and Beldade 2009; Massey and Wittkopp, 2016), and the dark stripes on the posterior edges of the abdominal cuticle segments vary in shape and pattern among species (reviewed in Wittkopp *et al*., 2003; Rebeiz and Williams, 2017). The cuticular pigments in *Drosophila* are synthesized by genes involved in the melanin biosynthetic pathway and are deposited in the developing cuticle during late pupal and early adult stages (reviewed in Massey and Wittkopp 2016). Furthermore, *ebony* involved in the pathway has been identified as the major causative gene that explains most of the pigmentation variation in *Drosophila melanogaster* (Takahashi *et al*., 2007; Pool and Aquadro, 2007; Rebeiz *et al*, 2009).

The Ebony protein is an enzyme that catalyzes the reaction from dopamine to N-β-alanyl dopamine (NBAD) in the melanin biosynthetic pathway in *Drosophila* (Wright, 1987; Walter *et al*., 1996). Since dopamine is the precursor of black and brown melanin and NBAD that is the precursor of yellow sclerotin, differences in the expression level of *ebony* during and after eclosion affect the body color of an adult fly via changes in the relative amount of each synthesized pigment (Takahashi *et al*, 2007; Rebeiz *et al*, 2009). The association between the variation in body color and the expression level of *ebony* quantified at around eclosion has been reported in Africa (Pool and Aquadro, 2007), Australia (Telonis-Scott *et al*., 2011), Japan (Takahashi and Takano-Shimizu 2011), and North America (Miyagi *et al*., 2015), therefore, this association is considered to be world-wide. Moreover, *D. melanogaster* has a black stripe pattern across the posterior end of the abdominal segments, and its midline area

expands in the anterior direction. It is known that *ebony* is not expressed in the area of the black stripe (Rebiez *et al*., 2009), suggesting that it is also involved in the formation of the epidermal pigmentation pattern. Thus, the expression of *ebony* around the eclosion and in the epidermis strongly links to body-color traits.

Therefore, a detailed investigation of the spatiotemporal regulatory system of *ebony* is expected to provide insights into the molecular mechanisms that maintain body color variation within species and how pigmentation pattern diversity among species is formed. Also, the body color and the *ebony* expression level in *D. melanogaster* show clinal variations along the latitude and altitude of the habitat, suggesting that they are under some kind of selective pressure (Pool and Aquadro, 2007; Parkash *et al*., 2009; Telonis-Scott *et al*., 2011). Furthermore, although *ebony* is well known to be a pleiotropic gene in *Drosophila* (reviewed in Wittkopp and Beldade, 2003; Pérez *et al*., 2010; Takahashi, 2013), physiological traits associated with *ebony* expression level have not been indicated clearly. The identification of such traits may help understand the clinal variation in body pigmentation and the underlying selective regime.

In this study, I conducted genetic studies by utilizing the abundant genetic tools available for *D. melanogaster* to improve our understanding of the spatiotemporal regulation and the pleiotropic effects of *ebony* in this species. In chapter Ⅰ, to elucidate the function of a known *cis*-regulatory element, I knocked out an enhancer element known to drive *ebony* expression in the epidermis during and after eclosion by genome editing. The knock-out revealed the presence of unknown epidermal enhancer(s) and a new silencer involved in the abdominal stripe pattern formation. In Chapter Ⅱ, to analyze the pleiotropic effect of *ebony* on physiological traits by changing its expression

level, I compared the cuticular hydrocarbon (CHC) profiles with the *ebony* expression levels in the developing epidermis in an inbred-strain collection originated from a natural population and showed that they covary. I also performed a genetic manipulation of the *ebony* expression level, which suggested that the epidermal *ebony* expression may affect desiccation tolerance. In the final part of the thesis, I discuss the implications of the findings above for the study of body color traits.

LITERATURE CITED

Brakefield, P. M., French, V., & Zwaan, B. J. (2003). Development and the genetics of evolutionary change within insect species. *Annual Review of Ecology, Evolution, and Systematics*, *34*(1), 633-660.

Carroll, S. B. (2008). Evo-devo and an expanding evolutionary synthesis: a genetic theory of morphological evolution. *Cell*, *134*(1), 25-36.

Carroll, S. B., Grenier, J. K., & Weatherbee, S. D. (2013). *From DNA to diversity: molecular genetics and the evolution of animal design*. John Wiley & Sons.

Castle, W. E., & Allen, G. M. (1903). The heredity of albinism. *Proceedings of the American Academy of Arts and Sciences* (Vol. 38, No. 21, pp. 603-622).

Endler, J. A. (1990). On the measurement and classification of colour in studies of animal colour patterns. *Biological Journal of the Linnean Society*, *41*(4), 315-352.

Jackson, D. M., & Westlind-Danielsson, A. (1994). Dopamine receptors: molecular biology, biochemistry and behavioural aspects. *Pharmacology & Therapeutics*, *64*(2), 291-370.

Lewontin, R. C. (1974). *The genetic basis of evolutionary change* (Vol. 560). New York: Columbia University Press.

Massey, J. H., & Wittkopp, P. J. (2016). The genetic basis of pigmentation differences within and between *Drosophila* species. *Current topics in Developmental Biology*, *119*, 27-61.

Miyagi, R., & Terai, Y. (2013). The diversity of male nuptial coloration leads to species diversity in Lake Victoria cichlids. *Genes & Genetic Systems*, *88*(3), 145-153.

Miyagi, R., Akiyama, N., Osada, N., & Takahashi, A. (2015). Complex patterns of cis‐regulatory polymorphisms in *ebony* underlie standing pigmentation variation in *Drosophila melanogaster*. *Molecular Ecology*, *24*(23), 5829-5841.

Nachman, M. W., Hoekstra, H. E., & D'Agostino, S. L. (2003). The genetic basis of adaptive melanism in pocket mice. *Proceedings of the National Academy of Sciences*, *100*(9), 5268-5273.

Parchem, R. J., Perry, M. W., & Patel, N. H. (2007). Patterns on the insect wing. *Current Opinion in Genetics & Development*, *17*(4), 300-308.

Pétavy, G., Moreteau, B., Gibert, P., & David, J. R. (2002). Phenotypic plasticity of body pigmentation in *Drosophila*: influence of a developmental thermoperiodic regime in two sibling species. *Physiological Entomology*, *27*(2), 124-135.

Parkash, R., Sharma, V., & Kalra, B. (2009). Impact of body melanisation on desiccation resistance in montane populations of *D. melanogaster*: analysis of seasonal variation. *Journal of Insect Physiology*, *55*(10), 898-908.

Pérez, M. M., Schachter, J., Berni, J., & Quesada-Allué, L. A. (2010). The enzyme NBAD-synthase plays diverse roles during the life cycle of *Drosophila melanogaster*. *Journal of Insect Physiology, 56*(1), 8-13.

Pool, J. E., & Aquadro, C. F. (2007). The genetic basis of adaptive pigmentation variation in *Drosophila melanogaster*. *Molecular Ecology*, *16*(14), 2844-2851.

Rebeiz, M., Pool, J. E., Kassner, V. A., Aquadro, C. F., & Carroll, S. B. (2009). Stepwise modification of a modular enhancer underlies adaptation in a *Drosophila* population. *Science*, *326*(5960), 1663-1667.

Rebeiz, M., & Williams, T. M. (2017). Using *Drosophila* pigmentation traits to study the mechanisms of cis-regulatory evolution. *Current Opinion in Insect Science, 19*, 1-7.

Schlager, G., & Dickie, M. M. (1966). Spontaneous mutation rates at five coat-color loci in mice. *Science*, *151*(3707), 205-206.

Sugumaran, M. (2002). Comparative biochemistry of eumelanogenesis and the protective roles of phenoloxidase and melanin in insects. *Pigment Cell Research*, *15*(1), 2-9.

Takahashi, A., Takahashi, K., Ueda, R., & Takano-Shimizu, T. (2007). Natural variation of *ebony* gene controlling thoracic pigmentation in *Drosophila melanogaster*. *Genetics*, *177*(2), 1233-1237.

Takahashi, A., & Takano-shimizu, T. (2011). Divergent enhancer haplotype of *ebony* on inversion In (3R) Payne associated with pigmentation variation in a tropical population of *Drosophila melanogaster*. *Molecular Ecology*, *20*(20), 4277-4287.

Takahashi, A. (2013). Pigmentation and behavior: potential association through pleiotropic genes in *Drosophila*. *Genes & Genetic Systems*, *88*(3), 165-174.

Telonis-Scott, M., Hoffmann, A. A., & Sgro, C. M. (2011). The molecular genetics of clinal variation: a case study of *ebony* and thoracic trident pigmentation in *Drosophila melanogaster* from eastern Australia. *Molecular Ecology*, *20*(10), 2100-2110.

Walter, M. F., Zeineh, L. L., Black, B. C., McIvor, W. E., Wright, T. R., & Biessmann, H. (1996). Catecholamine metabolism and in vitro induction of premature cuticle melanization in wild type and pigmentation mutants of *Drosophila melanogaster*. *Archives of Insect Biochemistry and Physiology: Published in Collaboration with the Entomological Society of America*, *31*(2), 219-233.

Wittkopp, P. J., Carroll, S. B., & Kopp, A. (2003). Evolution in black and white: genetic control of pigment patterns in *Drosophila*. *TRENDS in Genetics*, *19*(9), 495-504.

Wittkopp, P. J., & Beldade, P. (2009). Development and evolution of insect pigmentation: genetic mechanisms and the potential consequences of pleiotropy. *Seminars in Cell & Developmental Biology* (Vol. 20, No. 1, pp. 65-71).

Wright, T. R. (1987). The genetics of biogenic amine metabolism, sclerotization, and melanization in *Drosophila melanogaster*. *Advances in Genetics*, *24*, 127-222.

Part I

The role of the epidermis enhancer element on positive and negative transcriptional regulation of *ebony* in *Drosophila melanogaster*

INTRODUCTION

The spatiotemporal regulation of gene expression during the development of organisms results in diverse phenotypes. The *cis*-regulatory elements (CREs) are strings of nucleotides that differentially modulate the transcription levels of specific genes, typically in an allele-specific manner. The most common CREs, enhancers and silencers, are located within a certain distance from the transcription start site of the target gene and contain the binding sites for the transcription activators or repressors (Spitz and Furlong 2012; Long *et al*. 2016). While these CREs are generally unique to each expression unit (Arnone and Davidson 1997; Stern 2000; Wray *et al*. 2003; Prud'homme *et al*. 2007; Carroll 2008), various enhancers are reported to exhibit functional redundancy or to cooperatively define the expression site boundaries (Hong *et al*. 2008; Perry *et al*. 2009, 2010, 2011; Frankel *et al*. 2010; Bothma *et al*. 2015; El-Sherif and Levine 2016). Also, a number of enhancers with pleiotropic functions have been reported (Preger-Ben Noon *et al*. 2018; Nagy *et al*. 2018; Sabarís *et al*. 2019; Xin *et al*. 2020).

The CREs in genes involved in body pigmentation patterns have been well-characterized, and multiple modular enhancers that activate transcription in different body regions have been documented in detail (reviewed in Massey and Wittkopp 2016; Rebeiz and Williams 2017). For example, the distinct CREs of *yellow* that activate transcription in bristles, wing and body, and abdomen have been identified (Geyer and Corces 1987; Martin *et al*. 1989; Wittkopp *et al*. 2002; Jeong *et al*. 2006; Roeske *et al*. 2018). However, a recent study revealed that many sequence fragments in the regulatory region of *yellow* exhibit redundant and cryptic enhancer activities, suggesting that *cis*-

regulatory modules are not as distinct as described previously and more amenable to evolutionary changes (Kalay *et al*. 2019).

A complex architecture of *cis*-regulatory region has also been implicated from the within-species comparisons of *cis*-regulatory sequences of *ebony*. Polymorphisms in *ebony*, which encodes an enzyme of the melanin biosynthesis pathway, is the major causative factor determining the variation in body pigmentation intensity in *D. melanogaster* (Pool and Aquadro 2007; Takahashi *et al*. 2007; Rebeiz *et al*. 2009; Telonis-Scott *et al*. 2011). The sequence polymorphisms of the primary epidermis enhancer (priEE), which was identified to be located in the upstream intergenic region of *ebony*, were analyzed in detail. Some single-nucleotide polymorphisms (SNPs) first identified in the African populations affected the enhancer function but were not associated with body pigmentation intensity in the Japanese, European, North American, and Australian populations (Takahashi and Takano-Shimizu 2011; Telonis-Scott *et al*. 2011; Bastide *et al*. 2013; Dembeck *et al*. 2015; Miyagi *et al*. 2015; Telonis-Scott and Hoffmann 2018). Also, a priEE haplotype associated with light body color was identified in the Iriomote and Australian populations but not in the African populations (Telonis-Scott and Hoffmann 2018). Furthermore, there were no SNPs or indels in the priEE that showed complete association with the allele-specific expression levels in the developing epidermis in 20 strains sampled from the *Drosophila melanogaster* Genetic Reference Panel (Mackay *et al*. 2012), including some strains with identical priEE sequences exhibiting differential allele-specific expression levels (Miyagi *et al*. 2015). These analyses suggest the possibility of the presence of sequences that regulate the expression level of *ebony* in the epidermis outside the priEE region.

The priEE segment was the only segment within the approximately 10 kbp

regulatory region (including an upstream intergenic region and intron 1) that drove the expression of the reporter gene in the epidermis (Rebeiz *et al*. 2009). However, the previous findings mentioned above have indicated that the sequence variation within the priEE was not sufficient to explain the wide range of expression level variation of this gene. Therefore, I hypothesized that similar to *yellow*, *ebony* has other enhancers in addition to the priEE, possibly located outside the known approximately 10 kbp regulatory region and maybe taking part redundantly in activating transcription of *ebony* in the developing epidermis.

In comparison to the studies of enhancers, information on silencers is limited partly due to technical difficulties in detecting repressive activities by reporter assays. However, some studies conducting careful dissections of the *cis*-regulatory region of *ebony* have located the regions containing the silencers that repress transcription at the corresponding dark areas of the abdomen (Rebeiz *et al*. 2009; Johnson *et al*. 2015). In *D. melanogaster*, dark stripes are visible in the posterior regions of the A2–7 abdominal tergites in females and the A2–4 tergites in males (Fig. 1-1). Also, the abdominal pigmentation pattern exhibits sexual dimorphism with totally dark A5–7 tergites observed only in males (Fig. 1-1B). Furthermore, another characteristic dark line is present along the dorsal midline of the abdominal tergites in both males and females of this species. The pattern of the dark line varies among species (Markow and O'Grady 2005), but the expression of *ebony* is not present in this region in *D. melanogaster* (Rebeiz *et al*. 2009; Hughes *et al*. 2020). The locations of silencers responsible for the stripe repression and the male-specific repression in the posterior tergites have been indicated with a limited resolution (Rebeiz *et al*. 2009; Johnson *et al*. 2015). Moreover, no silencers to establish repression at the dorsal midline have been identified previously.

The transgenic reporter assay is a powerful approach to dissect regulatory sequences and identify CREs, such as enhancers and silencers. However, there are limitations because this assay does not test the activities of a genomic fragment in its native environment (Halfon 2019). Especially, the lengths and borders of a genomic fragment can markedly affect the results (Kalay *et al*. 2019). For the silencer screening, the target sequences need to be connected to or placed together with an enhancer in front of the reporter gene to test for negative regulations (Rebeiz *et al*. 2009; Johnson *et al*. 2015; Gisselbrecht *et al*. 2020).

In this study, I examined the genomic region by modifying the endogenous upstream sequence using the clustered regularly interspaced short palindromic repeats (CRISPR)-CRISPR associated protein 9 (Cas9) system (Kondo and Ueda, 2013), rather than conducting reporter gene assays. The deletion of the known priEE in a single genetic background enabled the examination of its contribution to the body color phenotype. I combined it with an assay using a reporter gene fused to the endogenous *ebony* to capture the changes in the expression pattern. As a result, I uncovered the presence of the enhancer activities outside the known priEE that drive the broad expression of *ebony* in the developing epidermis. I also show that the priEE fragment contains a silencer for repressing the expression of *ebony* in the dorsal midline of the abdominal tergites, which is necessary for developing the pigmentation pattern in abdominal midline. I discuss the consequences of such regulations on the pigmentation variation and the potential application of a similar approach to other genomic regions.

MATERIALS AND METHODS

Fly strains

y^{2} *cho*^{2} *v*^{1} P{*nos*-Cas9, *y*$^{+}$, *v*$^{+}$}1A/*FM7c*, *Kr*-GAL4 UAS-*GFP* (Cas-0002), *y*^{1} *v*^{1} P{*nos-phiC31¥int.NLS*}*X*; *attP40* (II) (TBX-0002), *y*^{2} *cho*^{2} *v*^{1}; *Sco*/*CyO* (TBX-0007), and *y*^{2} *cho*^{2} *v*^{1}; *Pr Dr*/*TM6C, Sb Tb* (TBX-0010) strains were obtained from the NIG-FLY Stock Center. *w*^{1118}; *wg*$^{Sp-1}$/ *CyO*; *Pr*^{1} *Dr*^{1}/ *TM3, Sb*^{1} *Ser*^{1} (DGRC#109551) and *e*^{1} (DGRC#106436) were obtained from the Kyoto Stock Center. The isogenized Cas-0002 strain (Cas-0002-iso) was established via the triple balancer by crossing DGRC#109551 with Cas-0002 (Fig. 1-2). The TBX-double-balancer (*y*^{2} *cho*^{2} *v*^{1}; *Sco*/*CyO*; *Pr Dr*/*TM6C, Sb Tb*) was generated from TBX-0007 and TBX-0010. The two attP strains *y*^{1} *w*^{1118}; *PBac*{*y*$^{+}$*-attP-3B*}*VK00033* (DGRC#130419) and *y*^{1} *w*^{1118}; *PBac*{*y*$^{+}$*-attP-3B*}*VK00037* (DGRC#130421) were used to generate transgenes at WellGenetics. All fly stocks were reared at 25ºC on a standard corn-meal fly medium.

Repair construct for *mCherry* knock-in

The repair construct (Fig. 1-3B) was designed following the method described by Hinaux *et al*. (2018). The construct *pJet-yellow_F4mut-mCherry* was gifted from Dr. Nicolas Gompel. A part of *ebony* gene region (2,610 bp, from approximately 1 kb upstream of exon 7 to approximately 1 kb downstream of 3'UTR) was amplified from Cas-0002-iso (Fig. 1-3A) using primers with the *Xho*I (5'-AGCctcgagTGGTGGATAAGGCCATTGTT-3') and *Xba*I (5'-CAGtctagaTGCAACTGGTTTGTGCGTAT-3') digestion site sequences. I performed PCR, using KAPA HiFi HotStart ReadyMix (Kapa Biosystems). The *pJet*-

yellow_F4mut-mCherry vector was digested with *Xho*I and *Xba*I, and the flanking sequences (including partial *yellow* and *mCherry* gene sequences) to incorporate the restriction sites into the PCR product, which were digested by these restriction enzymes to connect with the digested vector. The complete sequence of the resulting recombinant, excluding the *ebony* termination codon, was PCR-amplified with the following primers: 5'-GACGACCACCCGGTGGACGT-3' and 5'-TTTGCCCACCTCCTTCCAAT-3'.

Next, I PCR-amplified the *mCherry* sequence with a 5' linker (Waldo *et al*. 1999) from the *pJet-yellow_F4mut-mCherry* vector, using the primers with 15 bp flanking sequences (5'-AAGGAGGTGGGCAAAGGATCCGCTGGCTCCGCTGCTG-3' and 5'-CACCGGGTGGTCGTCTTACTTGTACAGCTCGTCCATGCC-3'). These two PCR products were then fused by using the In-Fusion HD Cloning Kit (TaKaRa) to generate the *pJet-ebony-mCherry* vector.

Finally, the two synonymous mutations were introduced in the target sequence of gRNA (5'-GCGCGCTATTGTCCATTGGA-3') to reduce the risk of the repair construct being cut during the knock-in reaction. To introduce mutations, I amplified two overlapping regions, including the gRNA target sequence, from the *pJet-ebony-mCherry* vector, using PCR with the following primer pairs: 5'-AATCCCCGCGAGAACATC-3' and 5'-TCCAGTGTACAATAGCGCGC-3'; 5'-GCGCTATTGTACACTGGAAG-3' and 5'-TTGTCTGGAAATCAAAGGCTTA-3'. These two PCR products were connected using overlap extension PCR to generate a mutated fragment. This mutated fragment was replaced with the original homologous sequence of the *pJet-ebony_mut-mCherry* vector by fusing the mutated fragment and the PCR product amplified from the *pJet-ebony-mCherry* vector using the In-Fusion HD

Cloning Kit (TaKaRa) with the following primers: 5'-GCCTTTGATTTCCAGACAA-3' and 5'-GTTCTCGCGGGGATTCAAC-3'. The constructed *pJet-ebony_mut-mCherry* vector was used as the repair construct for *mCherry* knock-in.

gRNA vector cloning

All the guide sequences of gRNAs were recombined with the pCFD5 vector (Addgene ##73914) according to the pCFD5 cloning protocol (Port and Bullock 2016). The guide sequences of gRNA1 (5'-GGAGCACGAGGTTCTGCGGG-3') and gRNA2 (5'-GCGCGCTATTGTCCATTGGA-3') were designed within exon 7 of *ebony* and recombined with separate pCFD5 vectors. The guide sequences of gRNA3 (5'-GTTAATAAGATCGGACAGAC-3') and gRNA4 (5'-GAAAGTACTATCAATATACA-3'), which were designed at both ends of the approximately 900-bp priEE fragment (Fig. 1-3D and 1-4), were recombined with a single the pCFD5 vector. Two additional guide sequences, gRNA5 (5'-TGAATAGTGATCAGCTGGTG-3') and gRNA6 (5'-TATGAGCATCCATATATCAG-3'), were designed within the priEE fragment (Fig. 1-5) and recombined with another single pCFD5 vector including gRNA3 and gRNA4. An In-Fusion HD Cloning Kit (TaKaRa) was used for cloning.

Construct for reporter gene assay

The sequence of the priEE of *ebony* was amplified from Cas-0002-iso by using the following primers with restriction enzyme digestion sites: 5'-CGGgaattcGGGCAAAGCAGGGTGAATA-3' (EcoRI site) and 5'-ACTgcggccgcTCACAGGGACTTATGGGAAA-3' (NotI site). These primers were designed to amplify most of the priEE knocked-out sequences including the whole

*e*_ECR0.9 (Takahashi and Takano-Shimizu 2011), *e*_core_*cis* (Miyagi *et al*. 2015), and "0.7 kb core abdominal element" (Rebeiz *et al*. 2009) (Fig. 1-4). The amplified product and the pEGFP-attB vector with a minimal Hsp70 promoter (*Drosophila* Genomics Resource Center) were digested with EcoRI and NotI. The PCR product was recombined with the pEGFP-attB vector at the multi-cloning site.

Embryonic microinjection

For *mCherry* knock-in, an *ebony* knockout strain was generated by injecting the gRNA1 guide-sequence-recombined pCFD5 vector (200 ng/μl) into the embryos of Cas-0002-iso. The embryos of *ebony* knockout strain were injected with a mixture of the gRNA2 guide-sequence-recombined pCFD5 vector (200 ng/μl) and the repair construct, *pJet-ebony_mut-mCherry* (400 ng/μl). Of the 250 adult flies that emerged from the injected embryos, four restored wild-type body color. The sequences of exon 7 of *ebony* and knocked-in *mCherry* were confirmed using Sanger sequencing with a BrilliantDye Terminator cycle sequencing kit (NimaGen) and an ABI PRISM 3130xl Genetic Analyzer (Applied Biosystems). The established strain was named Cas-0002-iso_*e*::*mCherry* (Fig. 1-3B).

The pCFD5 vector with guide sequences of gRNA3 and gRNA4 (200 ng/μl) was injected into the embryos of TBX-0002. The gRNA expression strain (y^2 *cho*^{2} v^1; attP40{gRNA v^+}; *Pr Dr*/*TM6c, Sb Tb*) was established by mating the successfully transformed individual with the TBX-double-balancer strain. The guide sequences of gRNAs of the established strains were confirmed using Sanger sequencing with a BrilliantDye Terminator cycle sequencing kit (NimaGen) and an ABI PRISM 3130xl Genetic Analyzer (Applied Biosystems). To induce partial deletions of priEE, the

embryos of *w*^{1118}; *e*::*mCherry* were injected with a mixture of the gRNA3–6 recombined pCFD5 and pBFv-nosP-Cas9 vectors (200 ng/μl each) (Kondo and Ueda, 2013).

The pEGFP-attB vector with the priEE fragment was prepared at a high concentration using Plasmid Midi Kit (Qiagen) and sent to WellGenetics (Taiwan) for injection into two attP strains (*y*^{1} *w*^{1118}; *PBac*{*y*$^{+}$*-attP-3B*}*VK00033* and *y*^{1} *w*^{1118}; *PBac*{*y*$^{+}$*-attP-3B*}*VK00037*).

Deletion strains generated by CRISPR-Cas9

The deletion strains with breakpoints at gRNA3 and gRNA4 targeting sites were generated by crossing gRNA expression strains with Cas-0002-iso or Cas-0002-iso_*e*::*mCherry* (the crossing scheme shown in Fig. 1-6). Deletions (Dels) occur in the germline cells of G1. Each of twelve G1 males was crossed with several TBX-0010 virgin females. Eight G2 males sampled from the progenies of each G1 male were subjected to PCR screening. DNA samples extracted from the mid-legs of G2 males, and the priEE region were amplified by using the primers e_-5029F (5'-CGTGTGCCTGATCGCTAGA-3') and e_-3391R (5'-ACTCGTGCCTTACTTAATCTGAA-3'). The G2 individuals were screened by a 1% agarose gel electrophoresis of the amplicons. The G2 individuals with deletions were crossed with TBX-0010. Then, the progeny, *y*^{2} *cho*^{2} *v*^{1}; +; Del/*TM6c, Sb Tb* (G3) was crossed with each other to establish G4 homozygous strains (*y*^{2} *cho*^{2} *v*^{1}; +; Del). The deletions were confirmed using Sanger sequencing with a BrilliantDye Terminator cycle sequencing kit (NimaGen) and an ABI PRISM 3130xl Genetic Analyzer (Applied Biosystems). The males from the G4 homozygous deletion strains were crossed twice

with the double balancer w^{1118}; $wg^{Sp\text{-}1}$/ *CyO*; Pr^1 Dr^1/ *TM3*, Sb^1 Ser^1 (DGRC#109551) to replace the y^2 cho^2 v^1 X chromosome with w^{1118}. Finally, the G7 homozygous deletion strains (w^{1118}; +; Del) were established (Fig. 1-6). Control strains (w^{1118}; +; + and w^{1118}; +; *e*::*mCherry*) were established with the same crosses using TBX-0002 instead of the gRNA expression strain (Fig. 1-6).

The deletion strains with breakpoints including gRNA5 and gRNA6 target sites were established by embryonic injection as described previously. The subsequent procedures were the same as above, and the crosses were performed as in Fig. 1-7.

Quantification of pigmentation intensity

At 5–7 days after eclosion, females were placed in 10% glycerol in ethanol at 4ºC for 1 h. Next, the flies were rotated in 10% glycerol in phosphate-buffered saline (PBS) at room temperature for 1 h after removing the head, legs, and wings. The images of the dorsal body of flies soaked in 10% glycerol in PBS were captured using a digital camera (DP73, Olympus) connected to a stereoscopic microscope (SZX16, Olympus). The same parameters (exposure time, zoom width and illumination) and reference grayscale (brightness = 128; ColorChecker, X-rite) were applied for capturing all images. White balance was corrected using the white scale (Brightness = 255; ColorChecker, X-rite) with cellSens Standard 1.6 software (Olympus). Pigmentation intensity was measured in manually selected areas of the thorax and abdomen (Fig. 1-8B) from RGB images of flies using ImageJ 1.53a (Schneider *et al*. 2012). The mode grayscale brightness values from thorax and abdomen were corrected by using the

reference grayscale of the background area at the bottom left corner of each image. The percent of darkness was calculated as follows:

$$\left(1 - \frac{\text{brightness}}{\text{background brightness}} \times \frac{128}{255}\right) \times 100\ (\%)$$

To test the statistical significans of pigmentation intensity difference, the data were analyzed by using Kruskal-Wallis rank sum test followed by Dunn's test. Statistical analyses were performed by using R version 4.0.3 (R Core Team 2020).

Confocal microscopy

The abdomen of females and males, and wings, front legs, and halteres of females were dissected from the adult flies 4 h after eclosion and collected in Phosphate-buffered saline (PBS). The dorsal abdominal cuticle and epidermis were separated from the rest of the abdomen. The fat body, internal organs, and genitalia were gently removed. The head of adult females collected 4–4.5 h after the light was turned on, and the intact brain was dissected and collected in PBS. Each brain sample was fixed in 4% paraformaldehyde for 1 h and washed with PBS for 1 h after the fixation.

Each specimen was mounted with VECTASHIELD Mounting Medium with DAPI (Vector Laboratories) and imaged under a C2 plus confocal microscope (Nikon). Max intensity images were composited from the XY overlapping images (abdomen: 12 images, wing: 10 images) with 1 μm wide Z-stacks using the NIS Elements AR 4.50.00 software (Nikon). The following laser wavelengths were applied for obtaining images: 488 nm for activation and 509 nm for imaging for EGFP; 561 nm for activation and 620 nm imaging for mCherry. The identical parameters of C2 plus settings (HV, offset, laser power, pinhole size, scan size, scan speed, scan direction, and zoom) were applied to

imaging the same tissue (mCherry or EGFP). The images were taken under the parameter settings that would not give saturated signals with no further corrections.

Quantification of *mCherry* fluorescent intensity

The fluorescent intensities of the confocal microscopic images of the abdomens from 10 individuals were quantified per strain for five strains. The mode pixel values (0–255) in the manually selected areas of the abdominal third, fourth and fifth segments (Fig. 1-9A) were measured by using ImageJ 1.53a (Schneider *et al*. 2012). The mode of the pixel values of the whole image, which reflects the background of each image was subtracted from the pixel values of the abdominal segments. To test the statistical significans of *mCherry* fluorescent intensity difference, the data was analyzed by using one-way analysis of variance, followed by Tukey HSD post-hoc test. Statistical analyses were performed using R version 4.0.3 (R Core Team 2020).

DNA sequence comparisons of the silencer region among strains from naturel populations

The DNA sequences of the midline silencer region from 68 wild-derived strains were obtained from previous studies (Table 1-1, Pool and Aquadro, 2007; Rebeiz *et al*., 2009; Takahashi and Takano-Shimizu, 2011; Miyagi *et al*., 2015). DNA sequences were aligned by using MEGA7: Molecular Evolutionary Genetics Analysis version 7.0 for bigger datasets (Kumar *et al*., 2016).

RESULTS

The priEE fragment was precisely excised by using the CRISPR-Cas9 system to examine whether transcriptional activation of *ebony* occurs in the absence of the priEE. First, to control the effects of genomic background, an isogenic Cas-0002 line (Cas-0002-iso) carrying the *nos*-Cas9 transgene was constructed (Fig. 1-3A and 1-2). Next, *mCherry* sequence was knocked-in to the 3' end of the *ebony* coding region in the Cas-0002-iso line by using the CRISPR-Cas9 system (Fig. 1-3B). The resultant transgenic line (Cas-0002-iso_*e*::*mCherry)* was designed to produce a Ebony-mCherry fusion protein. Cas-0002-iso and Cas-0002-iso_*e*::*mCherry* lines were crossed with guide RNA (gRNA) expression lines to drive a targeted deletion at the approximately 900-bp priEE fragment (Takahashi and Takano-Shimizu 2011; Miyagi *et al*. 2015) (Fig. 1-6). Additional crosses were performed to remove y^2 and replace the X chromosome with w^{1118} to avoid interference from *yellow*, which is involved in the same pigment synthesis pathway (Fig. 1-6). The following four priEE deletions were generated; two from Cas-0002-iso line (w^{1118}; $e^{\Delta 1028priEE}$ *and* w^{1118}; $e^{\Delta 1029priEE}$) and two from Cas-0002-iso_*e*::*mCherry* line (w^{1118}; $e^{\Delta 1017priEE}$::*mCherry* and w^{1118}; $e^{\Delta 1027priEE}$::*mCherry*) (Fig. 1-6).

If the priEE contains the only enhancer driving the expression of *ebony* in the epidermis, the priEE-deleted strains should exhibit a dark body color equivalent to the *ebony* null mutant (e^1). Contrary to this prediction, the body color of the priEE-deleted strains was similar to that of the control strain (Fig. 1-8A).

The percent darkness in the females of the two priEE-deleted strains (w^{1118}; $e^{\Delta 1028priEE}$ and w^{1118}; $e^{\Delta 1029priEE}$), the control strain (w^{1118}; +), and an *ebony* null mutant

(e^{1}) was compared. The percent darkness values of 20 DGRP strains were measured as indicators of pigmentation intensity (Miyagi *et al*., 2015), and the *ebony* expression levels of the same strains are available (Massey, Akiyama, *et al*., 2019). There was a significant correlation between these data (Spearman's $\rho = -0.53$, $P < 1.0 \times 10^{-2}$). The percent darkness in thoracic center of the 20 DGRP strains was in the range of 72.7-89.8. The relative expression level of *ebony* in the darkest strain (RAL-714) was 21.4 % of that in the lightest strain (RAL-852).

The percent darkness at the specific positions of the thoracic center and the fourth abdominal tergite (A4) was measured (10 flies per strain) (Fig. 1-8B). The pigmentation scores were significantly different between the strains (thorax, df = 6, $P < 10^{-9}$, Kruskal-Wallis rank sum test; abdomen, df = 6, $P < 10^{-6}$, Kruskal-Wallis rank sum test). The thoraces of one of the two priEE-deleted strains, w^{1118}; $e^{\Delta 1028priEE}$ and w^{1118}; $e^{\Delta 1029priEE}$, showed significantly but only slightly darker pigmentation than those of the control strain (Fig. 1-8C). The abdominal pigmentation in the two priEE-deleted strains was slightly lighter than that in the control strain (Fig. 1-8D). These subtle changes in pigmentation intensity suggest that the priEE deletion perturbs *ebony* transcription to some extent. However, the pigmentation in the thorax and abdomen of the two priEE-deleted strains was markedly lighter than that in the thorax and abdomen of e^{1} (Fig. 1-8C-D). Although the pigmentation intensity is an indirect measurement of the transcription level of *ebony,* the results suggested that the priEE deletion had limited effects on the overall transcription level regulation. These results indicate that an enhancer driving expression at the epidermis resides outside the primary enhancer.

To estimate the expression levels of *ebony* by different means, the *mCherry* knocked-in strain, w^{1118}; *e*::*mCherry*, and its priEE deleted strains, w^{1118};

$e^{\Delta 1017priEE}$::*mCherry* and w^{1118}; $e^{\Delta 1027priEE}$::*mCherry* were constructed (Fig. 1-3C). From body color, the *ebony* function was inferred to be not largely disrupted by the *mCherry* knock-in. Both w^{1118}; + strain and w^{1118}; *e*::*mCherry* strain showed light body color (Fig. 1-8 and 1-10). The percent darkness of thorax was significantly but only slightly lighter in the knock-in strain than in the control strain ($P < 0.001$, Student's t-test), and that of abdomen was not significantly different between these two strains ($P = 0.82$, Student's t-test). Also, the thoracic and abdominal pigmentation of w^{1118}; $e^{\Delta 1017priEE}$::*mCherry* and w^{1118}; $e^{\Delta 1027priEE}$::*mCherry* was largely consistent with the priEE-deleted strains without *mCherry* (w^{1118}; $e^{\Delta 1028priEE}$ *and* w^{1118}; $e^{\Delta 1029priEE}$) (Fig. 1-8 and 1-10). These results suggested that the catalytic function of Ebony in the pigmentation synthesis pathway is not disrupted upon fusion with mCherry at least.

The abdominal epidermis of the mCherry knocked-in strains were subjected to observation under fluorescence confocal microscopy, which enabled us to visualize signal intensities from Ebony-mCherry (Fig. 1-11A-B). The anterior regions of A3–5 tergites (Fig. 1-9A) were chosen as representative *ebony* expression domains with minimum effects of the bristles and stripes. The fluorescent intensities in these regions were quantified from ten females per strain and compared between strains. The intensities of w^{1118}; $e^{\Delta 1017priEE}$::*mCherry* and w^{1118}; $e^{\Delta 1027priEE}$::*mCherry* were slightly higher than that in the control strain (Fig. 1-9B). Therefore, the priEE was shown to be not only dispensable for driving the transcription of *ebony* in the developing epidermis but may have slightly lower activity than sequences outside itself.

Also, unexpectedly, the deletion of the priEE affected the pattern of pigmentation. In particular, the deletion of the priEE resulted in the loss of a dark pigmentation line along the dorsal midline of the abdominal tergites (Fig. 1-8A and 1-

10). This indicated that *ebony* expression is repressed in the midline area and that the priEE fragment is necessary for this suppression.

The area of *ebony* expression in the abdomen were investigated by confocal microscopy of the *mCherry* knocked-in strains (Fig. 1-11A-B). Endogenous *ebony* exhibited a broad epidermal expression, a suppressed expression at the posterior stripe region of each tergite (A1–6 of a female and A1–4 of a male), and tergite-wide suppression at A5 and A6 in males (Fig. 1-11A, D, and E). These expressions were consistent with those reported in previous studies (Rebeiz and Williams 2017; Hughes *et al*. 2020). Notably, predicted from the lack of dark pigmentation, the expression of *e::mCherry* at the dorsal midline was not repressed in the priEE-deleted strains (Figs 1-10B, D, and E).

The expression of *ebony* has been reported in other body regions (Hsouna *et al*. 2007; Suh and Jackson 2007; Rebeiz *et al*. 2009; Pérez *et al*. 2010), but the priEE has not been indicated to drive expression in tissues other than the developing epidermis (Rebeiz *et al*. 2009). As expected, the spatial expression pattern of *ebony* did not markedly change in other tissues upon deletion of the priEE (Fig. 1-12).

The results indicated that the deleted priEE fragment contained a silencer element for the dorsal midline as well as an epidermal enhancer element. In order to confirm that the deleted priEE contains both elements, a GFP reporter assay was performed. The priEE fragment was fused to an enhanced GFP (EGFP) gene (*priEE-EGFP*) with a minimal Hsp70 promoter and introduced into two attP strains (VK00033 and VK00037). The confocal images of GFP from the homozygous *priEE-EGFP* inserted to a third chromosome landing site in VK00033 (Fig. 1-11C and E) and a second chromosome landing site in VK00037 (Fig. 1-13) indicated that the priEE

autonomously drives the epidermal expression except at the flanking regions of the dorsal midline. However, the repression at the stripes and the male repression at the posterior segments were not observed (Fig. 1-11C-E and 1-13). Rebeiz *et al*. (2009) reported that the 0.7 kbp core element (included in the approximately 900-bp priEE) drove a similar expression pattern. The pattern clearly showed that a dorsal midline silencer is present in the priEE fragment, and it can silence the activity of the proximal enhancer element within the priEE fragment, which drives the broad expression of *ebony* in the developing abdominal epidermis.

To further narrow down the location of the silencer, the strains with partial deletions of the priEE were produced by injecting a mixture of pCFD5 vector that can produce four gRNAs (gRNA3–6) and pBFv-nosP-Cas9 vector into the embryos of w^{1118}; *e*::*mCherry*. The G1 individuals were screened for deletions by PCR-based genotyping (Fig. 1-7). Out of 319 individuals screened, 14 were detected to have a deletion. Among them, four individuals had breakpoints within the priEE. Two individuals had identical breakpoints described as $e^{\Delta 1092priEE\ (5'\_partial)}$, and another two had identical breakpoints described as $e^{\Delta 498priEE\ (3'\_partial)}$ (Fig. 1-5). Therefore, w^{1118}; $e^{\Delta 1092priEE(5'\_partial)}$ ::*mCherry* strain and w^{1118}; $e^{\Delta 498priEE(3'\_partial)}$ ::*mCherry* were established as in Fig. 1-7.

The two strains with partially deleted priEE had different breakpoints; w^{1118}; $e^{\Delta 1092priEE\ (5'\_partial)}$::*mCherry* and w^{1118}; $e^{\Delta 498priEE\ (3'\_partial)}$::*mCherry* had deletions in the 5' and 3' portions of the priEE, respectively (Fig. 1-14C). The midline pigmentation status and the expression of Ebony-mCherry domains of these strains indicate that the silencer is removed in w^{1118}; $e^{\Delta 1092priEE\ (5'\_partial)}$::*mCherry* but retained in w^{1118}; $e^{\Delta 498priEE\ (3'\_partial)}$::*mCherry* (Fig. 1-14A and B). The pattern indicates that the silencer resides in the 3' portion of the priEE. Together with the repressed midline expression of the

reporter driven by “0.7 kb abdominal core element” in Rebeiz *et al*. (2009), the silencer was indicated to be in the 351-bp overlapping region of this element and outside the deleted sequence of w^{1118}; $e^{\Delta 498priEE\ (3'\_partial)}$::*mCherry* (Fig. 1-14C).

The fluorescent intensity (pixel values) in the abdominal epidermis of w^{1118}; $e^{\Delta 1092priEE\ (5'\_partial)}$::*mCherry* was not significantly different from the control, but w^{1118}; $e^{\Delta 498priEE\ (3'\_partial)}$::*mCherry* was slightly higher than the control (Fig. 1-9). These results indicate that the effect of deletions may slightly vary due to the differences in the positions of breakpoints.

In addition, the RAL-852 strain, which exhibited no dark pigmentation line along the dorsal midline of the abdominal tergites (Fig. 1-15B), was among the 20 strains analyzed by Miyagi *et al*. (2015). The sequence comparison of the 351-bp silencer region between these 20 strains and the control strain (w^{1118}; +) in this study indicates that among 13 SNPs, the nucleotide variants at positions 123 and 340 were RAL-852 specific (Fig. 1-15A). To examine whether these two variants are present in other natural populations, 68 strains from different natural populations, data from Africa (Pool and Aquadro, 2007; Rebeiz *et al*., 2009) and from Iriomote (Takahashi and Takano-Shimizu, 2011), were added in the sequence comparison. Eight strains had the same variant as RAL-852 at the nucleotide position 340 (Fig. 1-15G). Also, the SNP at the nucleotide position 123 was not present in any of these strains, but two strains had the deletions containing that position (Fig. 1-15F). These patterns suggest the possibility that either or both of the two nucleotide variants in the 351-bp silencer region might be responsible for the loss of the dark pigmentation line along the dorsal midline of the abdominal tergites. However, as the midline pigmentation phenotypes of the 68 additional strains were not available, a large scale association study comparing the

phenotypic data and polymorphism within the 351-bp silencer region should be informative to investigate the association of two nucleotide variants resided in the silencer element.

DISCUSSION

Transcription-activating sequences other than the priEE reside in the *cis*-regulatory region of *ebony*

The removal of the endogenous priEE of *ebony* using the CRISPR-Cas9 system did not cause a drastic darkening as observed in the null mutant (e^1), although a slight perturbation of the pigmentation intensities in the thoracic and abdominal segments was observed (Fig. 1-8 and 1-10). A strong negative correlation between the darkness of body pigmentation and the expression level of *ebony* in the developing epidermis has been repeatedly detected in strains sampled from the natural populations of *D. melanogaster* (Pool and Aquadro 2007; Takahashi *et al*. 2007; Rebeiz *et al*. 2009; Takahashi and Takano-Shimizu 2011; Telonis-Scott *et al*. 2011; Miyagi *et al*. 2015). Thus, the dark pigmentation intensity of the cuticle could serve as a proxy indicator of local changes in the expression level of *ebony*, although compensation by other enzyme activities could influence the color. Therefore, the lack of a large increase in dark pigmentation in strains with the priEE deletion indicated that the expression of *ebony* was not largely disrupted.

Another indirect but relevant comparison of the expression levels of *ebony* was conducted by using the fluorescent intensity of mCherry fused to Ebony. The deletion of the whole priEE resulted in a slightly increased intensity of Ebony-mCherry (Fig. 1-9). These findings indicated that some endogenous sequences outside the priEE must have the ability to activate transcription of *ebony* in the developing epidermis, suggesting the presence of other enhancer element(s) in the surrounding genomic region. The complex arrangement of multiple CREs may be a reason for the scarcity of polymorphisms

association with pigmentation intensity or gene expression level within or near the enhancer element across worldwide populations (Telonis-Scott and Hoffmann 2018).

The locations of other transcription-activating sequences have not been determined. The results of a previous reporter assay revealed that no fragment other than those including the priEE segment was within the approximately 10 kb regulatory region that contains the 5' intergenic region and the first intron (Rebeiz *et al*. 2009). Therefore, any element that can drive epidermis expression is likely to be located elsewhere. However, unlike the recent reporter assay conducted with the *yellow* regulatory region (Kalay *et al*. 2019), many regions were tested using relatively large fragments (> 2 kbp), which may contain cryptic enhancers that are repressed by surrounding sequences in their native genomic context. Therefore, the possibility of the presence of redundant enhancer elements within the approximately 10 kb regulatory region cannot be ruled out. Some secondary enhancers were reported to be shadow enhancers that are more than 20 kb away from the transcription start site (Hong *et al*. 2008). Thus, there is a need for extensive search to elucidate the detailed spatial arrangement of CREs. Nevertheless, the advantage of deleting an endogenous enhancer, a strategy employed in this study, is the rapid capturing of redundant enhancer activity in the native genomic context. Such knockout assays using endogenous genome editing may reveal more cases of redundant enhancer activities in the *Drosophila* genome as in the study conducting similar experiments on mouse developmental genes (Osterwalder *et al*. 2018). Moreover, this approach can compensate for some potential bias in reporter gene assays caused by the choice of promoter and the genomic location of the transgenes (Halfon 2019).

Possible functions of redundant enhancers are to be investigated

The enhancer activities exhibited by sequences within and outside the priEE may be redundant in a sense that they both have abilities to drive transcription at the developing epidermis. However, how they coexist and function is not known. Redundant enhancer elements, which are often referred to as primary and shadow enhancers (Hong *et al*. 2008), have been suggested to confer robustness against environmental or genetic perturbations (Perry *et al*. 2009; Frankel *et al*. 2010; Pérez *et al*. 2010) or define sharp boundaries for gene expression (Perry *et al*. 2011; Bothma *et al*. 2015). The transcriptional activation of *ebony* by the sequences within and outside priEE appears to be largely overlapping but may not be completely redundant, suggested by the subtle changes in the pigmentation and Ebony-mCherry abundance upon deletion of the priEE (Fig. 1-8, 1-9 and 1-10). However, a wide range of variations in the transcription level of *ebony* have been reported within and among *D. melanogaster* populations (Pool and Aquadro 2007; Takahashi *et al*. 2007; Rebeiz *et al*. 2009; Takahashi and Takano-Shimizu 2011; Telonis-Scott *et al*. 2011; Miyagi *et al*. 2015). Thus, maintaining a robust transcription level of *ebony* might not be essential to *D. melanogaster*. The functional significance of redundant enhancers of *ebony* requires further investigation.

A silencer resides within an enhancer fragment

Spatially restricted suppression of focal gene transcription can be achieved by introducing a specific silencer that recruits repressive transcription factors (or repressors) expressed in the target cells. In contrast to enhancers, there is far limited information on the exact locations and features of silencers. This study demonstrated

that the priEE fragment contained a silencer of *ebony* in the abdominal dorsal midline based on two experimental evidences. First, the repression of *ebony* expression at the dorsal midline was not observed when the priEE fragment was deleted (Fig. 1-11B). Second, experiments with priEE fragment fused to a reporter gene revealed a broad epidermal expression driven by autonomous enhancer activity and the repression of gene expression at the dorsal midline (Fig. 1-11C). Furthermore, I obtained two partial priEE deletions and observed the effects on the Ebony-mCherry expression. By comparing the results with that of a previous reporter assay (Rebeiz *et al*. 2009), I was able to narrow down the effective silencer region to 351 bp (Fig 1-14). Thus, our study demonstrated that the combination of both deletion and reporter assays are effective in identifying silencer boundaries.

The *ebony* expression in the priEE-deleted strains implies that in the wildtype strain, in which the silencer is intact, overall enhancer activity at the dorsal midline is blocked. Although not known, if multiple enhancers are driving the *ebony* expression simultaneously in the developing epidermis, they are likely to be repressed altogether by the presence of a single silencer. The results of the *priEE-EGFP* reporter assay demonstrated that the repressor bound to the silencer within the fragment interferes with the neighboring enhancer activity of priEE. Taken together, although the underlying mechanisms have not been elucidated, the results suggest that the silencer is sufficient to overcome overall enhancer activity that drives epidermal expression of *ebony*, possibly by interfering with the basal transcription machinery at the promoter site. A chromatin conformation analysis may be effective to identify the direct physical interaction between the silencer and the promoter or enhancer.

Various models have been proposed to explain the functional categories of

silencers, and many silencers have been shown to act also as enhancers at different cellular contexts (Gray and Levine 1996; Courey and Jia 2001; Maston *et al*. 2006; Ogiyama *et al*. 2018; Gisselbrecht *et al*. 2020; Segert *et al*. 2021). The spatial configureuration of the epidermis enhancer and the midline silencer within the priEE sequence is yet to be investigated. An identification of the positive- and negative-acting transcription factor binding sites should help clarifying the picture. Among the 20 strains from the DGRP used in Miyagi *et al*. (2015) for nucleotide comparison, RAL-852 was the only strain that had no midline pigmentation and possessed two unique nucleotide variants in the 351-bp effective silencer region (Fig. 1-15A). These sites of nucleotide variant may be involved in transcription factor binding site necessary for the formation of midline pigmentation line. Several strains of the African population showed the same variant or a deletion spanning the SNP site (Fig. 1-15F-G). Examining the pigmentation at their abdominal midline may help identify the binding sites of the negatively acting transcription factors.

A schematic representation of the *cis*-regulatory transcriptional control of this gene is shown in Fig. 1-11F. As incorporated in the model, the repression of *ebony* in the dark stripes at the posterior regions of the abdominal tergites and the totally dark A5–6 tergites in males is not affected (Fig. 1-11A–D). This is consistent with the results of a previous study, which showed that the locations of these silencers are not within the deleted fragment (Rebeiz *et al*. 2009). The authors revealed that the male silencer was located approximately 1.5 kbp upstream of the transcription start site, and the stripe silencer was located within the first intron. A similar approach to exclude the putative silencer region can be effective for obtaining a comprehensive picture of the regulatory system of this gene.

At the molecular level, *omb*, *dpp*, and *wg*, are reported to be involved in the formation of sexually monomorphic pigmentation patterns in the abdomen of *D. melanogaster*, and *dpp*, which is expressed at the dorsal midline is essential for the formation of dark pigmentation along the midline (Kopp and Duncan 1997; Kopp *et al*. 1999; Wittkopp *et al*. 2003a). Additionally, *dpp* is known to activate the BMP signaling pathway, which regulates the transcription of numerous genes through a downstream transcription factor Mad (reviewed in Hamaratoglu *et al*. 2014). Kopp *et al*. (1999) showed that Mad^{12} clones at or near the dorsal midline promoted the loss of dark pigmentation, which suggested that Dpp signaling contributes to pigmentation. Furthermore, an RNAi screening revealed that 48 transcription factors, including Mad, are involved in abdominal pigmentation (Rogers *et al*. 2014). Therefore, although not investigated in this study, there is a possibility that the repression of *ebony* at the silencer is regulated through the Dpp signaling pathway.

Derepression of *ebony* is sufficient to diminish a taxonomic character

In the genus *Drosophila*, the pigmentation pattern of the abdominal midline is one of the traits used to distinguish between the subgenus *Sophophora*, which includes *D. melanogaster*, and the subgenus *Drosophila*. With some exceptions, the pigmentation stripes on the abdominal tergites of the subgenus *Sophophora* are mostly connected or expanded anteriorly at the dorsal midline forming a distinct dark area along the midline as in *D. melanogaster* (Markow and O'Grady 2005) (Fig. 1-8A and 1-11D). I have shown that the suppression of *ebony* by the abdominal midline silencer is necessary for the expanded midline pigmentation in *D. melanogaster*. The expression patterns of *pale*, *Ddc*, *ebony*, *tan*, and *yellow* in the developing abdominal epidermis of species

belonging to subgenus *Sophophora* were previously examined by using *in situ* hybridization (Hughes *et al*. 2020). The expression of *ebony* was not suppressed in the dorsal midline in *D. willistoni*, which does not show expanded midline pigmentation. Also, among the investigated genes, the suppression of *ebony* appears to be most pronounced in species with a typical dark dorsal midline. It is an interesting question whether the *ebony* is suppressed at the abdominal midline in other non-expanded *Sophophora* species (e.g., *D. ananasae*, *D. jamblina* and *D. kikkawai*).

In contrast, the stripes are narrowed or broken at the midline in most species of the subgenus *Drosophila* (Markow and O'Grady 2005). A pair of sister species within the subgenus *Drosophila*, *D. americana* and *D. novamexicana*, represent another case of distinct pigmentation patterns in the abdominal midline. *D. americana* has a dark body color with uniformly dark abdominal tergites, whereas *D. novamexicana* exhibits a light pigmentation along the abdominal midline (Wittkopp *et al*. 2003b), which is a typical pattern of the subgenus *Drosophila*. A recent study used reciprocal hemizygosity testing to demonstrate that the difference in abdominal midline pigmentation intensity between the two species was due to *ebony* (Lamb *et al*. 2020). The authors showed that *ebony* is required for the development of light pigmentation along the dorsal midline in wild-type *D. novamexicana*. It is interesting to examine whether the interspecific difference of *ebony* resides in the *cis*-regulatory region or not. However, the study also suggests that *ebony* suppression might be a key factor to determine this taxonomically important trait.

LITERATURE CITED

Arnone, M. I., & Davidson, E. H. (1997). The hardwiring of development: organization and function of genomic regulatory systems. *Development*, *124*(10), 1851-1864

Bastide, H., Betancourt, A., Nolte, V., Tobler, R., Stöbe, P., Futschik, A., & Schlötterer, C. (2013). A genome-wide, fine-scale map of natural pigmentation variation in *Drosophila melanogaster*. *PLoS Genetics*, *9*(6), e1003534.

Bothma, J. P., Garcia, H. G., Ng, S., Perry, M. W., Gregor, T., & Levine, M. (2015). Enhancer additivity and non-additivity are determined by enhancer strength in the *Drosophila* embryo. *Elife*, *4*, e07956.

Carroll, S. B. (2008). Evo-devo and an expanding evolutionary synthesis: a genetic theory of morphological evolution. *Cell*, *134*(1), 25-36.

Courey, A. J., & Jia, S. (2001). Transcriptional repression: the long and the short of it. *Genes & Development*, *15*(21), 2786-2796.

Dembeck, L. M., Huang, W., Magwire, M. M., Lawrence, F., Lyman, R. F., & Mackay, T. F. (2015). Genetic architecture of abdominal pigmentation in *Drosophila melanogaster*. *PLoS Genetics*, *11*(5), e1005163.

El-Sherif, E., & Levine, M. (2016). Shadow enhancers mediate dynamic shifts of *gap* gene

expression in the *Drosophila* embryo. *Current Biology*, *26*(9), 1164-1169.

Frankel, N., Davis, G. K., Vargas, D., Wang, S., Payre, F., & Stern, D. L. (2010). Phenotypic robustness conferred by apparently redundant transcriptional enhancers. *Nature*, *466*(7305), 490-493.

Geyer, P. K., & Corces, V. G. (1987). Separate regulatory elements are responsible for the complex pattern of tissue-specific and developmental transcription of the *yellow* locus in *Drosophila melanogaster*. *Genes & Development*, *1*(9), 996-1004.

Gisselbrecht, S. S., Palagi, A., Kurland, J. V., Rogers, J. M., Ozadam, H., Zhan, Y., *et al*. (2020). Transcriptional silencers in *Drosophila* serve a dual role as transcriptional enhancers in alternate cellular contexts. *Molecular Cell*, *77*(2), 324-337.

Gray, S., & Levine, M. (1996). Short-range transcriptional repressors mediate both quenching and direct repression within complex loci in *Drosophila*. *Genes & Development*, *10*(6), 700-710.

Halfon, S., & Bulut, P. (2019). Mentalization and the growth of symbolic play and affect regulation in psychodynamic therapy for children with behavioral problems. *Psychotherapy Research*, *29*(5), 666-678.

Hamaratoglu, F., Affolter, M., & Pyrowolakis, G. (2014). Dpp/BMP signaling in flies: from molecules to biology. In *Seminars in Cell & Developmental Biology* (Vol. 32, pp. 128-136).

Academic Press.

Hinaux, H., Bachem, K., Battistara, M., Rossi, M., Xin, Y., Jaenichen, R., *et al*. (2018). Revisiting the developmental and cellular role of the pigmentation gene *yellow* in *Drosophila* using a tagged allele. *Developmental Biology*, *438*(2), 111-123.

Hong, J. W., Hendrix, D. A., & Levine, M. S. (2008). Shadow enhancers as a source of evolutionary novelty. *Science*, *321*(5894), 1314-1314.

Hsouna, A., Lawal, H. O., Izevbaye, I., Hsu, T., & O'Donnell, J. M. (2007). *Drosophila* dopamine synthesis pathway genes regulate tracheal morphogenesis. *Developmental Biology*, *308*(1), 30-43.

Hughes, J. T., Williams, M. E., Johnson, R., Grover, S., Rebeiz, M., & Williams, T. M. (2020). Gene regulatory network homoplasy underlies recurrent sexually dimorphic fruit fly pigmentation. *Frontiers in Ecology and Evolution*, *8*, 80.

Jeong, S., Rokas, A., & Carroll, S. B. (2006). Regulation of body pigmentation by the Abdominal-B Hox protein and its gain and loss in *Drosophila* evolution. *Cell*, *125*(7), 1387-1399.

Johnson, W. C., Ordway, A. J., Watada, M., Pruitt, J. N., Williams, T. M., & Rebeiz, M. (2015). Genetic changes to a transcriptional silencer element confers phenotypic diversity within and between *Drosophila* species. *PLoS Genetics*, *11*(6), e1005279.

Kalay, G., Lachowiec, J., Rosas, U., Dome, M. R., & Wittkopp, P. (2019). Redundant and cryptic enhancer activities of the *Drosophila yellow* gene. *Genetics*, *212*(1), 343-360.

Kumar, S., Stecher, G., & Tamura, K. (2016). MEGA7: molecular evolutionary genetics analysis version 7.0 for bigger datasets. *Molecular Biology and Evolution*, *33*(7), 1870-1874.

Kondo, S., & Ueda, R. (2013). Highly improved gene targeting by germline-specific Cas9 expression in Drosophila. *Genetics*, *195*(3), 715-721.

Kopp, A., & Duncan, I. (1997). Control of cell fate and polarity in the adult abdominal segments of *Drosophila* by optomotor-blind. *Development*, *124*(19), 3715-3726.

Kopp, A., Blackman, R. K., & Duncan, I. (1999). Wingless, decapentaplegic and EGF receptor signaling pathways interact to specify dorso-ventral pattern in the adult abdomen of *Drosophila*. *Development*, *126*(16), 3495-3507.

Lamb, A. M., Wang, Z., Simmer, P., Chung, H., & Wittkopp, P. J. (2020). *ebony* affects pigmentation divergence and cuticular hydrocarbons in *Drosophila americana* and *D. novamexicana*. *Frontiers in Ecology and Evolution*, *8*, 184.

Long, H. K., Prescott, S. L., & Wysocka, J. (2016). Ever-changing landscapes: transcriptional enhancers in development and evolution. *Cell*, 167(5), 1170-1187.

Mackay, T. F., Richards, S., Stone, E. A., Barbadilla, A., Ayroles, J. F., Zhu, D., *et al*. (2012). The *Drosophila melanogaster* genetic reference panel. *Nature*, *482*(7384), 173-178.

Martin, M., Meng, Y. B., & Chia, W. (1989). Regulatory elements involved in the tissue-specific expression of the *yellow* gene of *Drosophila*. *Molecular and General Genetics MGG*, *218*(1), 118-126.

Markow, T. A., & O'Grady, P. (2005). *Drosophila: a guide to species identification and use*. Elsevier.

Massey, J. H., & Wittkopp, P. J. (2016). The genetic basis of pigmentation differences within and between *Drosophila* species. *Current topics in Developmental Biology*, *119*, 27-61.

Massey, J. H., Akiyama, N., Bien, T., Dreisewerd, K., Wittkopp, P. J., Yew, J. Y., & Takahashi, A. (2019). Pleiotropic effects of *ebony* and *tan* on pigmentation and cuticular hydrocarbon composition in *Drosophila melanogaster*. *Frontiers in Physiology*, *10*, 518.

Maston, G. A., Evans, S. K., & Green, M. R. (2006). Transcriptional regulatory elements in the human genome. *Annu. Rev. Genomics Hum. Genet.*, *7*, 29-59.

Miyagi, R., Akiyama, N., Osada, N., & Takahashi, A. (2015). Complex patterns of *cis*‐regulatory polymorphisms in *ebony* underlie standing pigmentation variation in *Drosophila melanogaster*. *Molecular Ecology*, *24*(23), 5829-5841.

Nagy, O., Nuez, I., Savisaar, R., Peluffo, A. E., Yassin, A., *et al*. (2018). Correlated evolution of two copulatory organs via a single *cis*-regulatory nucleotide change. *Current Biology, 28*(21), 3450-3457.

Ogiyama, Y., Schuettengruber, B., Papadopoulos, G. L., Chang, J. M., & Cavalli, G. (2018). Polycomb-dependent chromatin looping contributes to gene silencing during *Drosophila* development. *Molecular Cell, 71*(1), 73-88.

Osterwalder, M., Barozzi, I., Tissières, V., Fukuda-Yuzawa, Y., Mannion, B. J., Afzal, S. Y., et al. (2018). Enhancer redundancy provides phenotypic robustness in mammalian development. *Nature*, *554*(7691), 239-243.

Pérez, M. M., Schachter, J., Berni, J., & Quesada-Allué, L. A. (2010). The enzyme NBAD-synthase plays diverse roles during the life cycle of *Drosophila melanogaster*. *Journal of Insect Physiology, 56*(1), 8-13.

Perry, M. W., Cande, J. D., Boettiger, A. N., & Levine, M. (2009, January). Evolution of insect dorsoventral patterning mechanisms. *Cold Spring Harbor Symposia on Quantitative Biology* (Vol. 74, pp. 275-279).

Perry, M. W., Boettiger, A. N., Bothma, J. P., & Levine, M. (2010). Shadow enhancers foster robustness of *Drosophila* gastrulation. *Current Biology, 20*(17), 1562-1567.

Perry, M. W., Boettiger, A. N., & Levine, M. (2011). Multiple enhancers ensure precision of gap

gene-expression patterns in the *Drosophila* embryo. *Proceedings of the National Academy of Sciences*, *108*(33), 13570-13575.

Pool, J. E., & Aquadro, C. F. (2007). The genetic basis of adaptive pigmentation variation in *Drosophila melanogaster*. *Molecular Ecology*, *16*(14), 2844-2851.

Preger-Ben Noon E., Sabarís, G., Ortiz, D. M., Sager, J., Liebowitz, A., Stern, D. L., & Frankel, N. (2018). Comprehensive analysis of a *cis*-regulatory region reveals pleiotropy in enhancer function. *Cell Reports*, *22*(11), 3021-3031.

Prud'homme, B., Gompel, N., & Carroll, S. B. (2007). Emerging principles of regulatory evolution. *Proceedings of the National Academy of Sciences*, *104*(suppl 1), 8605-8612.

R Core Team. 2020. R: A language and environment for statistical computing. Vienna, Austria: R Foundation for Statistical Computing. https://www.R-project.org/.

Rebeiz, M., Pool, J. E., Kassner, V. A., Aquadro, C. F., & Carroll, S. B. (2009). Stepwise modification of a modular enhancer underlies adaptation in a *Drosophila* population. *Science*, *326*(5960), 1663-1667.

Rebeiz, M., & Williams, T. M. (2017). Using *Drosophila* pigmentation traits to study the mechanisms of *cis*-regulatory evolution. *Current Opinion in Insect Science*, *19*, 1-7.

Roeske, M. J., Camino, E. M., Grover, S., Rebeiz, M., & Williams, T. M. (2018). *Cis*-regulatory

evolution integrated the Bric-à-brac transcription factors into a novel fruit fly gene regulatory network. *Elife*, *7*, e32273.

Rogers, W. A., Grover, S., Stringer, S. J., Parks, J., Rebeiz, M., & Williams, T. M. (2014). A survey of the trans-regulatory landscape for *Drosophila melanogaster* abdominal pigmentation. *Developmental Biology*, *385*(2), 417-432.

Sabarís, G., Laiker, I., Preger-Ben Noon E., & Frankel, N. (2019). Actors with multiple roles: pleiotropic enhancers and the paradigm of enhancer modularity. *Trends in Genetics*, *35*(6), 423-433.

Schneider, C. A., Rasband, W. S., & Eliceiri, K. W. (2012). NIH Image to ImageJ: 25 years of image analysis. *Nature Methods*, *9*(7), 671-675.

Segert, J. A., Gisselbrecht, S. S., & Bulyk, M. L. (2021). Transcriptional silencers: Driving gene expression with the brakes on. *Trends in Genetics*, *37*(6), 514-527.

Spitz, F., & Furlong, E. E. (2012). Transcription factors: from enhancer binding to developmental control. *Nature Reviews Genetics*, *13*(9), 613-626.

Stern, D. L. (2000). Perspective: evolutionary developmental biology and the problem of variation. *Evolution*, *54*(4), 1079-1091.

Suh, J., & Jackson, F. R. (2007). *Drosophila ebony* activity is required in glia for the circadian

regulation of locomotor activity. *Neuron*, *55*(3), 435-447.

Takahashi, A., Takahashi, K., Ueda, R., & Takano-Shimizu, T. (2007). Natural variation of *ebony* gene controlling thoracic pigmentation in *Drosophila melanogaster*. *Genetics*, *177*(2), 1233-1237.

Takahashi, A., & Takano-shimizu, T. (2011). Divergent enhancer haplotype of *ebony* on inversion In (3R) Payne associated with pigmentation variation in a tropical population of *Drosophila melanogaster*. *Molecular Ecology*, *20*(20), 4277-4287.

Telonis-Scott, M., Hoffmann, A. A., & Sgro, C. M. (2011). The molecular genetics of clinal variation: a case study of *ebony* and thoracic trident pigmentation in *Drosophila melanogaster* from eastern Australia. *Molecular Ecology*, *20*(10), 2100-2110.

Telonis-Scott, M., & Hoffmann, A. A. (2018). Enhancing *ebony*? Common associations with a *cis*-regulatory haplotype for *Drosophila melanogaster* thoracic pigmentation in a Japanese population and Australian populations. *Frontiers in Physiology*, *9*, 822.

Waldo, G. S., Standish, B. M., Berendzen, J., & Terwilliger, T. C. (1999). Rapid protein-folding assay using green fluorescent protein. *Nature Biotechnology*, *17*(7), 691-695.

Wittkopp, P. J., Vaccaro, K., & Carroll, S. B. (2002). Evolution of *yellow* gene regulation and pigmentation in *Drosophila*. *Current Biology*, *12*(18), 1547-1556.

Wittkopp, P. J., Carroll, S. B., & Kopp, A. (2003a). Evolution in black and white: genetic control of pigment patterns in *Drosophila*. *TRENDS in Genetics*, *19*(9), 495-504.

Wittkopp, P. J., Williams, B. L., Selegue, J. E., & Carroll, S. B. (2003b). *Drosophila* pigmentation evolution: divergent genotypes underlying convergent phenotypes. *Proceedings of the National Academy of Sciences*, *100*(4), 1808-1813.

Wray, G. A., Hahn, M. W., Abouheif, E., Balhoff, J. P., Pizer, M., Rockman, M. V., & Romano, L. A. (2003). The evolution of transcriptional regulation in eukaryotes. *Molecular Biology and Evolution*, *20*(9), 1377-1419.

Xin, Y., Le Poul, Y., Ling, L., Museridze, M., Mühling, B., Jaenichen, R., *et al*. (2020). Ancestral and derived transcriptional enhancers share regulatory sequence and a pleiotropic site affecting chromatin accessibility. *Proceedings of the National Academy of Sciences*, *117*(34), 20636-20644.

Table 1-1 The list of sequences used for midline silencer region comparison

Strain name	Accession number	Original population	Reference
RAL-774	LC37995	North Carolina (DGRP)	[a]
RAL-786	LC37996	North Carolina (DGRP)	[a]
RAL-799	LC37997	North Carolina (DGRP)	[a]
RAL-820	LC37998	North Carolina (DGRP)	[a]
RAL-852	LC37999	North Carolina (DGRP)	[a]
RAL-365	LC38000	North Carolina (DGRP)	[a]
RAL-707	LC38001	North Carolina (DGRP)	[a]
RAL-517	LC38002	North Carolina (DGRP)	[a]
RAL-555	LC38003	North Carolina (DGRP)	[a]
RAL-358	LC38004	North Carolina (DGRP)	[a]
RAL-360	LC38005	North Carolina (DGRP)	[a]
RAL-380	LC38006	North Carolina (DGRP)	[a]
RAL-208	LC38007	North Carolina (DGRP)	[a]
RAL-335	LC38009	North Carolina (DGRP)	[a]
RAL-705	LC38010	North Carolina (DGRP)	[a]
RAL-303	LC38011	North Carolina (DGRP)	[a]
RAL-357	LC38012	North Carolina (DGRP)	[a]
RAL-399	LC38013	North Carolina (DGRP)	[a]
RAL-732	LC38014	North Carolina (DGRP)	[a]
U78	EF114370	Uganda	[b]
U76	EF114371	Uganda	[b]
U75a	EF114372	Uganda	[b]
U75b	EF114373	Uganda	[b]
U73	EF114374	Uganda	[b]
U70	EF114375	Uganda	[b]
U65	EF114376	Uganda	[b]
U64	EF114377	Uganda	[b]
U62	EF114378	Uganda	[b]
U56	EF114379	Uganda	[b]
U53	EF114380	Uganda	[b]
K71	EF114381	Kenya	[b]
K61a	EF114382	Kenya	[b]
K62b	EF114383	Kenya	[b]

Table 1-1 continued from the previous page

K60	EF114384	Kenya	[b]
K59	EF114385	Kenya	[b]
K58a	EF114386	Kenya	[b]
K58b	EF114387	Kenya	[b]
K53	EF114388	Kenya	[b]
K48	EF114389	Kenya	[b]
K46	EF114390	Kenya	[b]
cd11b	GU108064	Cameroon	[c]
cd16	GU108065	Cameroon	[c]
cd26	GU108066	Cameroon	[c]
cd30	GU108067	Cameroon	[c]
cd40a	GU108068	Cameroon	[c]
cn03	GU108069	Cameroon	[c]
cn04b	GU108070	Cameroon	[c]
cn07	GU108071	Cameroon	[c]
cn09b	GU108072	Cameroon	[c]
cn21b	GU108073	Cameroon	[c]
cn25	GU108074	Cameroon	[c]
co02	GU108075	Cameroon	[c]
co10b	GU108078	Cameroon	[c]
co16	GU108079	Cameroon	[c]
cw54	GU108081	Cameroon	[c]
cw82b	GU108083	Cameroon	[c]
er13	GU108084	Eritrea	[c]
er16a	GU108086	Eritrea	[c]
er17b	GU108087	Eritrea	[c]
er19b	GU108088	Eritrea	[c]
er20a	GU108089	Eritrea	[c]
er22a	GU108090	Eritrea	[c]
er23a	GU108091	Eritrea	[c]
er30	GU108092	Eritrea	[c]
rw1b	GU108093	Rwanda	[c]
rw3a	GU108095	Rwanda	[c]
rw5a	GU108096	Rwanda	[c]
ug02	GU108097	Uganda	[c]
ug06a	GU108099	Uganda	[c]

Table 1-1 continued from the previous page

ug08b	GU108100	Uganda	[c]
ug10b	GU108101	Uganda	[c]
ug12a	GU108102	Uganda	[c]
ug21	GU108103	Uganda	[c]
ug22b	GU108104	Uganda	[c]
ug24b	GU108105	Uganda	[c]
ug47a	GU108107	Uganda	[c]
IR03-1026	AB564311	Japan-Iriomote	[d]
IR03-1027	AB564312	Japan-Iriomote	[d]
IR03-1047	AB564313	Japan-Iriomote	[d]
IR03-1049	AB564314	Japan-Iriomote	[d]
IR03-1075	AB564315	Japan-Iriomote	[d]
IR03-1085	AB564317	Japan-Iriomote	[d]
IR03-1109	AB564318	Japan-Iriomote	[d]
IR03-1163	AB564319	Japan-Iriomote	[d]
IR03-1172	AB564320	Japan-Iriomote	[d]
IR03-1181	AB564321	Japan-Iriomote	[d]
IR03-1187	AB564322	Japan-Iriomote	[d]
IR03-1208	AB564323	Japan-Iriomote	[d]

[a] Miyagi *et al*. (2015)

[b] Rebeiz et al. (2009)

[c] Pool and Aquadro (2007)

[d] Takahashi and Takano-Shimizu (2011)

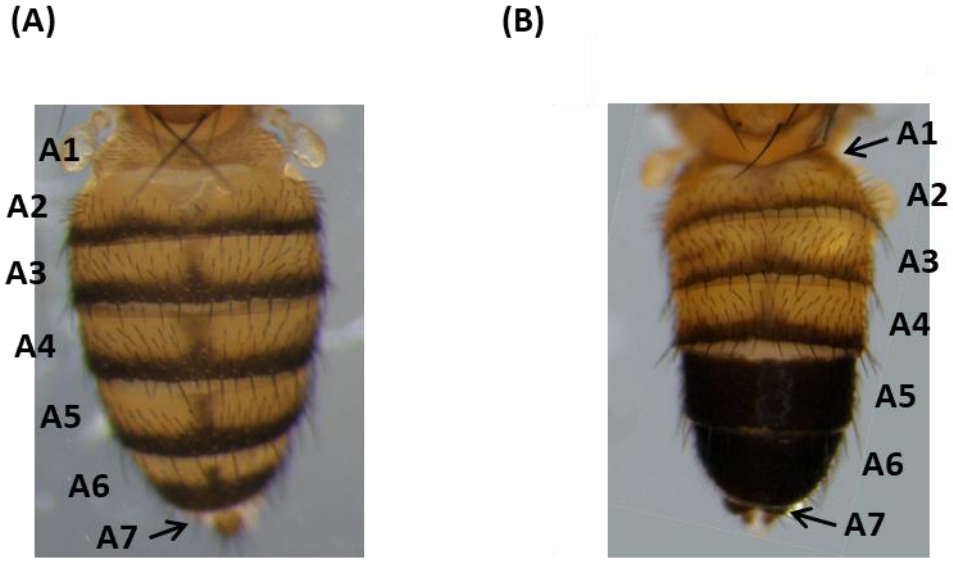

Fig. 1-1 Photo images of abdominal tergites in *D. melanogaster*

(A) Dorsal image of female abdomen (RAL-365). (B) Dorsal image of male adomen (RAL-365). A1–A7 indicate abdominal tergites.

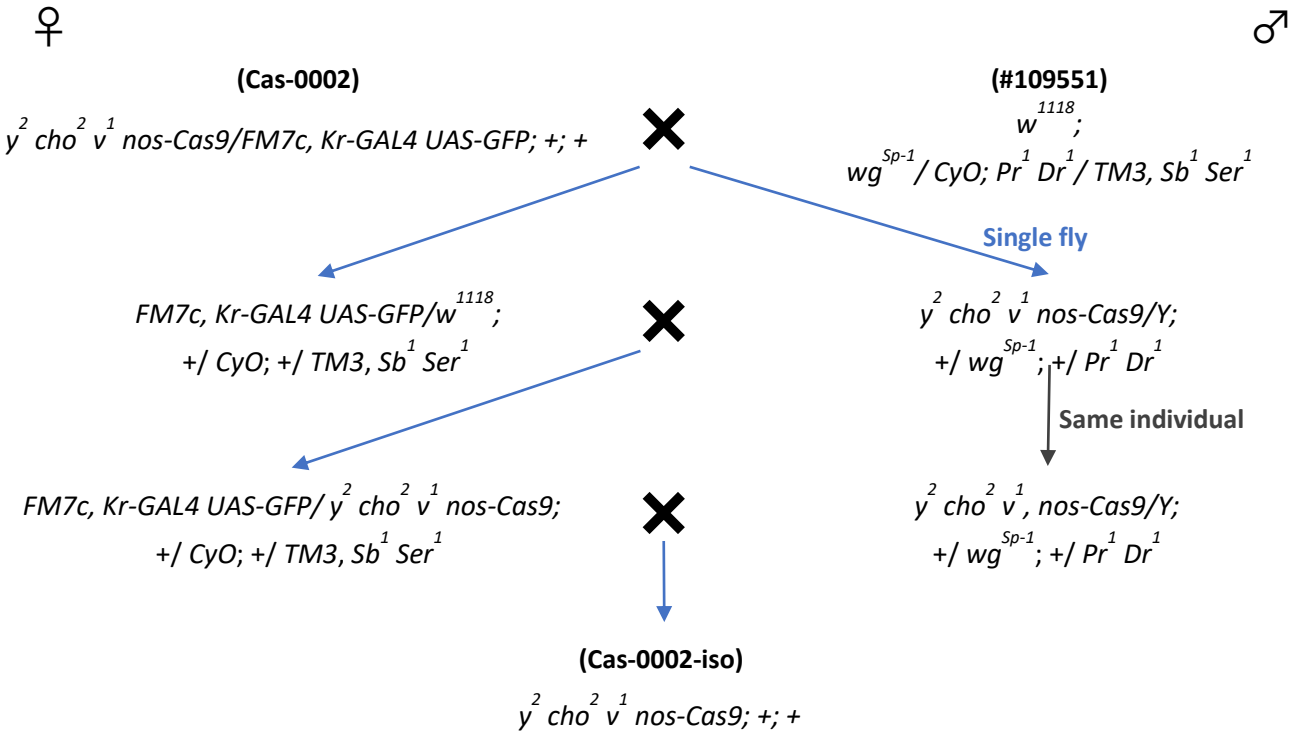

Fig. 1-2 Scheme for extracting an isogenized chromosome

To control for the genetic background of the genome-edited flies, each chromosome was originated from a single chromosome. The isogenized strain was named Cas-0002-iso.

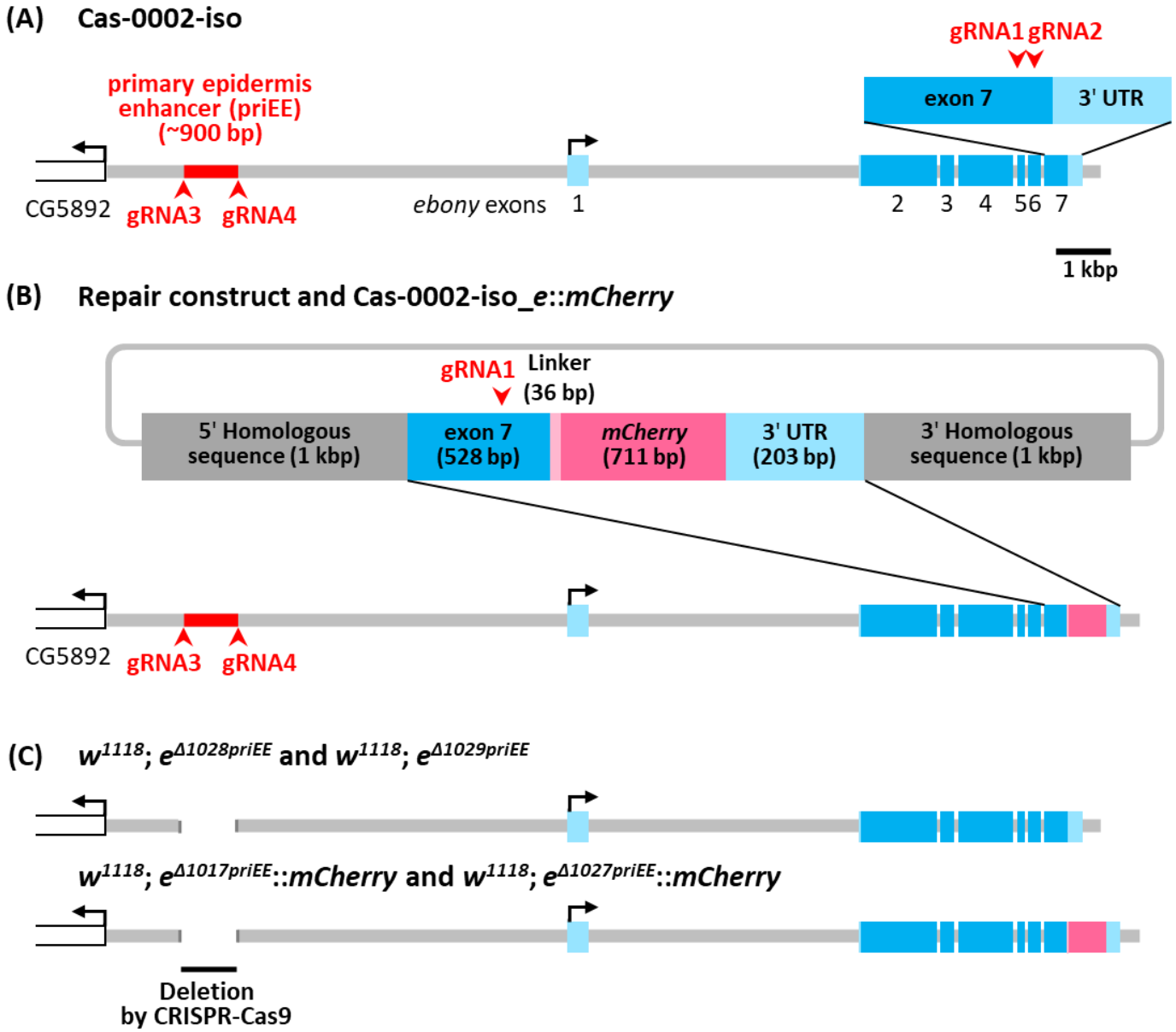
(A) Cas-0002-iso
gRNA1 gRNA2
primary epidermis enhancer (priEE) (~900 bp)
exon 7
3' UTR
CG5892
gRNA3
gRNA4
ebony exons
1
2
3
4
56
7
1 kbp
(B) Repair construct and Cas-0002-iso_e::mCherry
gRNA1
Linker (36 bp)
5' Homologous sequence (1 kbp)
exon 7 (528 bp)
mCherry (711 bp)
3' UTR (203 bp)
3' Homologous sequence (1 kbp)
CG5892
gRNA3
gRNA4
(C) w1118; eΔ1028priEE and w1118; eΔ1029priEE
w1118; eΔ1017priEE::mCherry and w1118; eΔ1027priEE::mCherry
Deletion by CRISPR-Cas9
(D)
priEE (~900 bp)
gRNA3 target sequence
gRNA4 target sequence
Control (w1118; +) AATGTTAATAAGATCGGACAGACGGGCA ..... TTTGAGAAAGTACTATCAATATACAAGGAAGC
eΔ1028priEE AATGTTAATAAG---------- ..... ----------AAGGAAGC
eΔ1028pr9EE AATGTTAATAAG---------- ..... ----------AGGAAGC
eΔ1017priEE::mCherry AATGTTAATAAGATCGGACT-------- ..... ----------TACAAGGAAGC
eΔ1027priEE::mCherry AATGTTAATAAGATCGGA---------- ..... ----------AGC
(988 bp)

Fig. 1-3 Construction of the primary epidermis enhancer (priEE) knockout strains

(A) The genomic region surrounding ebony in Cas-0002-iso, an isogenic line carrying *nos*-Cas9. (B) The genomic region surrounding *ebony* in Cas-0002-iso_*e*::*mCherry* is shown with the repair construct for *mCherry* knock-in. (C) The genomic region surrounding *ebony* in strains with deleted priEE after the removal of y^2 (Fig. 1-6). The light blue box indicates the untranlated region (UTR) and the blue box indicates the coding sequence (CDS). The red arrowhead indicates the target site of guide RNA (gRNA) sequences. (D) Partial sequence alignment around the priEE fragment in the control and priEE-deleted strains. w^{1118}; $e^{\Delta 1017priEE}$::*mCherry* had a single T of unknown origin within the deleted region.

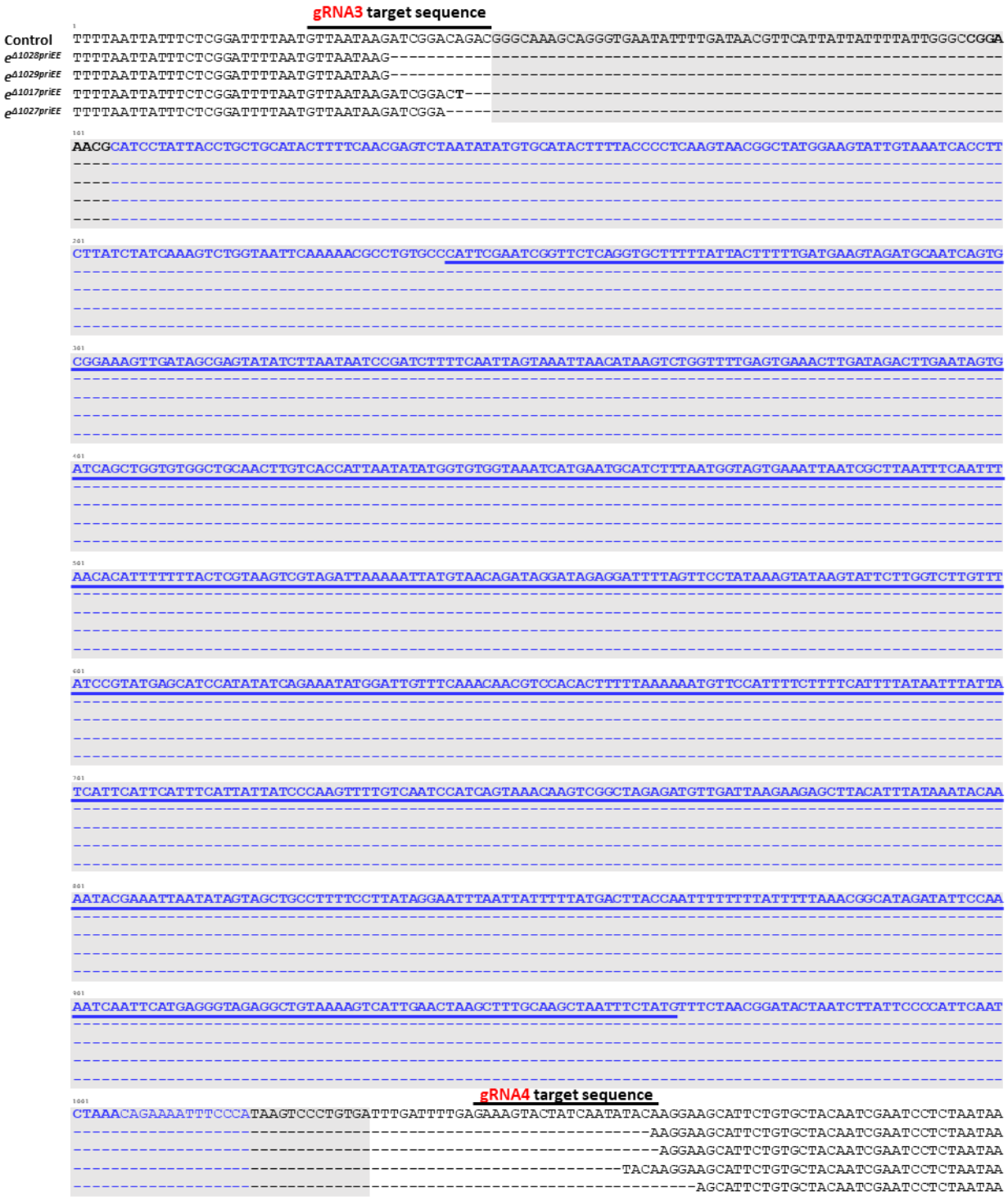
gRNA3 target sequence
Control
e^Δ1028priEE
e^Δ1029priEE
e^Δ1017priEE
e^Δ1027priEE
gRNA4 target sequence

Fig. 1-4 Alignment of sequences around the primary enhancer element (priEE) in the control and priEE knockout strains

The guide RNA (gRNA) target sequences are indicated above the sequence. Bases in bold indicate the 947-bp sequence of e_ECR0.9 from Takahashi and Takano-Shimizu (2011) (909-bp sequence in the control strain (Cas-0002-iso-derived w^{1118}; + strain)). Bases in blue indicate the 961-bp sequence of *e*_core_*cis* sequence from Miyagi *et al*. (2015) (915 bp in the control strain (Cas-0002-iso-derived w^{1118}; + strain) and the underlined bases indicate the "0.7 kb core abdominal element" from Rebeiz *et al*. (2009). Shaded bases indicate the sequence fragment (987 bp) used for the reporter assay in this study.

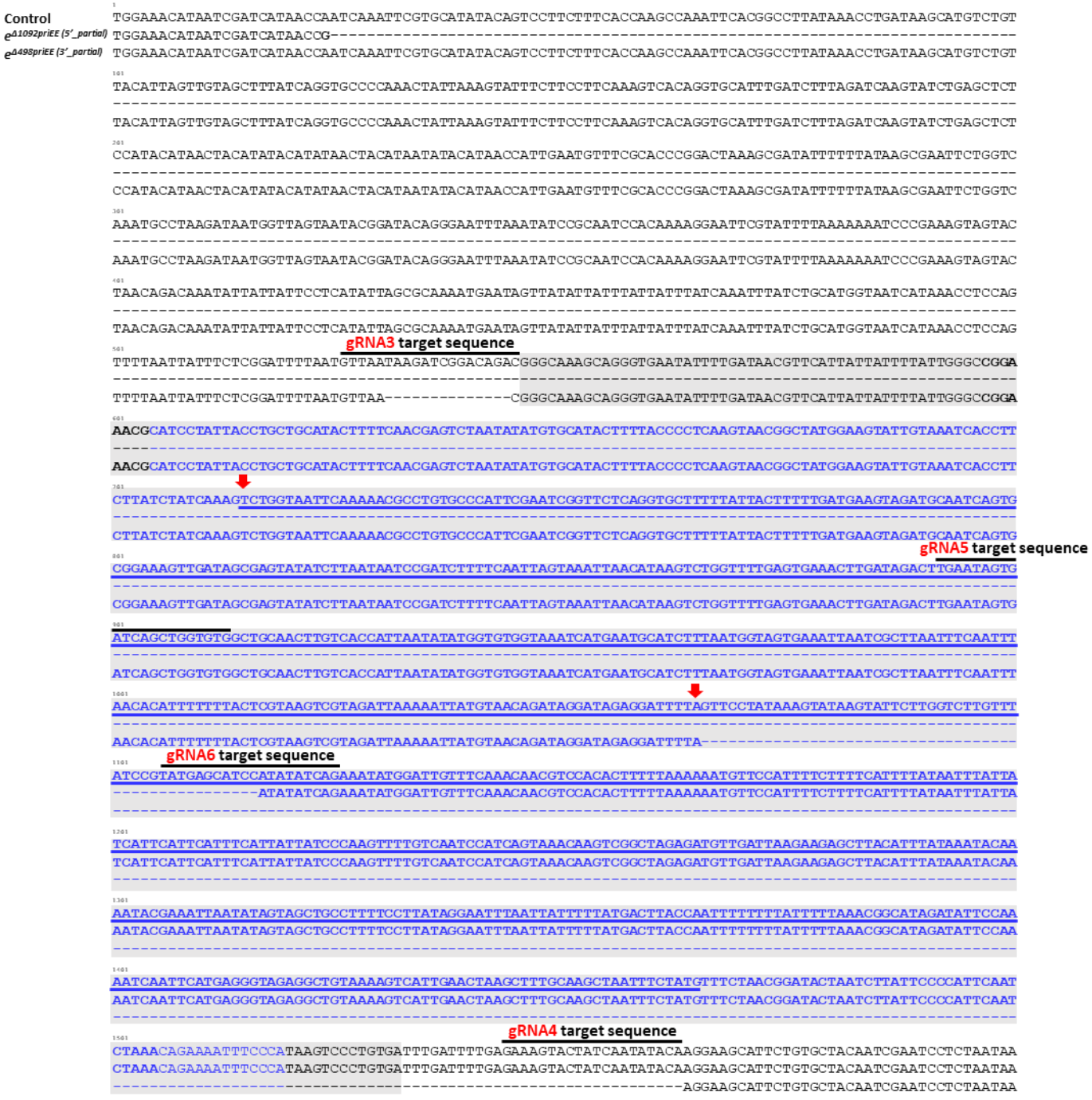
Control
e^Δ1092priEE (5'_partial)
e^Δ498priEE (3'_partial)
gRNA3 target sequence
gRNA5 target sequence
gRNA6 target sequence
gRNA4 target sequence

Fig. 1-5 Alignment of sequences around the primary enhancer element (priEE) in the control and the strains with partially deleted priEE

The guide RNA (gRNA) target sequences are indicated above the sequence. Bases in bold indicate the 947-bp sequence of e_ECR0.9 from Takahashi and Takano-Shimizu (2011) (909-bp sequence in the control strain (Cas-0002-iso-derived w^{1118}; + strain)). Bases in blue indicate the 961-bp sequence of *e*_core_*cis* sequence from Miyagi *et al*. (2015) (915 bp in the control strain (Cas-0002-iso-derived w^{1118}; + strain) and the underlined bases indicate the "0.7 kb core abdominal element" from Rebeiz *et al*. (2009). Shaded bases indicate the sequence fragment (987 bp) used for the reporter assay in this study. The red arrows indicate the first and the last nucleotides of the 351-bp abdominal midline silencer element.

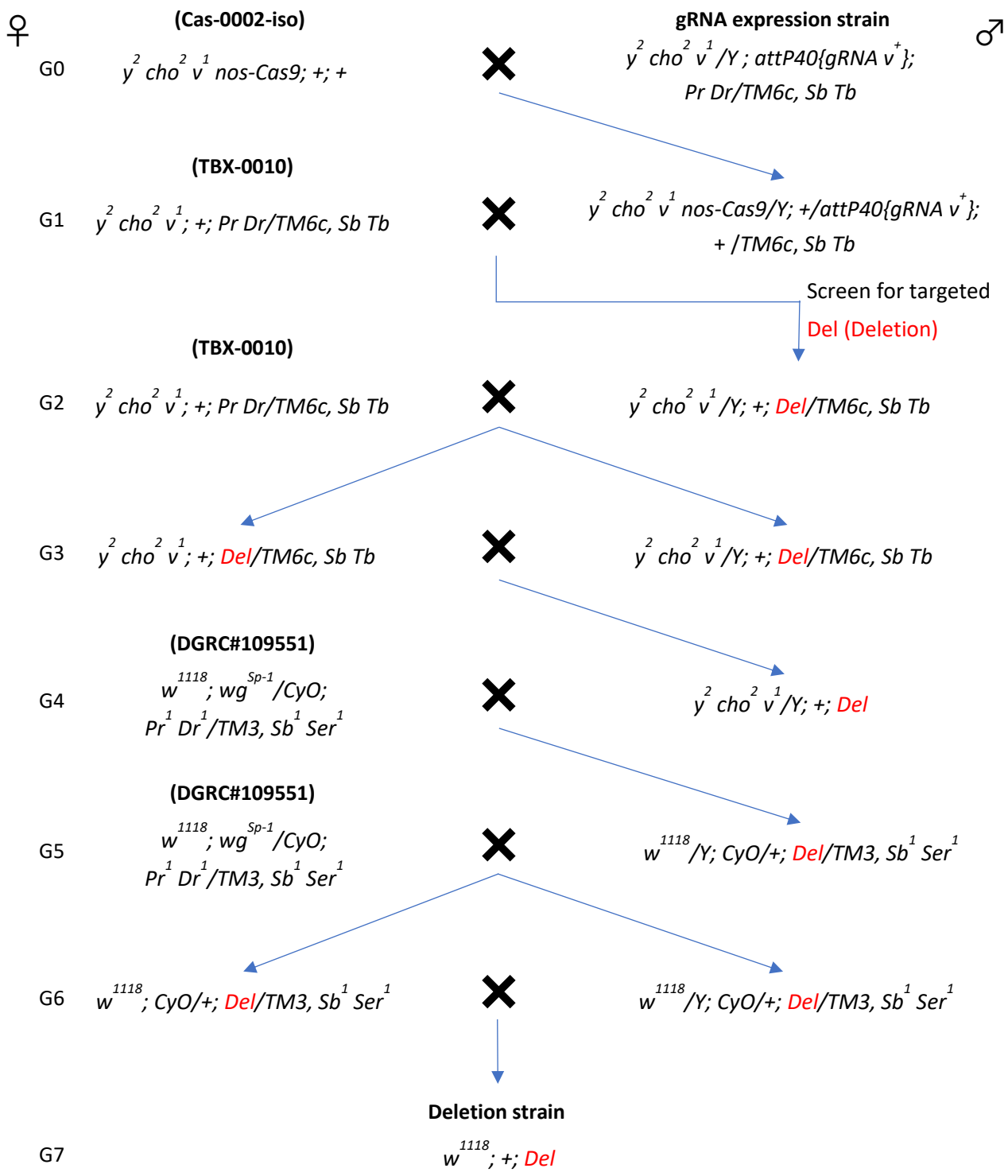
♀
♂
(Cas-0002-iso)
gRNA expression strain
G0
y2 cho2 v1 nos-Cas9; +; +
y2 cho2 v1 /Y ; attP40{gRNA v+};
Pr Dr/TM6c, Sb Tb
(TBX-0010)
G1
y2 cho2 v1; +; Pr Dr/TM6c, Sb Tb
y2 cho2 v1 nos-Cas9/Y; +/attP40{gRNA v+};
+ /TM6c, Sb Tb
Screen for targeted
Del (Deletion)
(TBX-0010)
G2
y2 cho2 v1; +; Pr Dr/TM6c, Sb Tb
y2 cho2 v1 /Y; +; Del/TM6c, Sb Tb
G3
y2 cho2 v1; +; Del/TM6c, Sb Tb
y2 cho2 v1 /Y; +; Del/TM6c, Sb Tb
(DGRC#109551)
G4
w1118; wgSp-1 /CyO;
Pr1 Dr1 /TM3, Sb1 Ser1
y2 cho2 v1 /Y; +; Del
(DGRC#109551)
G5
w1118; wgSp-1 /CyO;
Pr1 Dr1 /TM3, Sb1 Ser1
w1118 /Y; CyO/+; Del/TM3, Sb1 Ser1
G6
w1118; CyO/+; Del/TM3, Sb1 Ser1
w1118 /Y; CyO/+; Del/TM3, Sb1 Ser1
Deletion strain
G7
w1118; +; Del

Fig. 1-6 Scheme for generating primary enhancer element (priEE) deletion strains without y^2

CRISPR-Cas9-based genome editing was performed by crossing the Cas-0002-iso with the guide RNA (gRNA) expression strain (G0). The progenies from the G1 cross were screened for the presence of deletions. Homologous deletions were achieved by the crosses in G2 and G3. y^2 was removed by the crosses in G4 to G7 because it interferes with ebony in the pigment biosynthesis pathway. Deletion strains for mCherry fluorescence observation were established using the same scheme, except Cas-0002-iso_*e*::*mCherry* was used instead of Cas-0002-iso (G0). Control strains (w^{1118}; +; + and w^{1118}; +; *e*::*mCherry*) were established with the same crosses using TBX-0002 instead of the gRNA expression strain and using + instead of the Del genotype for the G2 cross.

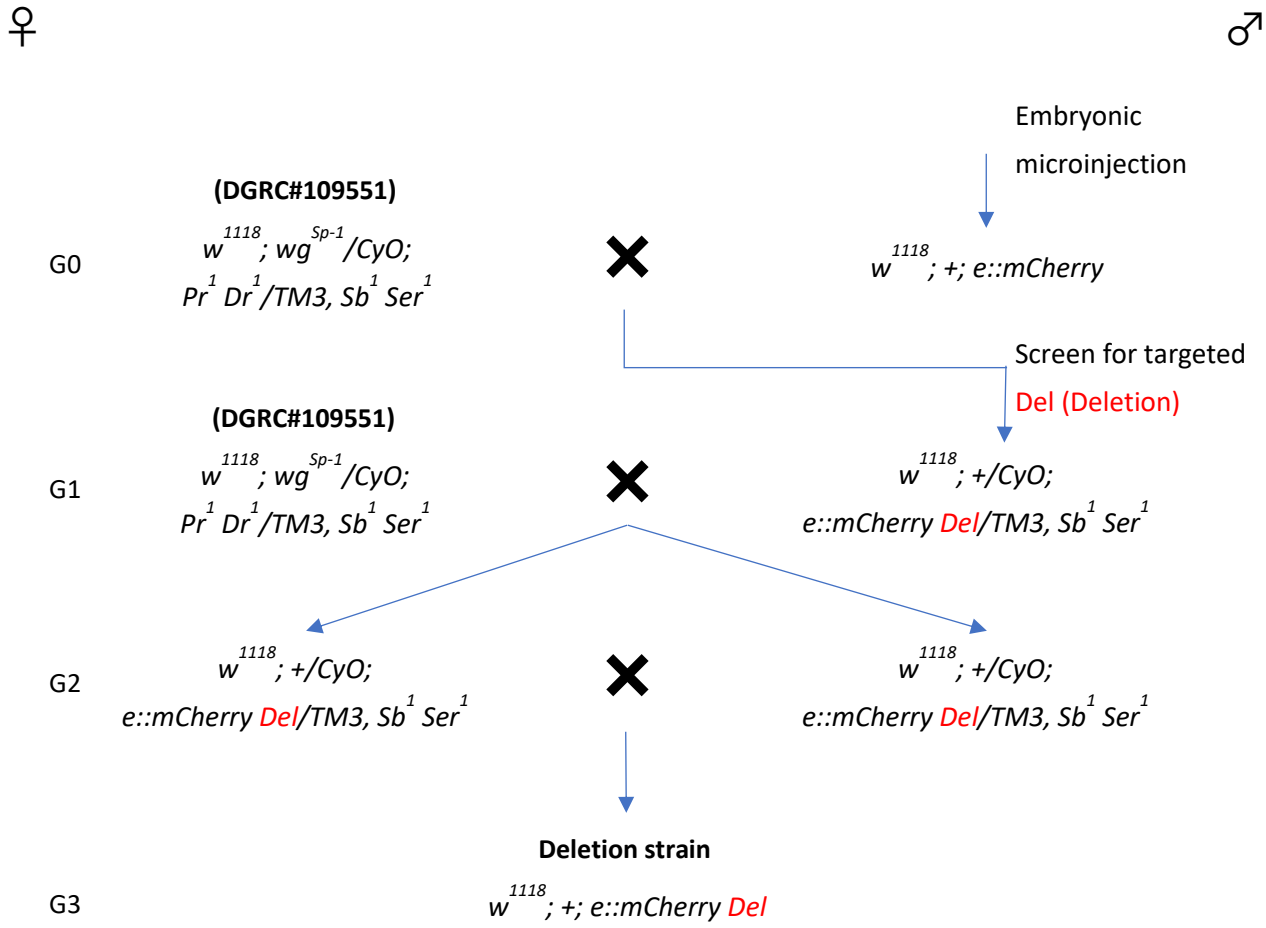

Fig. 1-7 Scheme for generating strains with partially deleted primary enhancer element (priEE)

CRISPR-Cas9-based genome editing was performed by embryonic microinjection of gRNA3–6 cloned pCFD5 and pBFv-nosP-Cas9 vectors. The progenies from the G0 cross were screened for the presence of deletions. Homologous deletions were achieved by the crosses in G1 and G2.

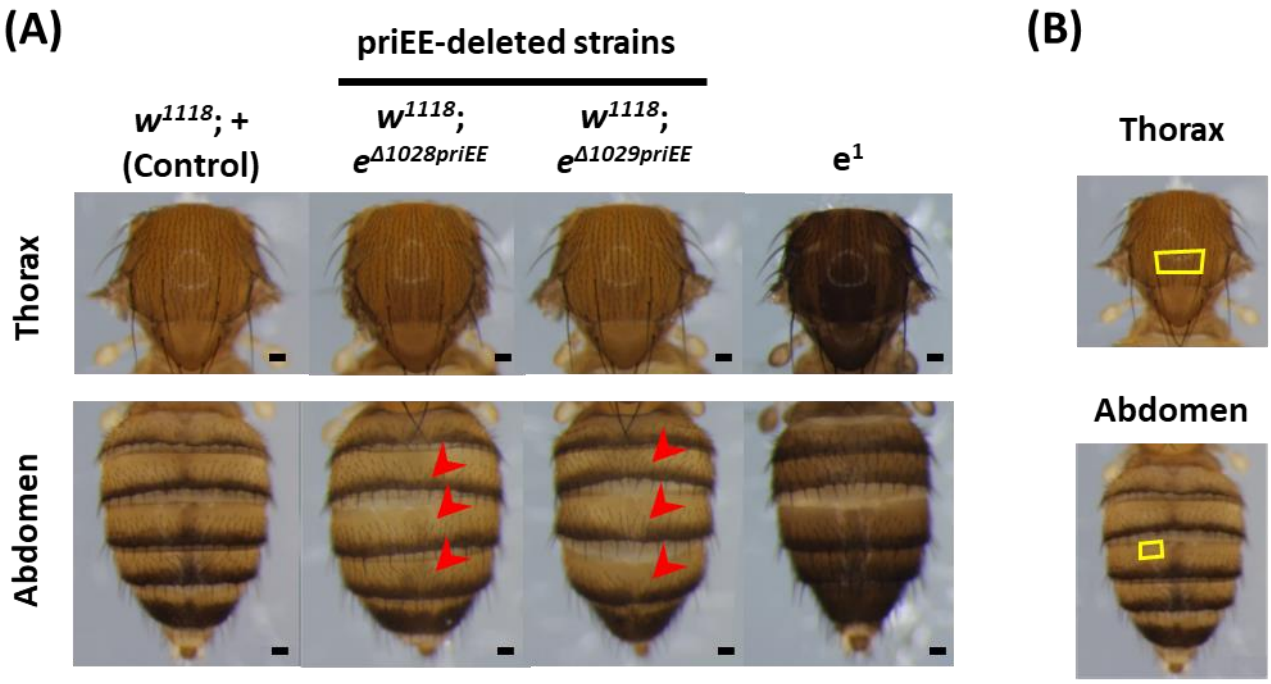
(A)
priEE-deleted strains
w1118; +
(Control)
w1118;
eΔ1028priEE
w1118;
eΔ1029priEE
e1
Thorax
Abdomen
(B)
Thorax
Abdomen

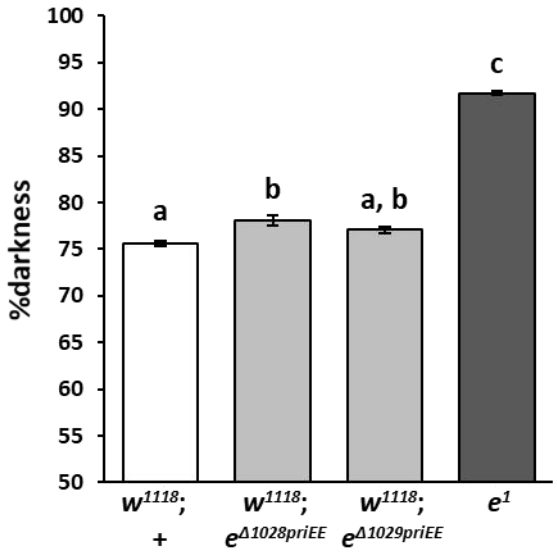
(C)
%darkness
100
95
90
85
80
75
70
65
60
55
50
a
b
a, b
c
w1118; +
w1118; eΔ1028priEE
w1118; eΔ1029priEE
e1

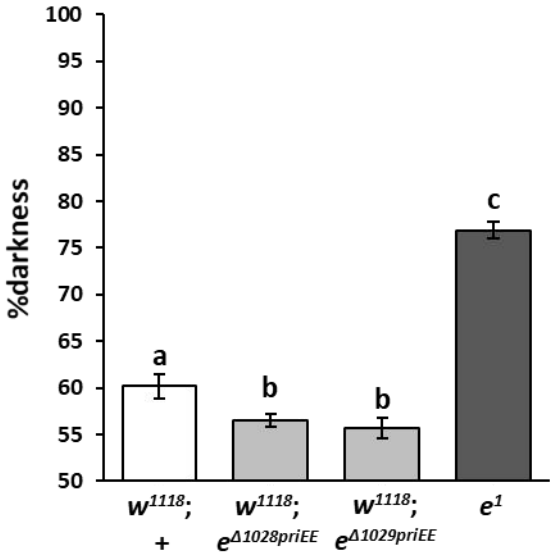
(D)
%darkness
100
95
90
85
80
75
70
65
60
55
50
a
b
b
c
w1118; +
w1118; eΔ1028priEE
w1118; eΔ1029priEE
e1

Fig. 1-8 Effect of primary epidermis enhancer (priEE) knockout on the intensity and patterns of pigmentation

(A) Images of the 5–7-day-old adult females. The red arrow indicates the area where the dark pigmentation in the dorsal midline is missing. (B) Yellow squares indicating the areas of thorax (upper panel) and abdomen (lower panel) where pigmentation was quantified. (C) Percent (%) darkness values obtained from the grayscale images of the thorax. (D) Percent (%) darkness values obtained from the grayscale images of the A4 abdominal segment. $N = 10$ for each strain. Different letters indicate significant differences between strains ($P < 0.05$; Kruskal-Wallis rank sum test followed by Dunn's test). Scale bars indicate 100 μm and error bars denote standard error.

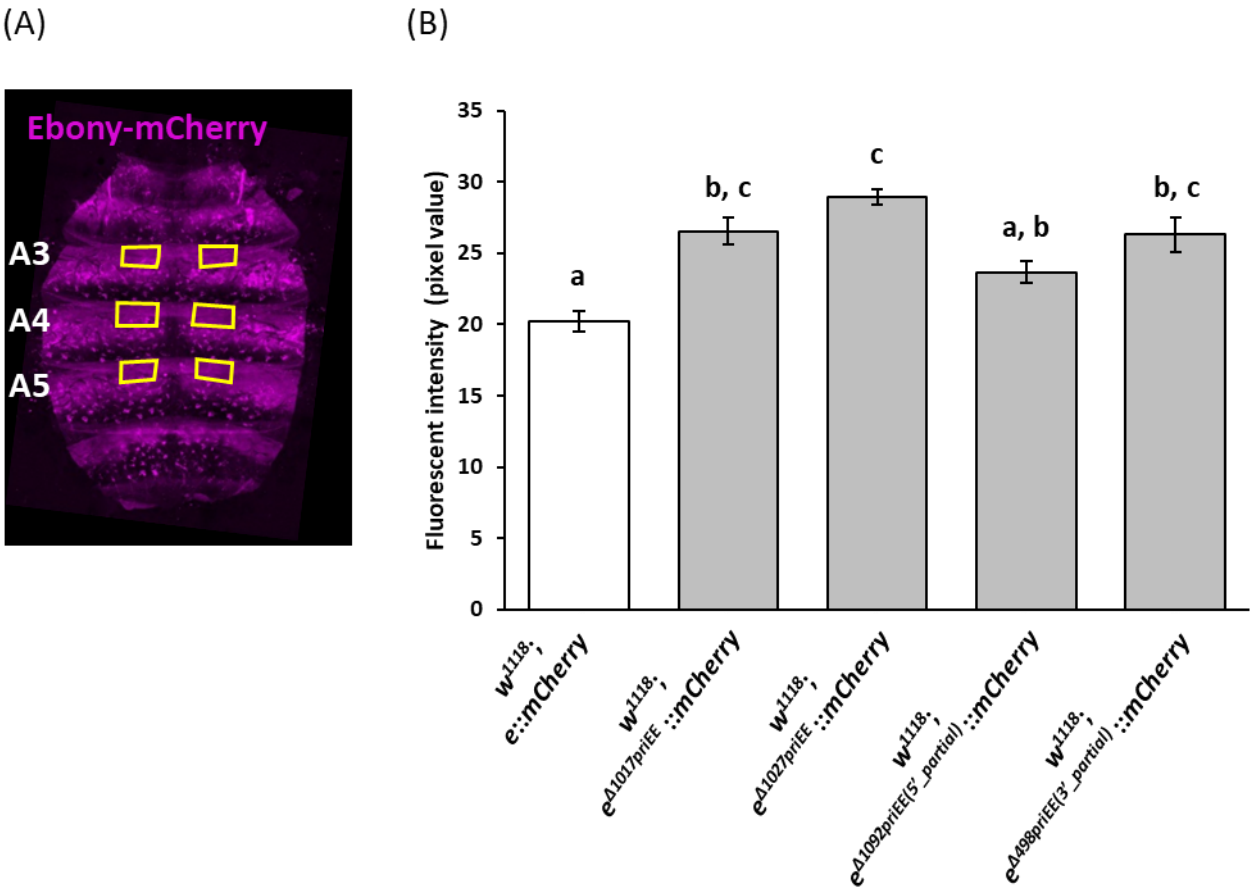

Fig. 1-9 Effect of primary epidermis enhancer (priEE) knockout on the fluorescent intensity of mCherry fused to Ebony

(A) Yellow squares indicating the areas of the abdominal tergites A3–5 where pigmentation was quantified in a confocal fluorescence image of the developing abdominal epidermis. (B) Fluorescence intensities in pixel values (0–255) quantified from the images of the control (w^{1118}; *e*::*mCherry*), the priEE-deleted strains (w^{1118}; $e^{\Delta 1017priEE}$::*mCherry* and w^{1118}; $e^{\Delta 1027priEE}$::*mCherry*), and the strains with partially deleted priEE (w^{1118}; $e^{\Delta 1092priEE(5'\_partial)}$::*mCherry* and w^{1118}; $e^{\Delta 498priEE(3'\_partial)}$::*mCherry*). $N = 10$ for each strain. Different letters indicate significant differences between strains ($P < 0.05$; one-way analysis of variance, followed by Tukey HSD post-hoc test). Error bars denote standard error.

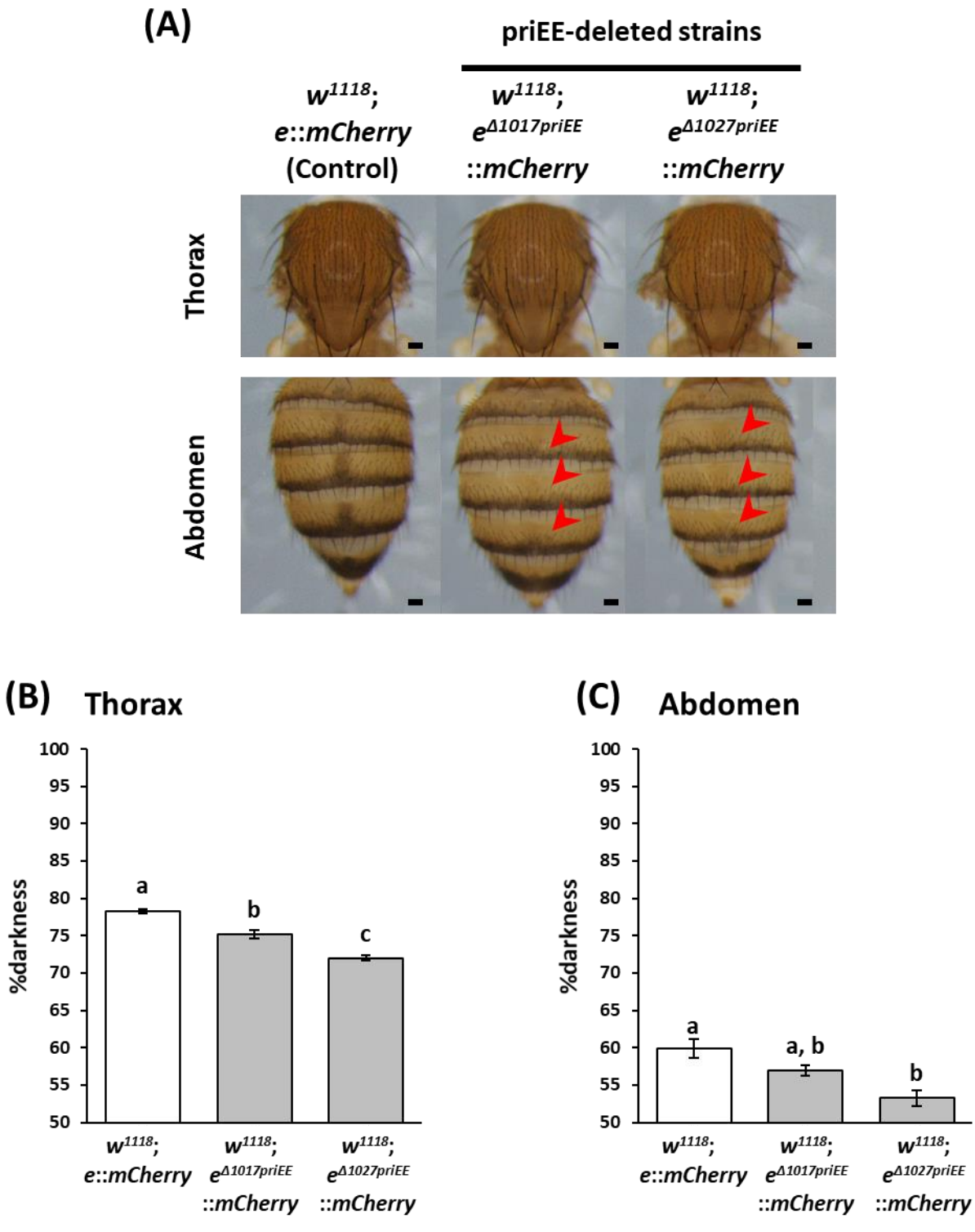
(A)
priEE-deleted strains
w1118; e::mCherry (Control)
w1118; eΔ1017priEE ::mCherry
w1118; eΔ1027priEE ::mCherry
Thorax
Abdomen
(B) Thorax
%darkness
100
95
90
85
80
75
70
65
60
55
50
a
b
c
w1118; e::mCherry
w1118; eΔ1017priEE ::mCherry
w1118; eΔ1027priEE ::mCherry
(C) Abdomen
%darkness
100
95
90
85
80
75
70
65
60
55
50
a
a, b
b
w1118; e::mCherry
w1118; eΔ1017priEE ::mCherry
w1118; eΔ1027priEE ::mCherry

Fig. 1-10 Effect of primary enhancer element (priEE) knockout on the intensity and patterns of pigmentation

(A) Images of the 5–7-day-old adult females. The red arrow indicates the area where the dark pigmentation in the dorsal midline is missing. (B) Percent (%) darkness values of the thorax. (C) Percent (%) darkness values of the A4 abdominal segment. Pigmentation of thorax and abdomen was quantified in the areas indicated by the yellow squares in the upper and lower panels, respectively, in Fig. 1-8B. $N = 10$ for each strain. Different letters indicate significant differences between strains ($P < 0.05$; Kruskal-Wallis rank sum test followed by Dunn's test with Bonferroni correction). Scale bars indicate 100 μm and error bars denote standard error.

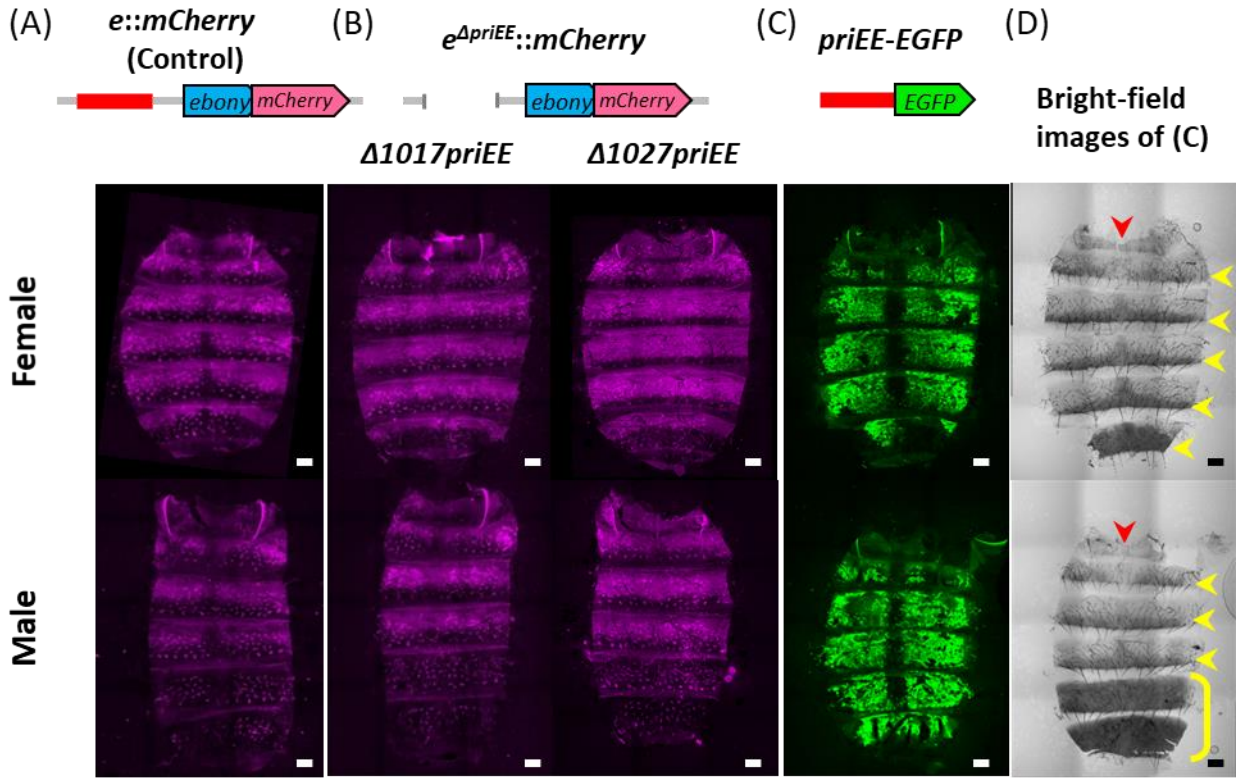

(E)

Broad abdominal expression	+	+	+
Dorsal midline expression	-	+	-
Stripe expression	-	-	+
Posterior segment expression in male	-	-	+

(F)

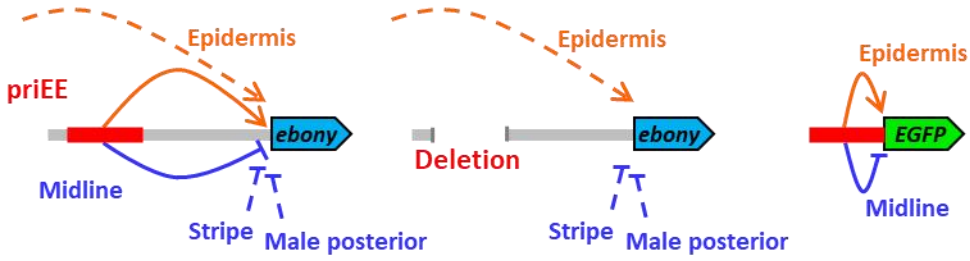

Fig. 1-11 *cis*-regulatory elements (CREs) regulate *ebony* expression in the developing epidermis

Confocal fluorescence images of the developing abdominal epidermis of w^{1118}*; e*::*mCherry* (A), w^{1118}; $e^{\Delta 1017priEE}$::*mCherry*, w^{1118}; $e^{\Delta 1027priEE}$::*mCherry* (B), and *priEE-EGFP* transformed to VK00033 (C). (D) Bright-field images of (C). Images of females and males are shown in the upper and lower panels, respectively. The red arrowhead indicates the dorsal midline. The yellow arrowhead indicates a dark stripe on the posterior area of each tergite. The yellow bracket indicates male-specific dark pigmentation in the A5 and A6 tergites. Scale bars indicate 100 μm. (E) Summary of the ebony expression sites for each strain determined from the fluorescence signals. (F) The suggested model for the regulation of *ebony* expression in the abdomen. The solid lines indicate the effects of priEE, while the dotted lines indicate the effects of other CREs. The priEE fragment was also equipped to function as a midline silencer.

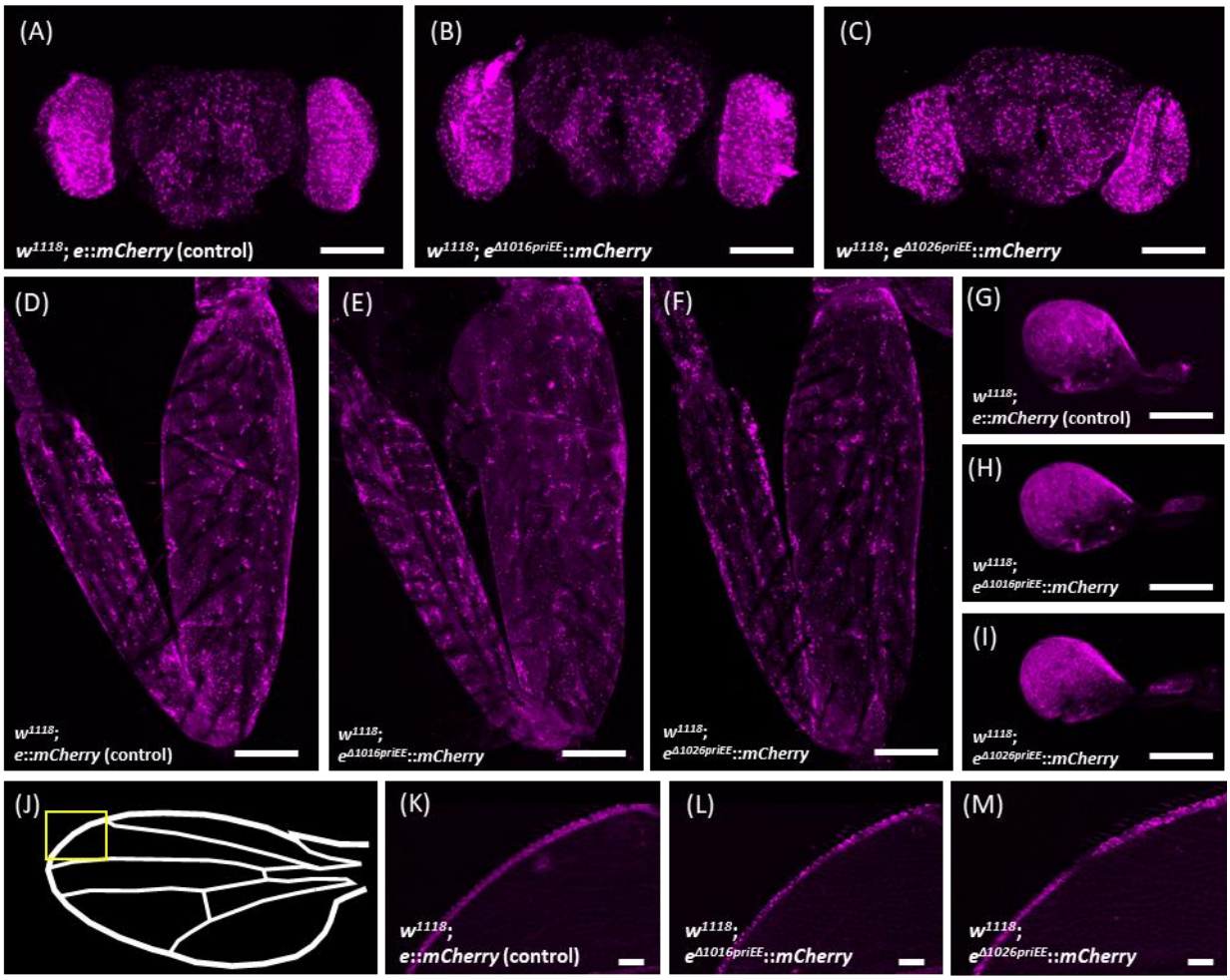

Fig. 1-12 *ebony* expression in tissues other than developing epidermis

Confocal images of the mCherry-fused Ebony in the brain (A, B, and C), the front leg (D, E, and F), the haltere (G, H, and I), and the wing (K, L, and M) at the area indicated by the yellow square (J). Each tissue was dissected from the control, w^{1118}; *e*::*mCherry* (A, D, G, and K), and the priEE-deleted strains, w^{1118}; $e^{\Delta 1017priEE}$::*mCherry* (B, E, H, and L) and w^{1118}; $e^{\Delta 1027priEE}$::*mCherry* (C, F, I, and M). Scale bars indicate 100 μm.

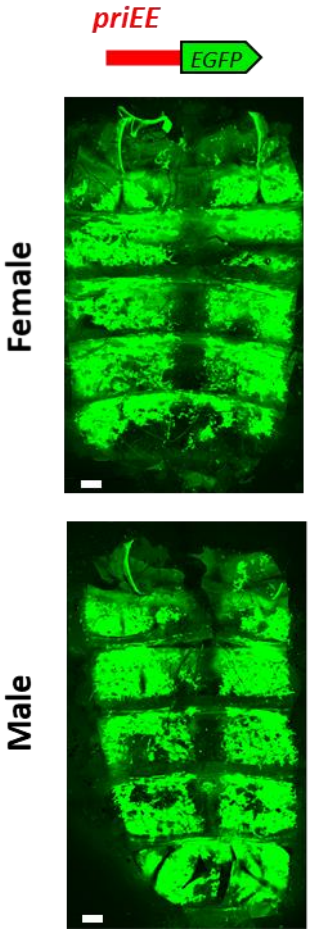

Fig. 1-13 Reporter assay using the enhanced GFP-fused primary enhancer element (*priEE-EGFP*) construct in the developing abdominal epidermis

Confocal fluorescence images of the developing abdominal epidermis of *priEE-EGFP* transformed to VK00037. Images of females and males are shown in the upper and lower panels, respectively. Scale bars indicate 100 μm.

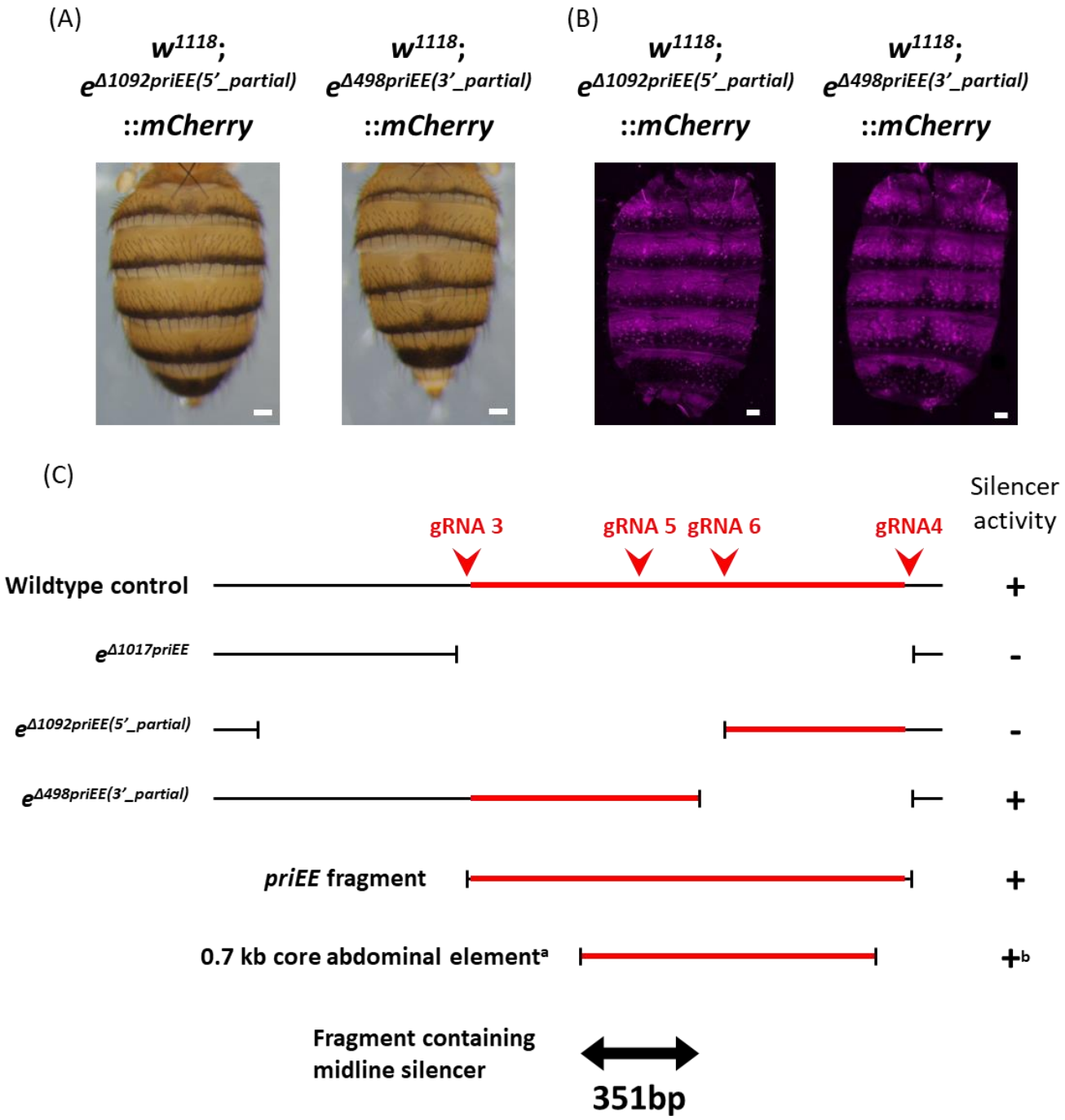
(A)
w1118;
eΔ1092priEE(5'_partial)
::mCherry
w1118;
eΔ498priEE(3'_partial)
::mCherry
(B)
w1118;
eΔ1092priEE(5'_partial)
::mCherry
w1118;
eΔ498priEE(3'_partial)
::mCherry
(C)
Silencer activity
gRNA 3
gRNA 5
gRNA 6
gRNA4
Wildtype control
+
eΔ1017priEE
-
eΔ1092priEE(5'_partial)
-
eΔ498priEE(3'_partial)
+
priEE fragment
+
0.7 kb core abdominal element[a]
+[b]
Fragment containing midline silencer
351bp

Fig. 1-14 Location of the dorsal abdominal midline silencer within the primary epidermis enhancer (priEE)

(A) The absence and presence of the dark pigmentation along the dorsal midline of the abdomen in w^{1118}; $e^{\Delta 1092priEE\ (5'\_partial)}$::*mCherry* (left panel) and in w^{1118}; $e^{\Delta 498priEE\ (3'\_partial)}$::*mCherry* (right panel), respectively. (B) The absence and presence of Ebony-mCherry repression along the dorsal midline of the abdomen w^{1118}; $e^{\Delta 1092priEE\ (5'\_partial)}$::*mCherry* (left panel) and in w^{1118}; $e^{\Delta 498priEE\ (3'\_partial)}$::*mCherry* (right panel), respectively. Scale bars indicate 100 μm. (C) The summary of the breakpoints of the deletions and the tested fragments by reporter assays and the midline silencer activity detected in the corresponding strains. The red arrowheads indicate the positions of the gRNA target sites used to generate partial deletions of the priEE. [a] and [b] are from Rebeiz *et al*. (2009). The double arrow indicates the position of the 351-bp fragment that include the silencer.

(A)

	Nucleotide position													Midline pigmentation
	23	28	32	68	123	186	259	263	274	298	300	340	342	
Control (w^{1118}; +)	T	A	G	G	T	G	A	A	T	T	A	T	G	+
RAL-852	.	G	.	.	**C**	.	G	T	A	A	.	**C**	.	–
RAL-208	.	.	.	.	.	.	.	.	.	.	.	.	.	+
RAL-303	.	G	.	T	.	.	.	T	A	A	.	.	.	+
RAL-324	.	G	A	T	.	.	G	T	A	A	T	.	.	+
RAL-335	.	G	.	T	.	A	G	T	A	A	.	.	T	+
RAL-357	.	.	.	.	.	.	.	T	A	A	.	.	.	+
RAL-358	.	G	A	T	.	.	G	T	A	A	.	.	.	+
RAL-360	.	G	.	T	.	.	G	T	A	A	.	.	.	+
RAL-365	.	G	.	T	.	.	.	T	A	A	T	.	.	+
RAL-380	.	.	.	.	.	.	.	.	.	.	.	.	.	+
RAL-399	C	G	A	T	.	A	G	T	A	A	.	.	.	+
RAL-517	.	.	.	.	.	.	.	.	.	.	.	.	.	+
RAL-555	.	G	A	T	.	.	G	T	A	A	.	.	.	+
RAL-705	.	G	.	T	.	A	G	T	A	A	.	.	.	+
RAL-707	.	G	A	T	.	.	G	T	A	A	.	.	.	+
RAL-732	C	G	A	T	.	.	G	T	A	A	.	.	.	+
RAL-774	.	G	.	T	.	A	G	T	A	A	.	.	.	+
RAL-786	.	.	.	.	.	A	G	T	A	A	.	.	.	+
RAL-799	C	G	A	T	.	.	G	T	A	A	.	.	.	+
RAL-820	.	G	A	T	.	.	G	T	A	A	.	.	.	+

(B)

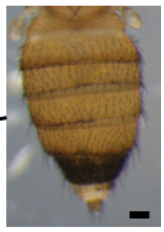

(C)

(D)

(E)

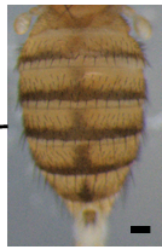

(F)

	108 -123	123
Control (w^{1118}; +)	+	T
RAL-852	+	C
cd30[a]	–	–
K61[b]	–	–
African 54 strains[a, b]	+	.
Iriomote 12 strains[c]	+	.

(G)

	340
Control (w^{1118}; +)	T
RAL-852	C
cn03[a]	C
cn04b[a]	C
er13[a]	C
ug06[a]	C
K71[b]	C
U64[b]	C
U70[b]	C
U73[b]	C
African 48 strains[a, b]	.
Iriomote 12 strains[c]	.

Fig. 1-15 Sequence comparison of silencer regions in natural populations

(A) SNP sites in the 351-bp silencer region. Dots indicate the same nucleotides as in the control strain. Bases in red letters are RAL-852 strain-specific SNPs. Sequences of 20 DGRP strains were obtained from Miyagi *et al*. (2015). (B-E) Dorsal abdominal images of adult flies. Scale bars indicate 100 μm. (F and G) Comparison of RAL-852-specific SNP positions shown in (A), including 56 African strains and 12 Japan-Iriomote strains. Dots indicate the same base as in the control strains, and － indicates deletion. The sequence of [a], [b] and [c] from Rebeiz *et al*. (2009), Pool and Aquadro (2007) and Takahashi and Takano-Shimizu (2011), respectively.

Part Ⅱ

Pleiotropic effect of *ebony* on epidermal cuticle associated traits in *Drosophila melanogaster*

INTRODUCTION

Genetic pleiotropy occurs when a gene affects more than one trait. The pleiotropic effects can be distinguished between cases where a genetic variant or a gene affects multiple phenotypes independently and cases where the affected phenotypes are causally related to each other (Solovief *et al*., 2013; Rheenen *et al*., 2019). Therefore, many studies have attempted to clarify whether the pleiotropic effects of the focal genes are antagonistic or synergistic (Medawar, 1952; Williams, 1957; Ostrowski *et al*., 2005; Leiby and Marx 2014). Identifying multiple functional outcomes of a genotype is important for understanding the diverse mechanisms and implications of pleiotropic genes.

In *Drosophila*, the effects of body pigmentation-associated genes are often pleiotropic. For examples, *pale* and *Ddc*, which encode enzymes involved in the melanin biosynthesis pathway, affect the synthesis of tyrosine-derived precursors of body pigments as well as melanin used for innate immune response (reviewed in Nappi, 2010; Takahashi, 2013). Similarly, *ebony* is known to have pleiotropic effects in addition to the effects on pigmentation. The expression of *ebony* in glial cells has been suggested to be necessary for the maintenance of circadian rhythms (Suh and Jackson, 2007). In the photoreceptor cells, it has been speculated to be involved in histamine metabolism (Borycz *et al*., 2002, True *et al*., 2005). Furthermore, *ebony* is predicted to be involved in the sclerotization of the tracheal cuticle (Pérez *et al*., 2010). Therefore, pigmentation-associated genes functioning together with *ebony* also act on phenotypes that are not related to the epidermal cuticle.

To date, the association between those pigment-synthesizing genes and the

cuticle properties other than pigmentation remains unclear. Several studies have shown that the levels of the biogenic amine, dopamine, affect the cuticular hydrocarbon (CHC) profiles in *D. melanogaster* (Marican *et al*., 2004; Wicker-Thomas and Hamann, 2008; Flaven-Pouchon *et al*., 2016). Since dopamine is one of the metabolites in the melanin biosynthetic pathway, the CHC profiles may also be affected by the pigmentation-associated genes.

CHCs are hydrophobic compounds produced by all insects to form a waxy outer layer on the epidermal cuticle. The CHCs on the cuticle are also used for chemical communication upon mating in some *Drosophila* species (Antony *et al*., 1985; Cobb and Jallon, 1990; Mas and Jallon, 2005; Chung *et al*., 2014) and have presumed to be functioning as a barrier against desiccation (Toolson and Kupersimbron, 1989; Hadley, 1981; Gibbs *et al*., 1997). The barrier function of the CHCs against desiccation is supported by a previous study, which showed that the desiccation tolerance of the CHC-free individuals was restored by applying the wild-type CHCs to their cuticle (Krupp *et al*., 2020). The CHCs are composed of unbranched, methyl-branched, saturated, and unsaturated hydrocarbons with 20 to 35 carbon chain (Blomquist et al., 1987; Lockey, 1988) and determine the physical properties of the cuticular barrier in general. Large proportions of long-chained, unbranched and saturated CHCs have been proposed to reduce cuticular permeability by increasing the melting temperature of the cuticular barrier (Gibbs, 2002). Positive correlations between the ratio of long-chain CHCs and desiccation resistance were detected in previous studies (Foley and Telonis-Scott, 2011; Chung and Carroll, 2015). The association between the CHC composition and desiccation resistance cannot be explained merely by the differences in the melting temperature, since a *D. melanogaster* population selected for high desiccation resistance

showed a low ratio of saturated CHCs (Ferveur *et al*., 2018).

In this study, I investigated whether there is an association between the pigmentation-associated gene, *ebony*, and the CHC profiles, using strains from the *Drosophila* Genetic Reference Panel (DGRP: Mackay *et al*., 2012). I found that the variations in the expression level of *ebony* co-vary with the CHC chain length. Considering the possibility that the expression level of *ebony* affects the desiccation tolerance of adult flies, I measured the dehydration speed in both *ebony* expression knocked-down and overexpressed individuals. The manipulations in either direction resulted in a higher dehydration speed than the control. However, the DGRP strains showed no correlation between the expression level of *ebony* and the dehydration speed. These results suggested that *ebony* affects the CHC length profile and may be involved in the cuticular water permeability. Nevertheless, it is not likely to be the main factor contributing to the variation of desiccation tolerance in natural populations.

MATERIALS AND METHODS

Fly strains

The inbred *D. melanogaster* strains, RAL-208, RAL-303, RAL-324, RAL-335, RAL- 357, RAL-358, RAL-360, RAL-365, RAL-380, RAL-399, RAL-437, RAL-517, RAL-555, RAL-705, RAL-707, RAL-714, RAL-732, RAL-774, RAL-786, RAL-799, RAL-820, RAL-852, and RAL-861 were obtained from the DGRP (Ayroles *et al*., 2009; Mackay *et al*., 2012; Huang *et al*., 2014). A ubiquitous GAL4 driver (*Act5C*-GAL4, BL 3954), a glial cell driver (*repo*-GAL4, BL 7415), and a trachea driver (*btl*-GAL4, BL 8807) were obtained from the Bloomington Drosophila Stock Center, and a partial epidermis GAL4 driver (*pnr*-GAL4, 106796) was obtained from Kyoto Stock Center (DGRC). The UAS strains, UAS-*e*-*IR* (*IR*: inverted repeat sequence) on the second (3331R-3) and the third (3331R-1) chromosomes were from NIG-Fly. The w^{1118} control strains with the identical genetic background as the UAS-*IR* strains were from Dr. Ryu Ueda (National Institute of Genetics). The strains w^{1118}; P[*w* UAS-*e*-cDNA], In(3R) e^{AFA}/*TM6*, *Sb* e^{1} (UAS-*e*-cDNA) and w^{1118}; P[*w* UAS-*e*-cDNA Ser^{611}-Ala], In(3R) e^{AFA}/*TM6*, *Sb* e^{1} (UAS-*e*-cDNA Ser611-Ala) were obtained from Dr. Bernhard T. Hovemann (Richard *et al*., 2003). The UAS-*e*-cDNA Ser611-Ala has a nonfunctional *ebony*-cDNA fused to UAS. All flies were grown at 25℃ with a 12 h light-dark cycle on the standard corn-meal fly medium.

CHC profiles

The CHC profiles of the DGRP females were obtained from Dembeck *et al*. (2015). They quantified the CHCs from each strain by gas chromatography/mass

spectrometry (GC/MS). The names and elemental formulas of the CHCs used in this study are summarized in Table 2-1. However, CHCs not detected in all strains were eliminated from the analyses. The relative abundance of each CHC signal was calculated by normalizing each CHC proportion to the hexacosane signal. To eliminate the multicolinearity among sample peak amounts, a log-contrast transformation was applied to the resulting proportional values, using nC27 as the denominator (Blows and Allen, 1998; Yew *et al*., 2011):

$$\text{log-contrast CHC}_n = \log_{10}\left(\frac{\text{proportion (CHC}_n\text{)}}{\text{proportion (C27 alkane)}}\right)$$

To determine the relative difference in CHC length between groups of DGRP strain, the difference in relative intensity of individual CHC intensities of each group (a and b) was calculated:

$$\text{Difference} = \text{log-contrast CHC}_a - \text{log-contrast CHC}_b$$

These values were then plotted against CHC chain length. In the case of a GC/MS peak composed of more than two combined CHC components that differed in CHC chain length, the non-branched CHC chain length was used.

The CHCs were decomposed into four structural categories: 10 alkanes, 21 monoenes, 15 dienes, and 12 methyl-branched (Table 2-1). In the case of a GC/MS peak containing multiple categories, the same log-contrast value was used in duplicate for the analysis of each category. Furthermore, if the chain length differed between categories, the length was selected according to the category of each CHC component (for example, for the combined peak of C26 monoene and C25 methyl-blanched, the value of chain length 26 for the monoene analysis was used for chain length 25 for the methyl-blanched analysis).

RNA extraction

Female virgin flies were collected within 1 h after eclosion, and the heads were removed in RNAlater (Ambion) to separate the effect from transcripts in non-epidermal head tissues. The remaining head-less bodies were stored in RNAlater at −80°C until use. Three body samples from each strain were placed in a 2 mL microtube with 400 μL TRIzol Reagent (Thermo Fisher Scientific, Tokyo, Japan) and an equivalent column of 1.2 mm zirconia silica beads (Bio Medical Science). After shaking, the tube at 3,200 rpm for 2 min using a Beads Crusher μT-12 (TAITEC, Koshigaya, Japan), 160 μL chloroform was added and mixed thoroughly. Total RNA in the aqueous phase was subsequently purified using silica-gel (Wakocil 5SIL, Wako, Osaka, Japan) based on the method in Boom *et al*. (1990) and was quantified using a NanoDrop 2000c spectrophotometer (Thermo Fisher Scientific).

Grouping DGRP strains based on expression level of *ebony*

The expression level of *ebony* was quantified by RT-qPCR. The first strand cDNA was synthesized from 1 μg total RNA by using a PrimeScript RT Reagent Kit with gDNA Eraser (Takara Bio, Kusatsu, Japan). The qPCR was performed in a 25 μL reaction volume with SYBR Premix Ex Taq II Tli RNaseH Plus (Takara Bio) on a Thermal Cycler Dice TP800 (Takara Bio). The primer set used for RT-qPCR were *ebony*: 5'-CTTAGTGTGAAACGGCCACAG-3' and 5'-GCAGCGAACCCATCTTGAA-3'; *Act57B*: 5'-CGTGTCATCCTTGGTTCGAGA-3' and 5'-ACCG CGAGCGATTAACAAGTG-3'; *Rp49*: 5'-TCGGATCGATAT GCTAAGCTG-3' and 5'-TCGATCCGTAACCGATGTTG-3'. The primer set *Act57B*

and *Rp49* were used as the internal controls. The PCRs were replicated twice for each cDNA sample, and three biological replicates were obtained for each strain.

The 23 DGRP strains with various expression levels of *ebony* were grouped into three categories, Low, Intermediate, and High expression strains, according to the results of RT-qPCR. Since the normalized quantities are continuous values, the grouping of strains was based on the standard deviations (SD). The strains were categorized into the following groups: Low (expression < mean – 0.5 SD, N = 9), Intermediate (mean – 0.5 SD ≤ expression ≤ mean + 0.5 SD, N = 6), and High (mean + 0.5 SD < expression, N = 8).

Dehydration speed

Ten virgin females were used for the desiccation resistance measurements. The flies were kept at 25℃ and 60% relative humidity (Rh) for 5−7 days after eclosion. A desiccation chamber consisted of a dry glass vial (13 mL) that contained 5 g silica gel at the bottom, and a piece of Parafilm (Bemis Company) was used to seal the top of each vial. Silica gel was covered with a piece of mesh in order to prevent the flies from touching it directly. The Rh inside the desiccation chamber was kept at ~2%.

Ten flies were used for one replicate. Flies were anesthetized by CO_2, and 10 individuals were weighed at a time (Weight A (mg)) before placing them into a desiccation chamber. After 5 h, the total weight of the flies (Weight B (mg)) was measured by the same procedure. If one or more flies died during the 5-h experiment, such cases were excluded from the analysis. Each sample was returned into the desiccation chamber and dried for more than 24 h to measure the weight of the completely dehydrated flies (Weight C (mg)) to control for the body size. The weight

was recorded at the 0.01 mg precision by using an electronic balance (AG285, METTLER TOLEDO). The dehydration speed was calculated as follows:

$$\text{Dehydration speed} = \frac{(\text{Weight A} - \text{Weight B})}{5}\ (\mu g/h)$$

and the residuals from the linear regression with $(\text{Weight C})^{2/3}$ were added to the mean speed to control for the differences in body surface area.

Fly imaging

At 5–7 days after eclosion, females were placed in 10% glycerol in ethanol at 4ºC for 1 h. Next, the flies were rotated in 10% glycerol in phosphate-buffered saline (PBS) at room temperature for 1 h after removing the head, legs, and wings. The images of the dorsal body of flies soaked in 10% glycerol in PBS were captured by using a digital camera (DP73, Olympus) connected to a stereoscopic microscope (SZX16, Olympus). The same parameters (exposure time, zoom width, and illumination) and reference grayscale (brightness = 128; ColorChecker, X-rite) were applied to all images. White balance was corrected using the white scale (Brightness = 255; ColorChecker, X-rite) with cellSens Standard 1.6 software (Olympus).

Statistics

All statistical analyses were performed by using R version 4.0.3 (R Core Team 2020). Spearman's rank correlation coefficient ρ was used to test for the significance of the association between the difference in log-contrast of relative abundance from the population average and the chain-length of each CHC component. The pairwise Student's t-test was used to test the differences in dehydration speed between the GAL4-UAS treated individuals and the control. The Kruskal-Wallis rank sum test was

used to test the differences in dehydration speed between each *ebony* expression group of the 23 DGRP strains.

RESULTS

The expression level of *ebony* covaries with CHC length profiles in the DGRP

The association between the expression level of *ebony* and the CHC profile was examined by using virgin females from 23 strains. The CHC data was obtained from Dembeck *et al*. (2015), where GC/MS analyses of the CHCs were performed for the most of the DGRP strains. The 23 strains consist of the set of 20 strains used in Miyagi *et al*. (2015), and additional three dark strains to avoid strain specific effects from a limited number of dark strains. The expression level of *ebony* within 1 h after eclosion, the stage of active production of pigments, was quantified by RT-qPCR. The 23 DGRP strains were categorized into three groups of Low (9 strains), Intermediate (6 strains), and High (8 strains) based on *ebony* expression levels obtained by the RT-qPCR (Fig 2-1). Next, the difference in the log-contrast of individual CHC abundance for the 23 strains from the average of each expression group was calculated and plotted against the chain length.

As the results, the Low-expression group showed lower levels of short-chain CHCs and higher levels of long-chain CHCs relative to the average value of the 23 strains (Fig. 2-2A, Spearman's $\rho = 0.67$, $P < 1.0 \times 10^{-6}$); the Intermediate-expression group showed no relationship with CHC chain length (Fig. 2-2B, Spearman's $\rho = -0.10$, $P = 0.50$); and the High-expression group showed the opposite pattern from the Low-expression group (Fig. 2-2C, Spearman's $\rho = -0.61$, $P < 1.0 \times 10^{-5}$). These results indicated that the variation in the expression level of *ebony* covaried with the CHC length profiles. Therefore, the variation in the *ebony* gene expression level has pleiotropic effects on the proportions of CHCs with different carbon chain lengths with

those on the pigmentation in a natural population of *D. melanogaster*.

The effect of *ebony* on CHC chain length profiles in different CHC categories

I further investigated whether the observed co-variation of the expression level of *ebony* and the CHC length profiles was dependent on the CHC categories. The CHCs were categorized into four types (Table 2-1), and the log-contrast differences from the 23-strain averages were plotted against the carbon chain length of each CHC component (Fig. 2-3). In alkanes, no correlation was found in the Low-expression group (Fig. 2-3A, Spearman's $\rho = 0.64$, $P = 0.054$), although a significant negative correlation was found in the High expression group (Fig. 2-3C, Spearman's $\rho = -0.71$, $P < 0.05$). Monoene and diene showed a significant positive correlation in the Low expression group (monoene: Fig. 2-3D, Spearman's $\rho = 0.56$, $P < 0.01$, diene: Fig. 2-3G, Spearman's $\rho = 0.75$, $P < 0.01$) and a significant negative correlation in the High expression group (monoene: Fig. 2-3F, Spearman's $\rho = -0.69$, $P < 0.001$, diene: Fig. 2-3I, Spearman's $\rho = -0.74$, $P < 0.01$). In Methyl-branched, a significant positive correlation was found in the Low expression group (Fig. 2-3J, Spearman's $\rho = 0.77$, $P < 0.01$), and the profile showed a bias toward short chains in the High expression group, but not significantly (Fig. 2-3L, Spearman's $\rho = -0.44$, $P = 0.155$). Also, none of the CHC categories showed any correlation in the Intermediate expression group (Fig. 2-3 B, E, H and K). Similar tendency was obtained from all CHC categories, but the effect of *ebony* on CHC length profiles seems to vary depending on the CHC category.

Manipulation of *ebony* expression levels in epidermis influences dehydration speed

Massey, Akiyama *et al*., (2019) showed that the knockout of *ebony* by CRISPR-Cas9 changes the CHC profiles in the same direction as the Low-expression group of the DGRP. Therefore, to verify whether the expression level of *ebony* also affects desiccation tolerance, I genetically manipulated the expression level using the GAL4-UAS system (Brand and Perrimon, 1993).

First, a ubiquitous GAL4 driver, *Act5C*-GAL4, was used to induce RNAi knockdown of *ebony* in the whole body. Two UAS-*e-IR* strains, Ⅲ and Ⅱ, with different transgenic insertion sites were crossed to *Act5C*-GAL4 strain. The *ebony* expression levels of knocked-down individuals were reduced by 85-99% compared to the control, and were lower than any DGRP strain (Fig. 2-1 and 2-4). The dehydration speeds of the whole-body *ebony* knocked-down individuals were significantly higher than the control (Fig. 2-5A, *Act5C*-GAL4 / UAS-*e-IR* (Ⅲ): $P < 0.01$, *Act5C*-GAL4 / UAS-*e-IR* (Ⅱ): $P < 0.05$, respectively).

Second, in order to identify the specific tissues in which *ebony* knockdown affects dehydration speed, tissue-specific GAL4 drivers, *pnr*-GAL4 (partial epidermis driver), *btl*-GAL4 (trachea driver), and *repo*-GAL4 (glial-cells driver) were used. In *pnr*-GAL4 / UAS-*e-IR* (Ⅱ or Ⅲ) flies, in which *ebony* was knocked down at about 1/3 of the dorsal epidermis area, the cuticle was darkly pigmented around the dorsal midline (Fig. 2-5D). The dehydration speeds of partial-epidermis *ebony* knocked-down individuals were significantly higher than the control (Fig. 2-5C, *pnr*-GAL4 / UAS-*e-IR* (Ⅲ): $P < 0.001$, *pnr*-GAL4 / UAS-*e-IR* (Ⅱ): $P < 0.01$, respectively), whereas no significant difference was found in the cases of trachea and glial-cell knockdown (Fig. 2-5E, G).

Finally, I performed an upregulation of *ebony* by using UAS-*e*-cDNA. The UAS-*e*-cDNA Ser611-Ala strain is the control strain for UAS-*e*-cDNA (see Materials and Methods). The *ebony* expression level of *Act5C*-GAL4 / UAS-*e*-cDNA Ser611-Ala individuals was not measured because the cDNAs with non-synonymous substitutions and normal cDNAs could not be distinguished by qPCR, but *ebony* expression level of *Act5C*-GAL4 / UAS-*e*-cDNA individuals was higher than any DGRP strain (Fig. 2-1 and 2-4). Similar desiccation experiments showed that the overexpression of *ebony* in the whole body and part of the epidermis showed significant increases in the dehydration speed (Fig. 2-6A and C, *Act5C*-GAL4 / UAS-*e*-cDNA: $P < 0.05$, *pnr*-GAL4 / UAS-*e*-cDNA: $P < 0.001$, respectively), while the overexpression of *ebony* in the trachea and glial-cells did not induce significant differences in the dehydration speed (Fig. 2-7E and G). The expression sites of *ebony* affecting the dehydration speed were consistent between the knockdown and overexpression experiments. However, both expression manipulations at the sites including epidermis increased the dehydration speed. These results suggested that the expression level of *ebony* in the epidermis may affect the degree of water retention. Nevertheless, the relationship may not be linear.

Dehydration speed is not associated with *ebony* in the DGRP

Based on the above results, I examined whether any association was present between the dehydration speed and the expression level of *ebony* among the DGRP strains. First, the dehydration speeds of the 23 DGRP strains were measured and compared among the different *ebony* expression groups. The results showed no significant difference among the expression groups (Fig. 2-7; $df = 2$, $\chi 2 = 0.71$, $P =$

0.7019, Kruskal-Wallis rank sum test). This result suggested that the expression level of *ebony* does not contribute to the variation in cuticular permeability in the DGRP.

DISCUSSION

CHC-related functions of *ebony* via dopamine

The Ebony protein is required for catalyzing the reaction from dopamine to NBAD in the tyrosine-dopa-dopamine-NBAD metabolic pathway involved in pigment biosynthesis (Wright, 1987, Walter *et al*., 1996). This study shows that *ebony* has a previously unknown role in CHC synthesis and accumulation. The influence of the pigment-related genes on the CHC composition has been suggested by previous studies showing that the dopamine levels affect CHC composition. For example, females homozygous for the loss-of-function Dopa-decarboxylase (*Ddc*) temperature-sensitive alleles showed changes in CHC composition, and the changes could be recovered by feeding dopamine (Marican *et al*., 2004; Wicker-Thomas and Hamann, 2008). Additionally, inhibiting dopamine synthesis by feeding wild-type females with the tyrosine hydroxylase inhibitor L-AMPT altered CHC composition in a similar direction as the loss-of-function alleles (Marican *et al*., 2004; Wicker-Thomas and Hamann, 2008). Also, in Massey, Akiyama, *et al*. (2019), the CHC profiles were strongly biased toward long-chain by knocking out *ebony* by CRISPR-Cas9, and the bias was reversed when feeding L-AMPT to the knockout mutant. Furthermore, *tan*, a gene that metabolizes NBAD to dopamine, was also suggested to affect the CHC profiles, and the direction of the effect was opposite to that of *ebony* (Massey, Akiyama *et al*., 2019). Based on these studies, the function of *ebony* regarding the CHC profile might be regulated by the dopamine level.

The pleiotropic effects of *ebony* on pigmentation and CHCs

ebony is a main causative gene for pigmentation variation in *D. melanogaster* (Takahashi *et al*., 2007; Pool and Aquadro, 2007; Rebeiz *et al*., 2009; Telonis-Scott *et al*., 2011), and my results showed that the expression level of *ebony* is associated with the CHC profile. Since both pigmentation and CHC profile are associated with cuticular traits, the question is whether the effects of *ebony* on pigmentation and the CHC profiles are related or independent. It has been known that the *ebony* expression in the epidermis affects pigmentation, whereas *ebony* expression in glial-cells is necessary for the normal circadian locomotor rhythms in *D. melanogaster* (Suh and Jackson, 2007). Therefore, pigmentation and locomotor rhythms are likely to be an example of independent pleiotropic effects. Also, although *ebony* is involved in the dopamine metabolism in the melanin biosynthetic pathway (Wright, 1987; Walter *et al*., 1996), it acts in a metabolic pathway that terminates the action of histamine in photoreceptor cells and is considered to be involved in histamine metabolism (Borycz *et al*., 2002; True *et al*., 2005). The pleiotropic effects of *ebony* on the epidermis and photoreceptor cells are possibly independent, since the associated biochemical processes are different.

In the case of the pleiotropic effect of *ebony* on CHC, we examined the CHC profiles by UV laser desorption/ionization mass spectrometry (UV-LDI MS) from each of the differently colored cuticle of *ebony* knocked-down individuals by *pnr*-GAL4. However, we did not detect differences in the short versus long CHCs between lightly and darkly pigmented cuticles (Massey, Akiyama *et al*., 2019). In addition, as mentioned above, the L-AMPT feeding individuals exhibited differences in CHC composition but not in pigmentation (Massey, Akiyama *et al*., 2019). Therefore, the function of *ebony* on CHC composition may not be related to its function on pigmentation. To clearly distinguish whether the CHC-related effect of is independent

of pigmentation, identifying cells where the expression of *ebony* affects CHC and elucidating the biochemical processes underlying the association are required.

Pleiotropic effect of *ebony* on desiccation tolerance

CHCs are thought to provide a barrier to prevent cuticular evaporation by covering the insect surface, and their composition defines the physical properties of the cuticular barrier (Gibbs, 2002). The lipid melting models suggest a higher proportion of long-chained, unbranched, and saturated CHCs augment the melting temperature of the barrier, resulting in reduced permeability (Gibbs, 2002). In addition, the survival time under desiccation was positively correlated with the ratio of long-chain CHCs in *D. melanogaster* females from a California population (Foley and Telonis-Scott, 2011). Thus, the CHC profile has been discussed in relation to desiccation tolerance. However, no difference in dehydration speed was observed among the three *ebony* expression level groups with different CHC length profiles in the DGRP strains used in this study (Fig. 2-7). There are various routes of water loss in insects besides cuticular evaporation. For example, respiration and excretion, and the desiccation tolerance determining factors include body size, behavior, and energy metabolism (reviewed in Wang *et al*., 2021). Several genes involved in desiccation tolerance through cuticle formation have also been identified, but they are not necessarily associated with CHC (Dembeck *et al*., 2015). Thus, different populations may have different traits to depend on the desiccation tolerance, since there are many different solutions to determine desiccation tolerance.

In previous studies, *ebony* expression and desiccation tolerance have not been directly compared. Also, the presence of the association between desiccation tolerance

and body color has been contradictory. The melanism-desiccation hypothesis, which claims that melanization reduces cuticular water permeability, was proposed early on (Kalmus, 1941). Although many studies support this hypothesis, many do not support it (reviewed in Wang *et al*., 2021). In this study, the association was not detected between the expression level of *ebony* involved in the melanization, and dehydration speed in the wild-derived inbred strains. Nevertheless, in the whole-body or tissue-specific expression manipulation by the GAL4-UAS system, significant changes in dehydration speed were detected when the *ebony* expression was manipulated at the epidermis-containing regions (Fig. 2-5A, C, 2-6A and C). Strictly speeking, *pnr-GAL4*, the driver used to drive expression in a partial epidermis region, is known to drive expression not only in the dorsal epidermis but also in the adult heart tube and the wing disc (Calleja *et al*., 1996, 2000; Qian and Bodmer, 2009). The possibility that *ebony* has unknown functions in these tissues or organs cannot be completely excluded. The more specific expression manipulation of *ebony* in the epidermal cells would help clarify whether there is an association between water retention and pigmentation.

Although there was no association between the *ebony* expression and dehydration speed in the 23 DGRP strains used in this study, the possibility remains that extreme difference in expression level of *ebony* were not included in these strains. Whether the quadratic model can be applied to correlations between the expression level of *ebony* and the dehydration speed in natural populations showing wider variation in *ebony* expression than in this study is an intriguing question. Such prospective investigations are expected to advance our understanding of the pleiotropic effects of this gene.

LITERATURE CITED

Antony, C., Davis, T. L., Carlson, D. A., Pechine, J. M., & Jallon, J. M. (1985). Compared behavioral responses of male *Drosophila melanogaster* (Canton S) to natural and synthetic aphrodisiacs. *Journal of Chemical Ecology*, *11*(12), 1617-1629.

Blomquist, G. J., Nelson, D. R., & De Renobales, M. (1987). Chemistry, biochemistry, and physiology of insect cuticular lipids. *Archives of Insect Biochemistry and Physiology*, *6*(4), 227-265.

Blows, M. W., & Allan, R. A. (1998). Levels of mate recognition within and between two *Drosophila* species and their hybrids. *The American Naturalist*, *152*(6), 826-837.

Boom, R. C. J. A., Sol, C. J., Salimans, M. M., Jansen, C. L., Wertheim-van Dillen, P. M., & Van der Noordaa, J. P. M. E. (1990). Rapid and simple method for purification of nucleic acids. *Journal of Clinical Microbiology*, *28*(3), 495-503.

Borycz, J., Borycz, J. A., Loubani, M., & Meinertzhagen, I. A. (2002). *tan* and *ebony* genes regulate a novel pathway for transmitter metabolism at fly photoreceptor terminals. *Journal of Neuroscience*, *22*(24), 10549-10557.

Brand, A. H., & Perrimon, N. (1993). Targeted gene expression as a means of altering cell fates and generating dominant phenotypes. *Development*, *118*(2), 401-415.

Calleja, M., Moreno, E., Pelaz, S., & Morata, G. (1996). Visualization of gene expression in living adult *Drosophila*. *Science*, *274*(5285), 252-255.

Calleja, M., Herranz, H., Estella, C., Casal, J., Lawrence, P., Simpson, P., & Morata, G. (2000). Generation of medial and lateral dorsal body domains by the *pannier* gene of *Drosophila*. *Development*, *127*(18), 3971-3980.

Chung, H., Loehlin, D. W., Dufour, H. D., Vaccarro, K., Millar, J. G., & Carroll, S. B. (2014). A single gene affects both ecological divergence and mate choice in *Drosophila*. *Science*, *343*(6175), 1148-1151.

Chung, H., & Carroll, S. B. (2015). Wax, sex and the origin of species: dual roles of insect cuticular hydrocarbons in adaptation and mating. *BioEssays*, *37*(7), 822-830.

Cobb, M., & Jallon, J. M. (1990). Pheromones, mate recognition and courtship stimulation in the *Drosophila melanogaster* species sub-group. *Animal Behaviour*, *39*(6), 1058-1067.

Dembeck, L. M., Böröczky, K., Huang, W., Schal, C., Anholt, R. R., & Mackay, T. F. (2015). Genetic architecture of natural variation in cuticular hydrocarbon composition in *Drosophila melanogaster*. *Elife*, *4*, e09861.

Ferveur, J. F., Cortot, J., Rihani, K., Cobb, M., & Everaerts, C. (2018). Desiccation resistance: effect of cuticular hydrocarbons and water content in *Drosophila melanogaster* adults. *PeerJ*, *6*, e4318.

Flaven-Pouchon, J., Farine, J. P., Ewer, J., & Ferveur, J. F. (2016). Regulation of cuticular hydrocarbon profile maturation by *Drosophila* tanning hormone, bursicon, and its interaction with desaturase activity. *Insect Biochemistry and Molecular Biology*, *79*, 87-96.

Foley, B. R., & Telonis-Scott, M. (2011). Quantitative genetic analysis suggests causal association between cuticular hydrocarbon composition and desiccation survival in *Drosophila melanogaster*. *Heredity*, *106*(1), 68-77.

Gibbs, A. G., Chippindale, A. K., & Rose, M. R. (1997). Physiological mechanisms of evolved desiccation resistance in *Drosophila melanogaster*. *The Journal of Experimental Biology*, *200*(12), 1821-1832.

Gibbs, A. G. (2002). Lipid melting and cuticular permeability: new insights into an old problem. *Journal of Insect Physiology*, *48*(4), 391-400.

Hadley, N. F. (1981). Cuticular lipids of terrestrial plants and arthropods: a comparison of their structure, composition, and waterproofing function. *Biological Reviews*, *56*(1), 23-47.

Kalmus, H. (1941). The resistance to desiccation of *Drosophila* mutants affecting body colour. *Proceedings of the Royal Society of London. Series B-Biological Sciences*, *130*(859), 185-201.

Krupp, J. J., Nayal, K., Wong, A., Millar, J. G., & Levine, J. D. (2020). Desiccation resistance is

an adaptive life-history trait dependent upon cuticular hydrocarbons, and influenced by mating status and temperature in *D. melanogaster*. *Journal of Insect Physiology*, *121*, 103990.

Leiby, N., & Marx, C. J. (2014). Metabolic erosion primarily through mutation accumulation, and not tradeoffs, drives limited evolution of substrate specificity in *Escherichia coli*. *PLoS Biology*, 12(2), e1001789.

Lockey, K. H. (1988). Lipids of the insect cuticle: origin, composition and function. *Comparative Biochemistry and Physiology Part B: Comparative Biochemistry*, *89*(4), 595-645.

Mackay, T. F., Richards, S., Stone, E. A., Barbadilla, A., Ayroles, J. F., Zhu, D., *et al*. (2012). The *Drosophila melanogaster* genetic reference panel. *Nature*, *482*(7384), 173-178.

Marican, C., Duportets, L., Birman, S., & Jallon, J. M. (2004). Female-specific regulation of cuticular hydrocarbon biosynthesis by dopamine in *Drosophila melanogaster*. *Insect Biochemistry and Molecular Biology*, *34*(8), 823-830.

Mas, F., & Jallon, J. M. (2005). Sexual isolation and cuticular hydrocarbon differences between *Drosophila santomea* and *Drosophila yakuba*. *Journal of Chemical Ecology*, *31*(11), 2747-2752.

Massey, J. H., Akiyama, N., Bien, T., Dreisewerd, K., Wittkopp, P. J., Yew, J. Y., & Takahashi, A. (2019). Pleiotropic effects of *ebony* and *tan* on pigmentation and cuticular hydrocarbon

composition in *Drosophila melanogaster*. *Frontiers in Physiology*, *10*, 518.

Medawar, P. B. (1952). A biological analysis of individuality. *American Scientist*, *40*(4), 632-639.

Miyagi, R., Akiyama, N., Osada, N., & Takahashi, A. (2015). Complex patterns of *cis*‐regulatory polymorphisms in *ebony* underlie standing pigmentation variation in *Drosophila melanogaster*. *Molecular Ecology*, *24*(23), 5829-5841.

Nappi, A. J. (2010). Cellular immunity and pathogen strategies in combative interactions involving *Drosophila* hosts and their endoparasitic wasps. *Invertebrate Survival Journal*, *7*(2), 198-210.

Ostrowski, E. A., Rozen, D. E., & Lenski, R. E. (2005). Pleiotropic effects of beneficial mutations in *Escherichia coli*. *Evolution*, *59*(11), 2343-2352.

Pérez, M. M., Schachter, J., Berni, J., & Quesada-Allué, L. A. (2010). The enzyme NBAD-synthase plays diverse roles during the life cycle of *Drosophila melanogaster*. *Journal of Insect Physiology*, *56*(1), 8-13.

Pool, J. E., & Aquadro, C. F. (2007). The genetic basis of adaptive pigmentation variation in *Drosophila melanogaster*. *Molecular Ecology*, *16*(14), 2844-2851.

Qian, L., & Bodmer, R. (2009). Partial loss of GATA factor Pannier impairs adult heart function

in *Drosophila*. *Human Molecular Genetics*, *18*(17), 3153-3163.

R Core Team. 2020. R: A language and environment for statistical computing. Vienna, Austria: R Foundation for Statistical Computing. https://www.R-project.org/.

Rebeiz, M., Pool, J. E., Kassner, V. A., Aquadro, C. F., & Carroll, S. B. (2009). Stepwise modification of a modular enhancer underlies adaptation in a *Drosophila* population. *Science*, *326*(5960), 1663-1667.

Rheenen, V. W., Peyrot, W. J., Schork, A. J., Lee, S. H., & Wray, N. R. (2019). Genetic correlations of polygenic disease traits: from theory to practice. *Nature Reviews Genetics*, *20*(10), 567-581.

Richardt, A., Kemme, T., Wagner, S., Schwarzer, D., Marahiel, M. A., & Hovemann, B. T. (2003). Ebony, a novel nonribosomal peptide synthetase for β-alanine conjugation with biogenic amines in *Drosophila*. *Journal of Biological Chemistry*, *278*(42), 41160-41166.

Solovieff, N., Cotsapas, C., Lee, P. H., Purcell, S. M., & Smoller, J. W. (2013). Pleiotropy in complex traits: challenges and strategies. *Nature Reviews Genetics*, *14*(7), 483-495.

Suh, J., & Jackson, F. R. (2007). *Drosophila ebony* activity is required in glia for the circadian regulation of locomotor activity. *Neuron*, *55*(3), 435-447.

Takahashi, A., Takahashi, K., Ueda, R., & Takano-Shimizu, T. (2007). Natural variation of

ebony gene controlling thoracic pigmentation in *Drosophila melanogaster*. *Genetics*, *177*(2), 1233-1237.

Takahashi, A. (2013). Pigmentation and behavior: potential association through pleiotropic genes in *Drosophila*. *Genes & Genetic Systems*, *88*(3), 165-174.

Telonis-Scott, M., Hoffmann, A. A., & Sgro, C. M. (2011). The molecular genetics of clinal variation: a case study of *ebony* and thoracic trident pigmentation in *Drosophila melanogaster* from eastern Australia. *Molecular Ecology*, *20*(10), 2100-2110.

Toolson, E. C., & Kuper-Simbron, R. (1989). Laboratory evolution of epicuticular hydrocarbon composition and cuticular permeability in *Drosophila pseudoobscura*: effects on sexual dimorphism and thermal-acclimation ability. *Evolution*, *43*(2), 468-473.

True, J. R., Yeh, S. D., Hovemann, B. T., Kemme, T., Meinertzhagen, I. A., Edwards, T. N., *et al*. (2005). *Drosophila tan* encodes a novel hydrolase required in pigmentation and vision. *PLoS Genetics*, *1*(5), e63.

Walter, M. F., Zeineh, L. L., Black, B. C., McIvor, W. E., Wright, T. R., & Biessmann, H. (1996). Catecholamine metabolism and in vitro induction of premature cuticle melanization in wild type and pigmentation mutants of *Drosophila melanogaster*. *Archives of Insect Biochemistry and Physiology: Published in Collaboration with the Entomological Society of America*, *31*(2), 219-233.

Wang, Y., Ferveur, J. F., & Moussian, B. (2021). Eco-genetics of desiccation resistance in *Drosophila*. *Biological Reviews*, *96*(4), 1421-1440.

Wicker-Thomas, C., & Hamann, M. (2008). Interaction of dopamine, female pheromones, locomotion and sex behavior in *Drosophila melanogaster*. *Journal of Insect Physiology*, *54*(10-11), 1423-1431.

Williams, G. C. (1957) Pleiotropy, Natural Selection, and the Evolution of Senescence. *Evolution*, *11*, 398-411.

Wright, T. R. (1987). The genetics of biogenic amine metabolism, sclerotization, and melanization in *Drosophila melanogaster*. *Advances in Genetics*, *24*, 127-222.

Yew, J. Y., Dreisewerd, K., De Oliveira, C. C., & Etges, W. J. (2011). Male-specific transfer and fine scale spatial differences of newly identified cuticular hydrocarbons and triacylglycerides in a *Drosophila* species pair. *PLoS One*, *6*(2), e16898.

Table 2-1 The list of CHCs in *D. melanogaster* female from Dembeck *et al*. (2015)

Structural category	Elemental formula	Common notation	Abbreviations according to Dembeck *et al*. (2015)
alkane	C21 H44	nC21	n-C21
monoene	C22 H46		x-C22:1 *
monoene	C22 H46		x-C22:1 *
alkane	C22 H44	nC22	n-C22
diene	C23 H44	7.11TD	7,11-C23:2
methyl branched	C23 H46	22Br	2-Me-C22
			NI *
monoene	C23 H46	9-T	9-C23:1
monoene	C23 H46	7-T	7-C23:1
monoene	C23 H46		6-C23:1
monoene	C23 H46	5-T	5-C23:1
monoene	C23 H46		x-C23:1
alkane	C23 H48	nC23	n-C23
methyl branched	C24 H50		11- & 9-Me-C23 *
diene	C24 H46		7,11-C24:2 *
diene	C24 H46		x,y-C24:2
methyl branched	C24 H50	23Br	3-Me-C23
monoene	C24 H48		7-C24:1 *
monoene	C24 H48		9-C24:1
			NI *
monoene	C24 H48		6-C24:1
alkane	C24 H50	nC24	n-C24
diene	C25 H48		9,13-C25:2 *
diene	C25 H48	7.11PD	7,11-C25:2
methyl branched	C25 H52	24Br	2-Me-C24
diene	C25 H48		6,10-C25:2
diene	C25 H48		5,9-C25:2
monoene	C25 H50	9-P	9-C25:1
monoene	C25 H50		8-C25:1 *
monoene	C25 H50	7-P	7-C25:1
monoene	C25 H50		6-C25:1
monoene	C25 H50		5-C25:1
alkane	C25 H52	nC25	n-C25

Table 2-1 continued from the previous page

			NI *
			NI *
methyl branched	C26 H54		13-Me-C25
methyl branched	C26 H54		11-Me-C25
methyl branched	C26 H54		5-Me-C25
diene	C26 H50		8,12-C26:2 *
diene	C26 H50		7,11-C26:2 *
methyl branched	C26 H54		2-Me-C25 *
diene	C26 H50		6,10-C26:2
methyl branched	C26 H54		3-Me-C25
monoene	C26 H52		9-C26:1
monoene	C26 H52		7-C26:1
monoene	C26 H52		6-C26:1
alkane	C26 H54	internal standard	n-C26
diene	C27 H52		9,13-C27:2
diene	C27 H52	7.11HD	7,11-C27:2
methyl branched	C27 H54	26Br	
diene	C27 H52		5,9-C27:2
monoene	C27 H54	9-H	9-C27:1
monoene	C27 H54	7-H	7-C27:1
monoene	C27 H54		5-C27:1
alkane	C27 H56	nC27	n-C27
diene	C28 H54		8,12-C28:2
diene	C28 H54		7,11-C28:2
methyl branched	C28 H56		2-Me-C27
methyl branched	C28 H56		3-Me-C27
diene	C28 H54		6,10-C28:2
			NI *
monoene	C28 H56		9-C28:1
alkane	C28 H58		n-C28
diene	C29 H56		9,13-C29:2
methyl branched	C29 H58	28Br	2-Me-C28
diene	C29 H56	7.11ND	7,11-C29:2
monoene	C29 H58		9-C29:1
diene	C29 H56		5,9-C29:2
monoene	C29 H58		7-C29:1

Table 2-1 continued from the previous page

alkane	C29 H60	nC29	n-C29
methyl branched	C30 H60		2-Me-C29
diene	C30 H58		8,12-C30:2
methyl branched	C31 H62		2-Me-C30
diene	C31 H60		7,11-C31:2 *
alkane	C31 H64		n-C31

Br: methyl branched

T: tricosene

P: pentacosene

H: heptacosene

TD: tricosadiene

PD: pentacosadiene

HD: heptacosadiene

ND: nonacosadiene

*: Excluded from the analysis in this study.

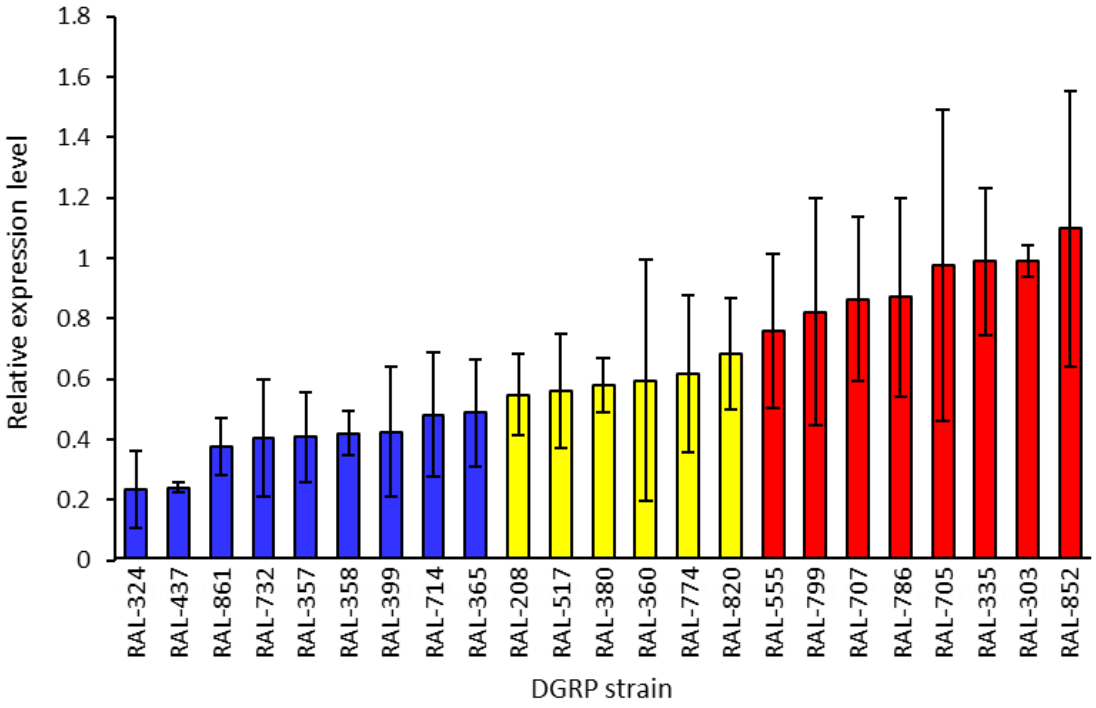

Fig. 2-1 Grouping DGRP strains based on expression level of *ebony*

The expression level of *ebony* was quantified by RT-qPCR with three biological replications. Graph colors indicate expression level categories of the 23 DGRP strains: Low (expression < mean – 0.5 SD, blue), Intermediate (mean – 0.5 SD ≤ expression ≤ mean + 0.5 SD, yellow), and High (mean + 0.5 SD < expression, red). Error bar denotes standard error.

(A)

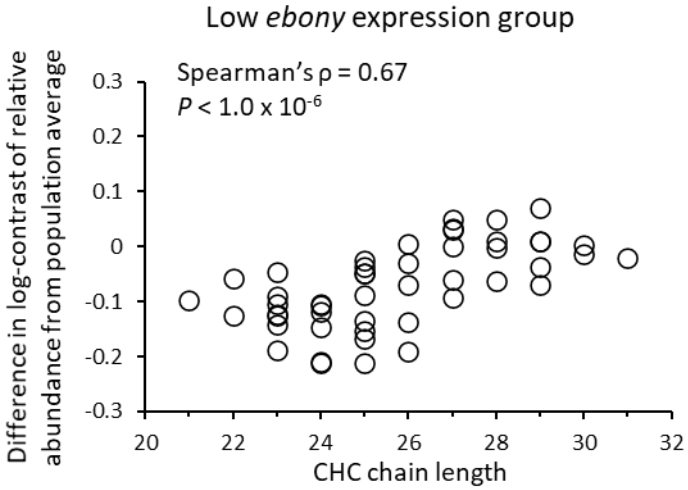
Low *ebony* expression group
Spearman's ρ = 0.67
P < 1.0 x 10-6
Difference in log-contrast of relative abundance from population average
0.3
0.2
0.1
0
-0.1
-0.2
-0.3
20
22
24
26
28
30
32
CHC chain length

(B)

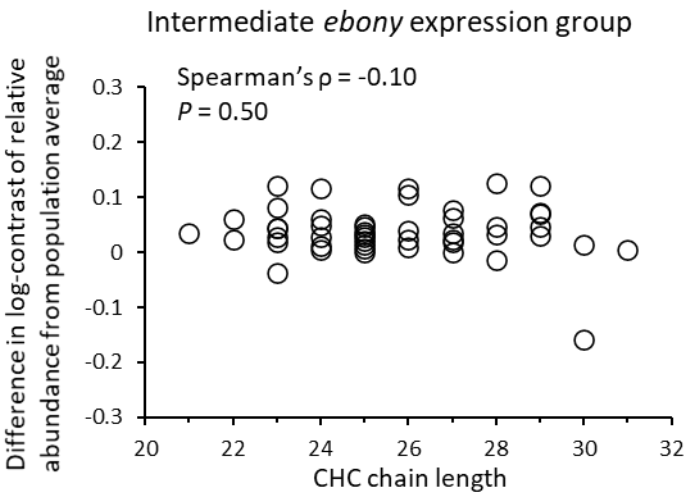
Intermediate *ebony* expression group
Spearman's ρ = -0.10
P = 0.50
Difference in log-contrast of relative abundance from population average
0.3
0.2
0.1
0
-0.1
-0.2
-0.3
20
22
24
26
28
30
32
CHC chain length

(C)

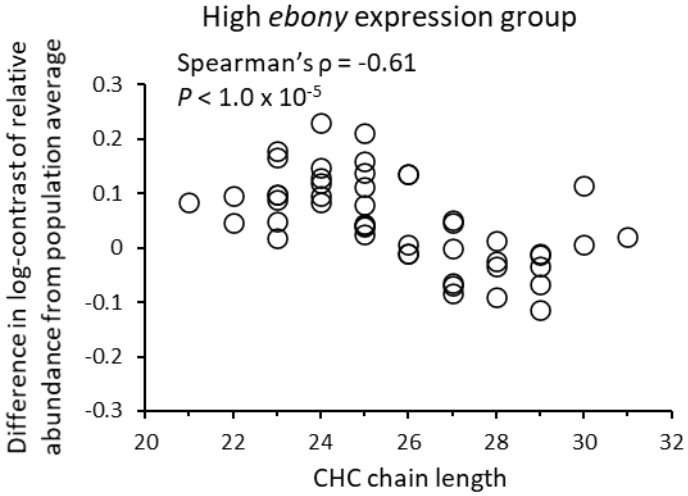
High *ebony* expression group
Spearman's ρ = -0.61
P < 1.0 x 10-5
Difference in log-contrast of relative abundance from population average
0.3
0.2
0.1
0
-0.1
-0.2
-0.3
20
22
24
26
28
30
32
CHC chain length

Fig. 2-2 Difference in log-contrast of relative CHC abundance between the *ebony* expression groups and the population average plotted against the chain length in DGRP

The CHC data was obtained from Dembeck *et al*. (2015), and the expression level of *ebony* was quantified by RT-qPCR. Difference in log-contrast of relative CHC proportion between the average of each expression level group and the average of the 23 DGRP strains; (A) Low group (9 strains), (B) Intermediate group (6 strains) and (C) High group (8 strains).

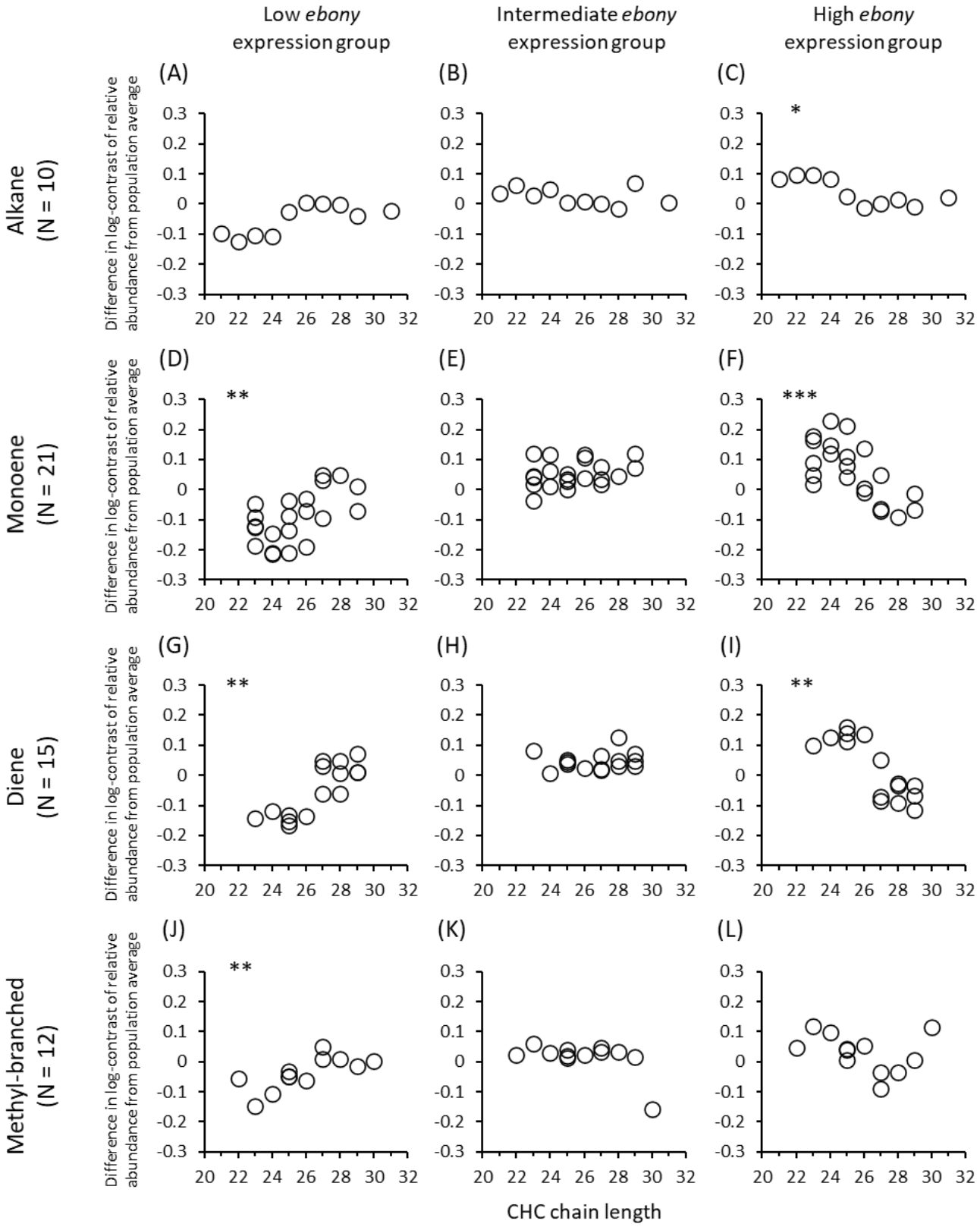
Low *ebony* expression group
Intermediate *ebony* expression group
High *ebony* expression group
Alkane (N = 10)
Monoene (N = 21)
Diene (N = 15)
Methyl-branched (N = 12)
Difference in log-contrast of relative abundance from population average
CHC chain length
(A)
(B)
(C)
(D)
(E)
(F)
(G)
(H)
(I)
(J)
(K)
(L)
*
**
***
**
**

Fig. 2-3 Difference in log-contrast of relative CHC abundance between the *ebony* expression groups and the population average plotted against the chain length in DGRP

The CHCs were categorized into four structural categories and plotted as in Fig. 2-2. CHC categories; (A, B and C) Alkane, (D, E, and F) Monoene, (G, H and I) Diene, (J, K and L) Methyl-branched. *ebony* expression group; (A, D, G and J) Low group (9 strains), (B, E, H and K) Intermediate group (6 strains) and (C, F, I and L) High group (8 strains). Each Spearman's rank correlation coefficient ρ is follows; (A) 0.64, (B) -0.43, (C) -0.71, (D) 0.56, (E) 0.25, (F) -0.69, (G) 0.75, (H) 0.15, (I) -0.74, (J) 0.77, (K) -0.32 and (L) -0.44. *, ** and *** indicate $P < 0.05$, $P < 0.01$ and $P < 0.001$ estimated from Spearman's ρ, respectively.

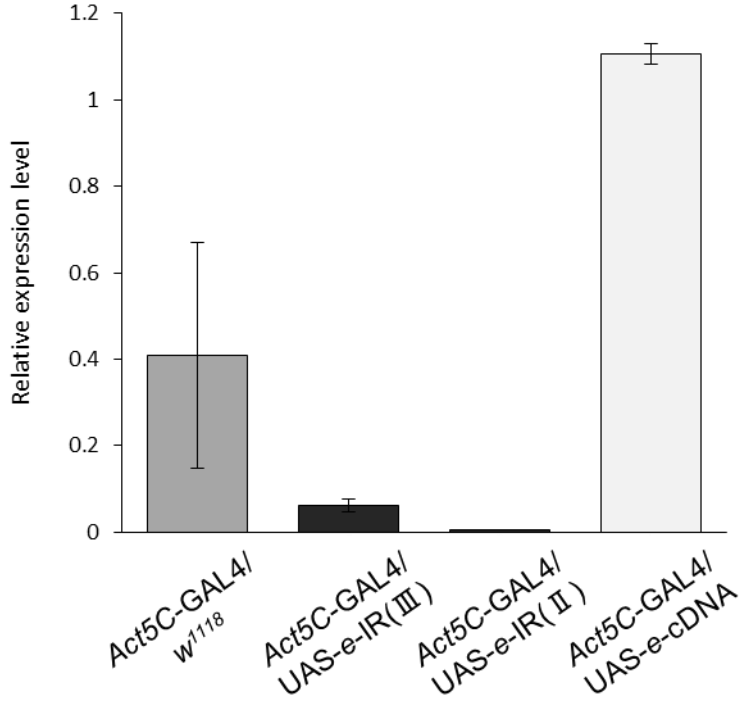

Fig. 2-4 The expression level of *ebony* of expression manipulated individuals

The expression level of *ebony* was quantified by RT-qPCR with three biological replications. *Act5C*-GAL4/w^{1118} is the control of *Act5C*-GAL4/UAS-*e*-IR(III) and *Act5C*-GAL4/UAS-*e*-IR(II). Error bar denotes standard error.

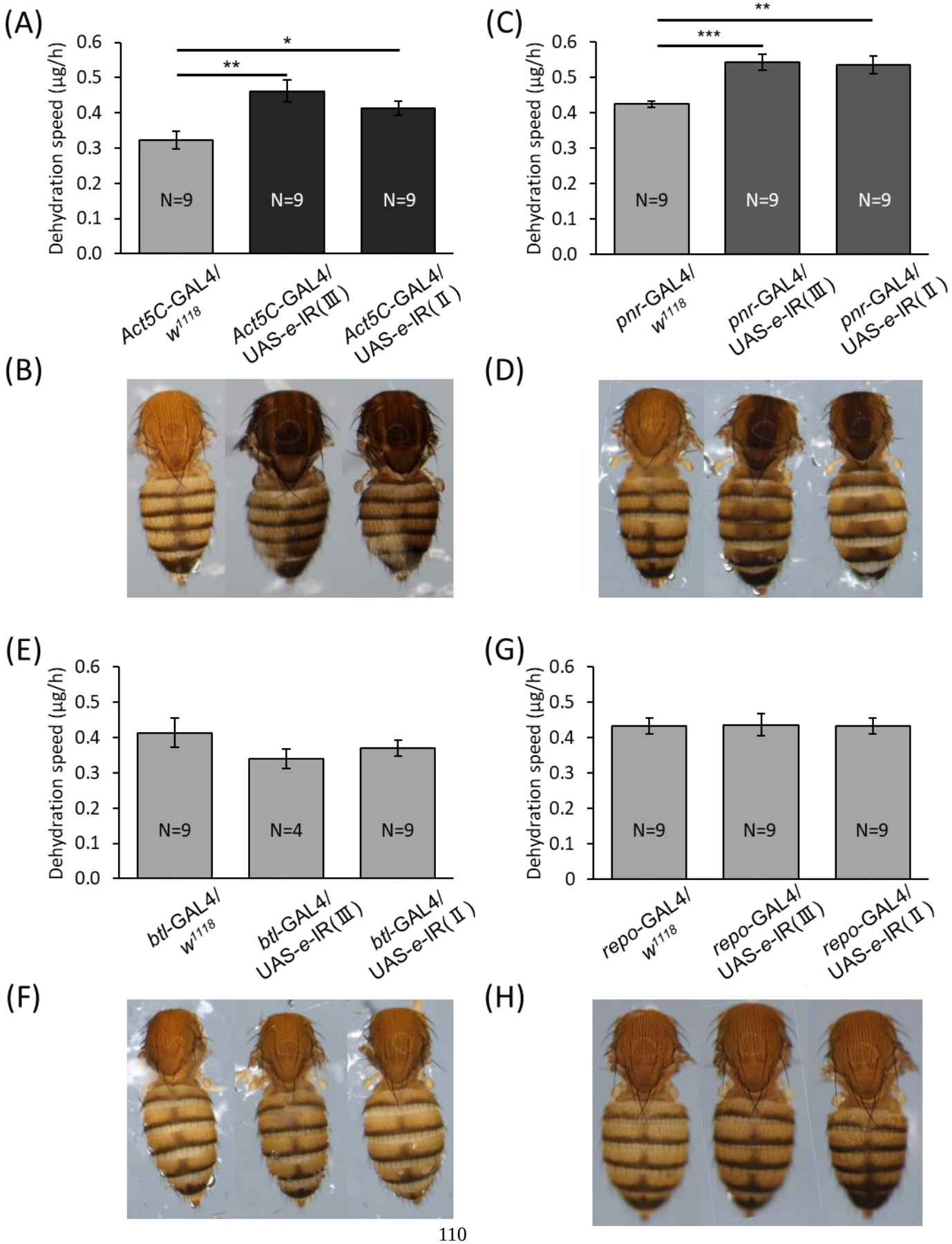
(A)
Dehydration speed (μg/h)
0.6
0.5
0.4
0.3
0.2
0.1
0.0
*
**
N=9
N=9
N=9
Act5C-GAL4/ w1118
Act5C-GAL4/ UAS-e-IR(Ⅲ)
Act5C-GAL4/ UAS-e-IR(Ⅱ)
(C)
**
***
N=9
N=9
N=9
pnr-GAL4/ w1118
pnr-GAL4/ UAS-e-IR(Ⅲ)
pnr-GAL4/ UAS-e-IR(Ⅱ)
(B)
(D)
(E)
0
N=9
N=4
N=9
btl-GAL4/ w1118
btl-GAL4/ UAS-e-IR(Ⅲ)
btl-GAL4/ UAS-e-IR(Ⅱ)
(G)
N=9
N=9
N=9
repo-GAL4/ w1118
repo-GAL4/ UAS-e-IR(Ⅲ)
repo-GAL4/ UAS-e-IR(Ⅱ)
(F)
(H)

Fig. 2-5 Changes in dehydration speed by *ebony* knockdown

(A) Dehydration speed of individuals whose *ebony* is knocked-down in the whole-body. (B) Dorsal images of the thorax and abdomen used in (A). (C) Dehydration speed of individuals whose *ebony* is knocked-down in the partial epidermis. (D) Fly images used in (C). (E) Dehydration speed of individuals whose *ebony* is knocked-down in the trachea. (F) Fly images used in (E). (G) Dehydration speed of individuals whose *ebony* is knocked-down in the glial cells. (H) Fly images used in (G). Student's *t*-test was performed. *, ** and *** indicate $P < 0.05$, $P < 0.01$ and $P < 0.001$, respectively.

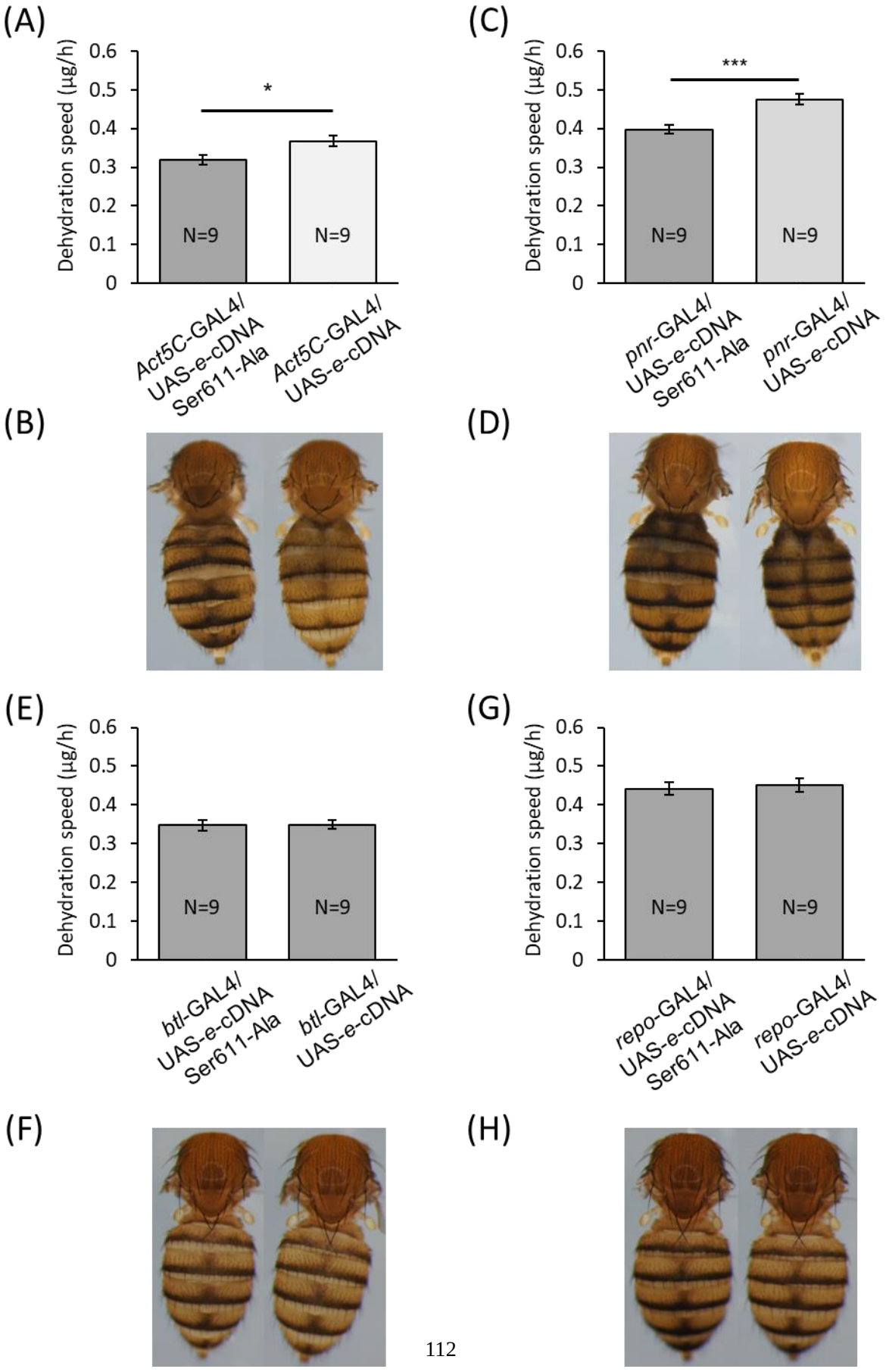
(A)
Dehydration speed (µg/h)
0.6
0.5
0.4
0.3
0.2
0.1
0
*
N=9
N=9
Act5C-GAL4/ UAS-e-cDNA Ser611-Ala
Act5C-GAL4/ UAS-e-cDNA
(C)
Dehydration speed (µg/h)
***
N=9
N=9
pnr-GAL4/ UAS-e-cDNA Ser611-Ala
pnr-GAL4/ UAS-e-cDNA
(B)
(D)
(E)
Dehydration speed (µg/h)
N=9
N=9
btl-GAL4/ UAS-e-cDNA Ser611-Ala
btl-GAL4/ UAS-e-cDNA
(G)
Dehydration speed (µg/h)
N=9
N=9
repo-GAL4/ UAS-e-cDNA Ser611-Ala
repo-GAL4/ UAS-e-cDNA
(F)
(H)

Fig. 2-6 Changes in dehydration speed by *ebony* upregulation

(A) Dehydration speed of individuals whose *ebony* is upregulated in the whole-body. (B) Fly images used in (A). (C) Dehydration speed of individuals whose *ebony* is upregulated in the partial epidermis. (D) Fly images used in (C). (E) Dehydration speed of individuals whose *ebony* is upregulated in the trachea. (F) Fly images used in (E). (G) Dehydration speed of individuals whose *ebony* is upregulated in the glial cells. (H) Fly images used in (G). Student's *t*-test was performed. * and *** indicate $P < 0.05$ and $P < 0.001$, respectively.

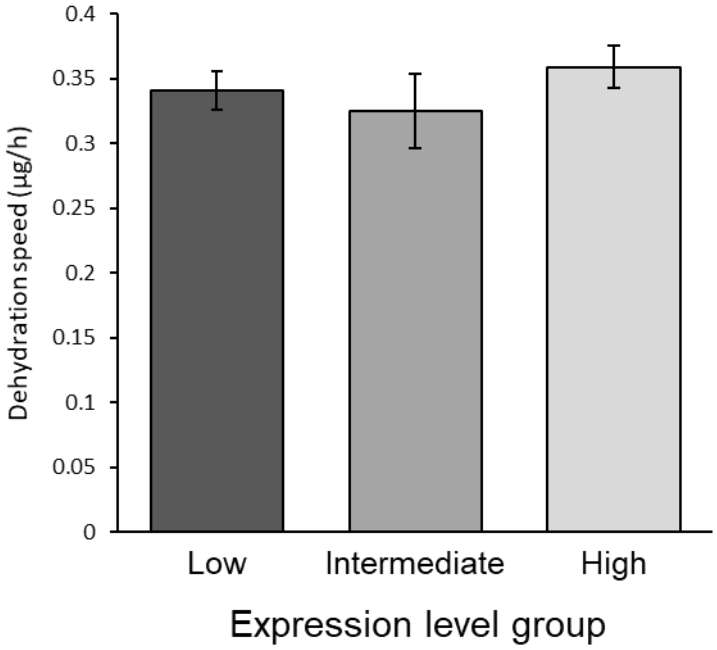

Fig. 2-7 Dehydration speed of three groups of *ebony* expression in DGRP

The average dehydration speed in each expression level group of the DGRP strains (Low: 9 strains, Intermediate: 6 strains, High: 8 strains). Three to nine replications were performed for each strain. Error bar denotes standard error.

GENERAL DISCUSSION

Many studies have focused on how the wide range of variations in pigmentation in insects have been acquired and maintained. Approaches from different fields, including developmental biology, ecology, and genetics, have been taken to elucidate this question. In this study, the main causative gene for pigmentation variation in *D. melanogaster*, *ebony*, was used to advance our understanding of its spatiotemporal regulatory system involved in the formation of body pigmentation and pleiotropy effects. In this section, I discuss the prospects of these results offer for studies on pigmentation.

The results presented in this study suggested the presence of multiple epidermis enhancers of *ebony* by knocking out the primary epidermis enhancer (priEE). The locations of other epidermal enhancers have not been identified in this study. A Chromosome conformation capture-on-chip method (4C, Simonis *et al*., 2006) may be helpful for identifying the candidate. The genomic regions interacting with the promoter of *ebony* can be detected by 4C, and the enhancer activity in the developing epidermis can be confirmed by a reporter assay.

The identification of multiple epidermis enhancers may allow further investigation of the variations that have similar effects on the *ebony* regulation. The *ebony* haplotypes strongly associated with dark body color identified in different worldwide populations are not similar (Rebeiz *et al*. 2009; Takahashi and Takano-Shimizu, 2011; Miyagi *et al*. 2015; Telonis-Scott and Hoffmann 2018). The combinations of nucleotide variants in different epidermis enhancers of *ebony* might be a reason for the complexity. Those variants at scattered sites in the *ebony cis*-regulatory

region may have occurred independently but act similarly in different populations.

The studies on spatial regulation of the genes involved in pigmentation patterns have been conducted mainly in some *Drosophila* and butterfly species (reviewed in Prud'homme *et al*., 2007; Rebeiz and Williams, 2017; Livraghi *et al*., 2018). The pigmentation patterns in these species are associated with the spatial regulation of the gene expression. The method used in this study that allows genome editing in the germ cells to establish non-mosaic knockout individuals could be applied to these insects with remarkable pigmentation pattern diversity. Dissecting and narrowing down the *cis*-regulatory elements by genome editing is helpful in elucidating the mechanisms of pigmentation pattern diversity. Furthermore, one could ask whether or not the pigmentation pattern has occurred through the convergent evolution of the same *cis*-regulatory elements.

Also, the establishment of genome-edited individuals is superior to expression site labeling, such as in-situ hybridization or reporter assays, because the phenotype can be directly observed and the individuals can be repeatedly used from the established stocks. In addition, it is possible to confirm whether a phenotype can be reproduced by enhancer replacements. For example, replacing a limb-specific enhancer in the mouse *Shh* gene with a snake-derived sequence resulted in snake-like mice without normal leg formation (Kvon *et al*., 2016). A simple understanding of the pigmentation pattern evolution may be achieved by replacing a single factor, such as the midline silencer of *ebony* shown in this study, with the orthologous sequences in other species.

Pigmentation-associated genes in insects are often associated with other phenotypes and considered to be pleiotropic. In this study, I investigated a new aspect of *ebony* and showed that the expression level of *ebony* and the CHC profiles co-vary in a

natural population of *D. melanogaster*. After these results were published (Massey, Akiyama *et al*., 2019), the association between *ebony* and CHC profiles in two other species, *D. americana* and *D. novamexicana*, were also reported (Lamb *et al*., 2020). Whether this association is universally observed in other dipteran species and a wide range of insect species is also of interest. Also, CHCs are thought to affect cuticular permeability and sexual selection depending on their composition and amount (reviewed in Yew and Chung, 2015; Wang *et al*., 2021). Although no association between CHC profiles and cuticular permeability was found in the natural population investigated in this study, CHCs may be valuable candidates for elucidating concrete mechanisms of adaptation to desiccation and reproductive isolation related to body color.

This study has advanced the understanding of the genetic basis of how *ebony*-mediated pigmentation variation is regulated at the transcriptional level and the features of its pleiotropic effects on ecologically relevant physiological traits that co-varies with body color.

LITERATURE CITED

Kvon, E. Z., Kamneva, O. K., Melo, U. S., Barozzi, I., Osterwalder, M., Mannion, B. J., ... & Visel, A. (2016). Progressive loss of function in a limb enhancer during snake evolution. *Cell*, *167*(3), 633-642.

Lamb, A. M., Wang, Z., Simmer, P., Chung, H., & Wittkopp, P. J. (2020). *ebony* affects pigmentation divergence and cuticular hydrocarbons in *Drosophila americana* and *D. novamexicana*. *Frontiers in Ecology and Evolution*, *8*, 184.

Livraghi, L., Martin, A., Gibbs, M., Braak, N., Arif, S., & Breuker, C. J. (2018). CRISPR/Cas9 as the key to unlocking the secrets of butterfly wing pattern development and its evolution. *Advances in Insect Physiology* (Vol. 54, pp. 85-115).

Massey, J. H., Akiyama, N., Bien, T., Dreisewerd, K., Wittkopp, P. J., Yew, J. Y., & Takahashi, A. (2019). Pleiotropic effects of *ebony* and *tan* on pigmentation and cuticular hydrocarbon composition in *Drosophila melanogaster*. *Frontiers in Physiology*, *10*, 518.

Miyagi, R., Akiyama, N., Osada, N., & Takahashi, A. (2015). Complex patterns of *cis*‐regulatory polymorphisms in *ebony* underlie standing pigmentation variation in *Drosophila melanogaster*. *Molecular Ecology*, *24*(23), 5829-5841.

Prud'homme, B., Gompel, N., & Carroll, S. B. (2007). Emerging principles of regulatory evolution. *Proceedings of the National Academy of Sciences*, *104*(suppl 1), 8605-8612.

Rebeiz, M., Pool, J. E., Kassner, V. A., Aquadro, C. F., & Carroll, S. B. (2009). Stepwise modification of a modular enhancer underlies adaptation in a *Drosophila* population. *Science*, *326*(5960), 1663-1667.

Rebeiz, M., & Williams, T. M. (2017). Using *Drosophila* pigmentation traits to study the mechanisms of *cis*-regulatory evolution. *Current Opinion in Insect Science*, *19*, 1-7.

Simonis, M., Klous, P., Splinter, E., Moshkin, Y., Willemsen, R., De Wit, E., *et al*. (2006). Nuclear organization of active and inactive chromatin domains uncovered by chromosome conformation capture–on-chip (4C). *Nature Genetics*, *38*(11), 1348-1354.

Takahashi, A., & Takano-shimizu, T. (2011). Divergent enhancer haplotype of *ebony* on inversion In (3R) Payne associated with pigmentation variation in a tropical population of *Drosophila melanogaster*. *Molecular Ecology*, *20*(20), 4277-4287.

Telonis-Scott, M., & Hoffmann, A. A. (2018). Enhancing *ebony*? Common associations with a *cis*-regulatory haplotype for *Drosophila melanogaster* thoracic pigmentation in a Japanese population and Australian populations. *Frontiers in Physiology*, *9*, 822.

Wang, Y., Ferveur, J. F., & Moussian, B. (2021). Eco‐genetics of desiccation resistance in *Drosophila*. *Biological Reviews*, *96*(4), 1421-1440.

Yew, J. Y., & Chung, H. (2015). Insect pheromones: An overview of function, form, and

discovery. *Progress in Lipid Research*, *59*, 88-105.

COMPLIANCE STATEMENT IN DISSERTATIONS

Conflict of Interest

There is no conflict of interest to declare.

Publication

Massey, J. H., Akiyama, N., Bien, T., Dreisewerd, K., Wittkopp, P. J., Yew, J. Y., & Takahashi, A. (2019). Pleiotropic effects of *ebony* and *tan* on pigmentation and cuticular hydrocarbon composition in *Drosophila melanogaster*. *Frontiers in Physiology*, *10*, 518. doi: 10.3389/fphys.2019.00518

Akiyama, N., Sato, S., Tanaka, K. M., Sakai, T., & Takahashi, A. (2022). The role of the epidermis enhancer element in positive and negative transcriptional regulation of *ebony* in *Drosophila melanogaster*. *G3 Genes| Genomes| Genetics*. doi: 10.1093/g3journal/jkac0106506522

ACKNOWLEDGEMENTS

I would like to express my deepest gratitude to Dr. Aya Takahashi for her guidance during the course of this study and for critical reading of the manuscript for the thesis and publication. I also wish to express my great appreciation to Dr. Koichiro Tamura and Dr. Takaomi Sakai for their invaluable advice and reviewing my thesis. I also appreciate Dr. Shoma Sato for kindly teaching experimental techniques and for providing valuable comments to my study. I would also like to thank Dr. Nikolas Gompel for *pJet-yellow_F4mut-mCherry* vector, Dr. Ryu Ueda for w^{1118} strain, Dr. Bernhard T. Hovemann for UAS-*e*-cDNA and UAS-*e*-cDNA Ser611-Ala, WellGenetics for embryonic injection, and Bloomington *Drosophila* Stock Center, VDRC Stock Center, NIG-Fly and Kyoto Stock Center for fly stocks. I also thank the stock maintaining staffs and the Evolutionary Genetics laboratory members for their support.